

8-14-2017

Hydroformylation and Aldehyde-Water Shift Catalysis by Dirhodium Tetrphosphine Complexes

Marshall Douglas Moulis

Louisiana State University and Agricultural and Mechanical College, mmouli5@lsu.edu

Follow this and additional works at: https://digitalcommons.lsu.edu/gradschool_dissertations



Part of the [Inorganic Chemistry Commons](#)

Recommended Citation

Moulis, Marshall Douglas, "Hydroformylation and Aldehyde-Water Shift Catalysis by Dirhodium Tetrphosphine Complexes" (2017).
LSU Doctoral Dissertations. 4095.

https://digitalcommons.lsu.edu/gradschool_dissertations/4095

This Dissertation is brought to you for free and open access by the Graduate School at LSU Digital Commons. It has been accepted for inclusion in LSU Doctoral Dissertations by an authorized graduate school editor of LSU Digital Commons. For more information, please contact gradetd@lsu.edu.

HYDROFORMYLATION AND ALDEHYDE-WATER SHIFT
CATALYSIS BY DIRHODIUM TETRAPHOSPHINE COMPLEXES

A Dissertation

Submitted to the Graduate Faculty of the
Louisiana State University and Agricultural and
Mechanical College
in partial fulfillment of the
requirement for the degree of
Doctor of Philosophy

in

The Department of Chemistry

by
Marshall Douglas Moulis
B.S. University of Dallas, 2011
December 2017

Acknowledgements

Above all else, I would like to thank the Lord our God, Jesus the Christ, for His continued blessing on me and my family. My life, abilities, and passions are by His will, and it is through His guidance and encouragement that I was able to achieve the following research and document. To my advising professor, Dr. George Stanley, I'd like to thank you for your continued support. You have giving me more understanding and guidance of the materials than anyone before and likely anyone to come, which allowed me to grasp the broad subject of catalysis. I thank you too for your generosity in finding funding for and additional funding of my research. I too would like to thank the Louisiana Board of Regents for the fellowship that supported most of my research.

To my brother Malloy, thank you for giving me a hard time. Your support of my wellbeing the first two years of this long journey were able to fuel my body for the many hours that I was needed in the lab. Furthermore, your constraint appearance for the remaining four years brought me much joy. It is thanks to you and your beautiful wife Hannah that I had much of a social life giving balance to my studies. As a final note, I just wanted to congratulate you two on your wedding, and I love you both.

To my father and mother, I will start with I love you. You have given me everything that I could ever want. You instilled in my life values and faith. You persistently have sustained me even though I have had faults that made me question my resolve. The support of your home eased the hardships that most might face in pursuit of higher education. I am not sure how I can repay you, but as a start I accredit this document below to you.

I would like to thank the members of my committee, Dr. Donghui Zhang, Dr. Andrew Maverick, and Dr. Ye Xu for your patience and flexibility. I thank Dr. Connie David in the Mass

Spec facility, Dr. Thomas Weldeghiorghis in the NMR facility, and Dr. Frank Fronczek in the X-ray crystallography lab for each of their assistance in analysis of various materials and understanding of the processes; it is from you I have learned vital techniques and I thank you for your time and your attribution to my research. Finally, I am honored to thank past members of the Stanley research group Rider Barnum, Ekaterina Kalachnikova, Ranelka Fernando, and Ciera Gasery and current members Drew Hood and Ryan Johnson. Your friendships over the past years are treasured and made many days bearable. Your training, advice, and discussions gave knowledge and insight to the project that I could not do without.

Table of Contents

Acknowledgements	ii
List of Abbreviations	v
Abstract	vii
Chapter 1: Hydroformylation of Olefins by Rhodium Systems	1
1.1 Discovery of Hydroformylation	1
1.2 The Use of Phosphines as Ligands	3
1.3 Chelating Ligands	8
1.4 Bimetallic Hydroformylation.....	10
1.5 Discovery of Aldehyde-Water Shift Reaction	14
1.6 Design of a New Tetraphosphine Ligand	16
1.7 Continued Research on Hydroformylation and Aldehyde-Water Shift	17
1.8 References.....	19
Chapter 2: Ligand Synthesis and Complex Characterization	22
2.1 Introduction	22
2.2 Results and Discussion	28
2.3 References	45
Chapter 3: Hydroformylation and Aldehyde-Water Shift Catalysis	49
3.1 Introduction	49
3.2 Results and Discussion	62
3.3 References	81
Chapter 4: Experimental Procedures	83
4.1 General Considerations	83
4.2 General Hydroformylation Procedures	84
4.3 General Aldehyde-Water Shift Procedures (Tandem Hydroformylation).....	85
4.4 Synthesis of Cl-Bridge	85
4.5 Synthesis of I-Small Arm	86
4.6 Synthesis of Br-Small Arm	86
4.7 Synthesis of et,ph-P4-Ph via I-Small Arm	87
4.8 Synthesis of et,ph-P4-Ph via Br-Small Arm	88
4.9 Column Chromatography for the Removal of Impurities from et,ph-P4-Ph.....	88
4.10 Column Chromatography for the Separation of <i>meso</i> - and <i>rac</i> -et,ph-P4-Ph.....	89
4.11 Synthesis of [Rh(nbd) ₂]PF ₆	89
4.12 Synthesis of [Rh(nbd) ₂ (<i>rac</i> -et,ph-P4-Ph)](BF ₄) ₂	90
4.13 Synthesis of [Rh(nbd) ₂ (<i>rac</i> -et,ph-P4-Ph)](PF ₆) ₂	90
4.14 Synthesis of [Rh(μ-CO)(CO) ₃ (<i>rac</i> -et,ph-P4-Ph)](BF ₄) ₂	90
4.15 References	91
Vita	92

List of Abbreviations

AWS	aldehyde-water shift
bridge	H(Ph)PCH ₂ P(Ph)H
Br-small arm	1-(diethylphosphino)-2-bromobenzene
¹³ C NMR	carbon NMR
¹³ C { ¹ H} NMR	carbon, proton decoupled, NMR
chlorobridge	Cl(Ph)PCH ₂ P(Ph)Cl
COSY	correlation spectroscopy
DCM	dichloromethane
DFT	density functional theory
DMF	N,N-dimethylformamide
DMSO	dimethylsulfoxide
dddd	doublet of doublet of doublet of doublets
dppb	1,2-bis(diphenylphosphino)butane
dppe	1,2-bis(diphenylphosphino)ethane
dppm	1,2-bis(diphenylphosphino)methane
dppp	1,2-bis(diphenylphosphino)propane
eq.	equivalents
FT-IR	Fourier transform-inferred spectrometry
GC-MS	gas chromatography-mass spectrometry
¹ H NMR	proton NMR
hydro	hydrogenation
Hz	Hertz

I-small arm	1-(diethylphosphino)-2-iodobenzene
iso	isomerization
L:B	linear:branched
min	minute
<i>meso</i>	<i>mesomeric</i>
mL	milliliters
mM	millimolar (mmol/L)
mmol	millimole
NMR	nuclear magnetic resonance
ORTEP	Oak Ridge thermal ellipsoid plot program
³¹ P NMR	phosphorus NMR
³¹ P { ¹ H} NMR	phosphorus, proton decoupled, NMR
ppm	parts per million
psi	pounds per square inch
psig	pounds per square inch, gauge
<i>rac</i>	<i>racemic</i>
syn-gas	synthesis gas (H ₂ /CO)
THF	tetrahydrofuran
TOF	turnover frequencies
vol	volume

Abstract

The use of a unique tetraphosphine ligand (et,ph-P4) allows for the chelating of two rhodium centers to perform bimetallic cooperativity in hydroformylation reactions to better the yields the linear aldehyde product. The proposed catalyst is $[\text{Rh}_2(\mu\text{-H})_2(\text{CO})_4(\text{rac-et,ph-P4})]^{2+}$ and has been studied by *in situ* FT-IR and NMR. When tested in a polar phasic acetone/water (30 % by vol.), the catalyst forms a monocationic system $[\text{Rh}_2(\mu\text{-H})_2(\text{CO})_4(\text{rac-et,ph-P4})]^+$ that has an initial TOF of 26 min^{-1} , selectivity of 27:1 L:B, and low byproducts of 4.6 % alkene isomerization and 1.3 % hydrogenation for the conversion of 1-hexene to heptanal. Previous *in situ* FT-IR and NMR research as well as DFT calculations have determined the active catalyst and mechanism for both the dicationic and monocationic systems.

A new stronger chelating tetraphosphine ligand (et,ph-P4-Ph) as been built to function similarly to the et,ph-P4 ligand. After a preliminary synthetic scheme for the production of et,ph-P4-Ph, optimization of the key synthetic steps has been accomplished. This optimization allows for the increase in yields of those steps and the separation of the *rac*- and *meso*-diastereomers of the ligand. Use of this ligand to chelate two rhodium centers has occurred and a crystal structure of $[\text{Rh}_2(\text{nbd})_2(\text{rac-et,ph-P4-Ph})](\text{BF}_4)_2$ has been obtained.

This complex has been studied by *in situ* FT-IR and NMR experiments to determine the nature of the catalytic system. Out of these studies the highly active complex $[\text{Rh}_2(\mu\text{-CO})(\text{CO})_3(\text{rac-et,ph-P4})](\text{BF}_4)_2$ has been synthesized and characterized by X-ray diffraction. When used in hydroformylation in a polar phasic DMF/water (25 % by vol.), the new catalyst has initial TOF of 35 min^{-1} , an aldehyde L:B selectivity of 18:1, 1.9 % alkene isomerization, and < 1 % alkene hydrogenation. Attempts have also been made to use this complex for aldehyde-water shift reactions. Further work is underway to further these studies for publication.

Chapter 1: Hydroformylation of Olefins by Rhodium Systems

1.1 Discovery of Hydroformylation

Early in the twentieth century, Otto Roelen revolutionized the production of aldehydes by his serendipitous discovery of hydroformylation.¹ While working on Fischer-Tropsch chemistry, Roelen found that cobalt metal would dissolve into solution under H₂/CO pressure and temperature. When ethylene was introduced to the mixture, propanal was produced: discovering the catalysis of hydroformylation. This reaction is the conversion of olefins, hydrogen, and carbon monoxide with a metal center, usually Co or Rh, to form aldehydes (Figure 1.1). The aldehyde produced can exist as one of two forms dependent on where the carbonyl adds to the olefin. If it were to end up on the terminal carbon of the double bond, then a linear or normal aldehyde is formed. If it were to add to the internal carbon of the double bond, then a branched or iso aldehyde is formed. Industry generally wants the linear aldehyde as it is more valuable than the branched aldehyde. Likewise, another aspect of the research into hydroformylation is the limitation of side products via alkene isomerization and hydrogenation to alkanes.

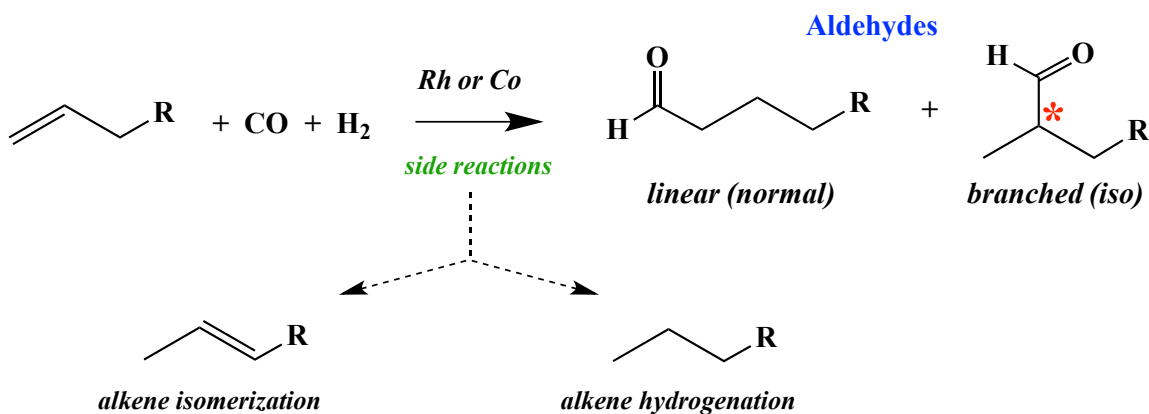


Figure 1.1. Hydroformylation catalysis

Hydroformylation is the largest homogeneous catalysis in the world producing over 6,000,000 tons of aldehydes a year. Some of the applications of the aldehydes include the

formation of alcohols, amines, carboxylic acids, acroleins, diols, acetals, and ethers, which in turn are used to make solvents, plasticizers, and detergents.^{2,3} After Roelen's initial discovery in 1938, it was not until 1961 that Heck and Brewslo proposed what is now the accepted mechanism for the catalysis (Figure 1.2).⁴ Using $\text{Co}_2(\text{CO})_8$ as the initial catalyst, they found $\text{Co}_2(\text{CO})_8$ oxidatively adds H_2 forming two equivalents of monometallic $\text{HCo}(\text{CO})_4$, which is the active catalyst.

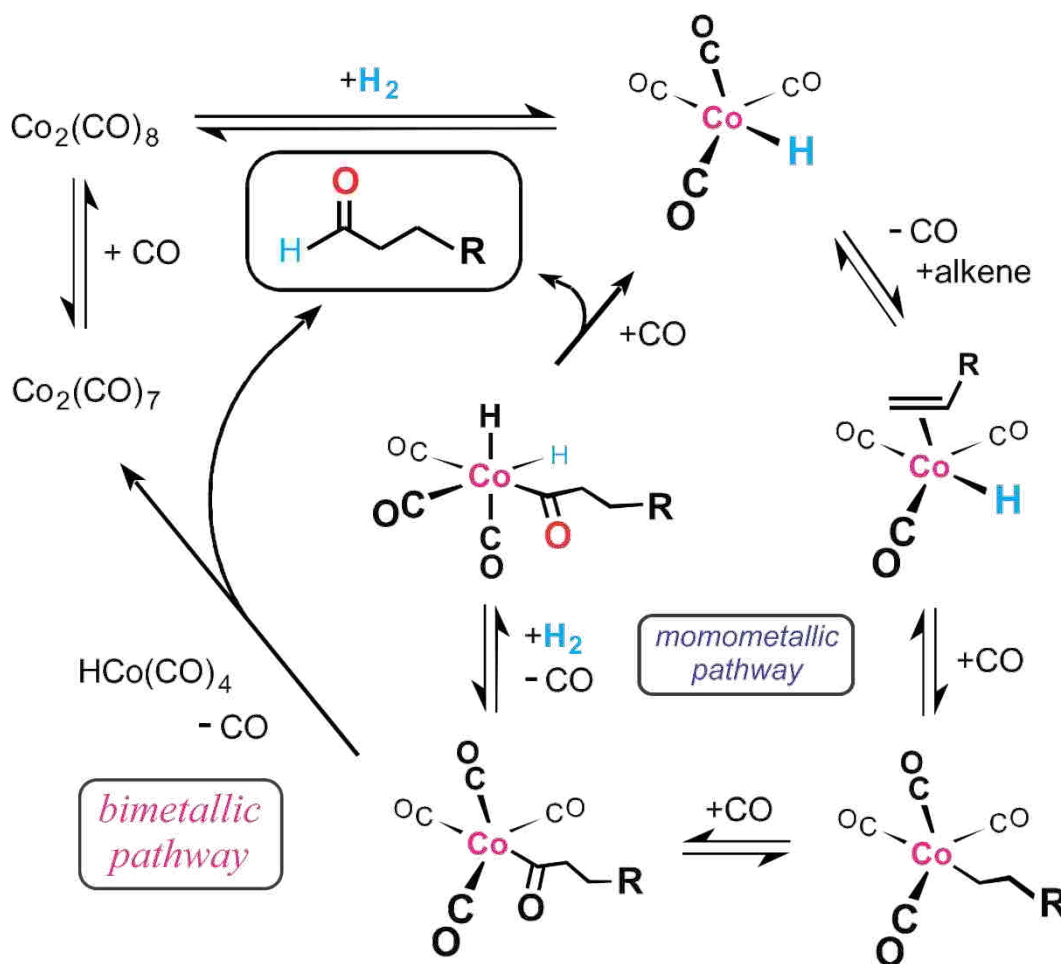


Figure 1.2. Heck and Brewslo's mechanism for Roelen's cobalt hydroformylation

The first reaction step is the exchange of a carbonyl for the olefin. The $\text{HCo}(\text{CO})_4$ species contains an 18 electron cobalt that is saturated, so the dissociation of a carbonyl ligand must first occur in order to allow coordination of the alkene. The hydride then does a migratory insertion

with the alkene, adding to the internal carbon of the double bond producing the linear alkyl ligand. The hydride could also add to the terminal carbon of the double bond to form the branched alkyl species, which is not shown in Figure 1.2. A new carbonyl ligand adds to the empty coordination site formed from the reaction of the hydride and alkene. The alkyl ligand then does a migratory insertion with a cisoidal carbonyl making an acyl ligand, followed by the addition of another carbonyl to the resulting empty coordination site on the cobalt.

The favored pathway has a carbonyl dissociating from the metal followed by oxidative addition of H_2 to the metal to generate a dihydride complex. One of the hydrides reductively eliminates with the acyl producing the linear aldehyde and the regenerated $HCo(CO)_4$ catalyst. Heck also proposed a pathway involving carbonyl dissociation and the intermolecular transfer of a hydride from a second $HCo(CO)_4$ catalyst to reductively eliminate aldehyde. $Co_2(CO)_8$ is the other product formed from this reductive elimination, which can react with H_2 to regenerate two equivalents of $HCo(CO)_4$. Under normal catalytic conditions the concentration of the cobalt catalyst is too low to favor this bimetallic mechanism. However, this intermolecular hydride transfer step is a form of bimetallic cooperativity that encouraged Prof. Stanley to design a binucleating ligand system that keeps two metal centers in close proximity to promote an intramolecular hydride transfer.

1.2 The Use of Phosphines as Ligands

Most research after Heck's mechanism proposal focused on monometallic complexes. Roelen's original system suffered from $HCo(CO)_4$ decomposing to cobalt metal. To counter this, high CO partial pressures are needed to keep the carbonyl ligand bound to the cobalt. However, as the CO partial pressures increased, the dependence on higher temperatures are

needed to keep an active catalyst system. The $\text{HCo}(\text{CO})_4$ catalyst requires temperatures in the range of 150 – 300 °C and pressures of 200 – 300 bar.

Carbonyls are known to have the ability to π -backbond to a metal center. This involves the d-electrons from the metal center being donated to the empty π^* orbital of the carbonyl ligand. This π -backbonding strengthens the overall bond between the metal and carbonyl, making it stronger and less likely to dissociate. The π -backbonding weakens the π -bonding between C-O, and it lowers CO infrared stretching frequency. Stronger σ -donating ligands, such as phosphines, make the metal center more electron-rich, and favors π -backdonation to the carbonyls.

Slaugh and Mullineaux at Shell Chemical recognized this, and added trialkylphosphines to $\text{HCo}(\text{CO})_4$.⁶ The donating ability of these phosphines increased the electron richness of the cobalt center, which in turn increased the π -backbonding to the carbonyl ligands, and reduced their tendency to dissociate. Although this slows the hydroformylation catalysis, it stabilizes the $\text{HCo}(\text{CO})_3(\text{PR}_3)$ catalyst so it does not decompose to cobalt metal as easily. This allowed Shell to run hydroformylation under considerably lower CO partial pressures relative to $\text{HCo}(\text{CO})_4$. With the addition of phosphines, the pressures could be reduced to 720 – 1455 psi.⁵

Slaugh's examination into which phosphine and arsine ligands promoted hydroformylation showed interesting trends. Ligands such as PEt_3 or PBu_3 could convert the olefins to aldehydes, which were then hydrogenated to the desired alcohol products. As the alkyl groups were exchanged for the less electron donating phenyl group, aldehydes production dominated. With arsines, even greater production of aldehydes was seen, but at the cost of selectivity. Arsines were also found to be more sensitive to degradation at higher temperatures.

Furthermore, bulkier phosphine ligands lead to higher yields with fair selectivity. The overall trends can be reviewed in this excerpt of Slaugh *et al.*'s data table below, (Table 1.1).

Table 1.1. Hydroformylation of 1-pentene using $\text{Co}(\text{CO})_3\text{L}^*$

Ligand (L)	% Conv. of 1-Pentene	% Yield of Alcohols	% Yield of Aldehydes	Linear Selectivity	Branched Selectivity
PEt_3	100	79.8	0	80.9	19.1
PBu_3	100	77.0	0	84.1	15.9
PEt_2Ph	100	75.6	2.8	79.0	21.0
PEtPh_2	100	74.5	4.3	74.5	25.5
PBu_2Ph	100	72.0	0	80.0	20.0
PPh_3	39.9	60.7	10.3	66.0	34.0
AsBu_3	82.8	51.9	28.7	67.8	32.2
AsEt_2Ph	98.9	66.6	18.4	55.7	44.3

* $\text{Co}_2(\text{CO})_8$ was mixed with two eq. of the ligand to make the complex. Hydroformylation was run at 150 °C for the arsine complexes and 195 °C for the phosphine complexes.

Osborn, Young, and Wilkinson found that rhodium phosphine complexes not only could catalyze hydroformylation reactions, but did so under much milder conditions.⁷⁻¹¹ The activity of rhodium was shown to be 1000× that of cobalt. Some of Wilkinson's early experiments were actually run under ambient conditions. Originally, their research was done with $\text{RhCl}(\text{PPh}_3)_3$ as it was a common starting material, however, halides were later found to inhibit the reaction. Since research by Slaugh *et al.* had shown the remarkable effect of phosphines, PPh_3 was used as the ligand for most of their research. The industry standard $\text{HRh}(\text{CO})(\text{PPh}_3)_3$ catalyst was based on these observations. The accepted mechanism for the Rh/PPh_3 catalyst is shown below as Figure 1.3. The steps in this system mimic those in Heck's monometallic cobalt mechanism.

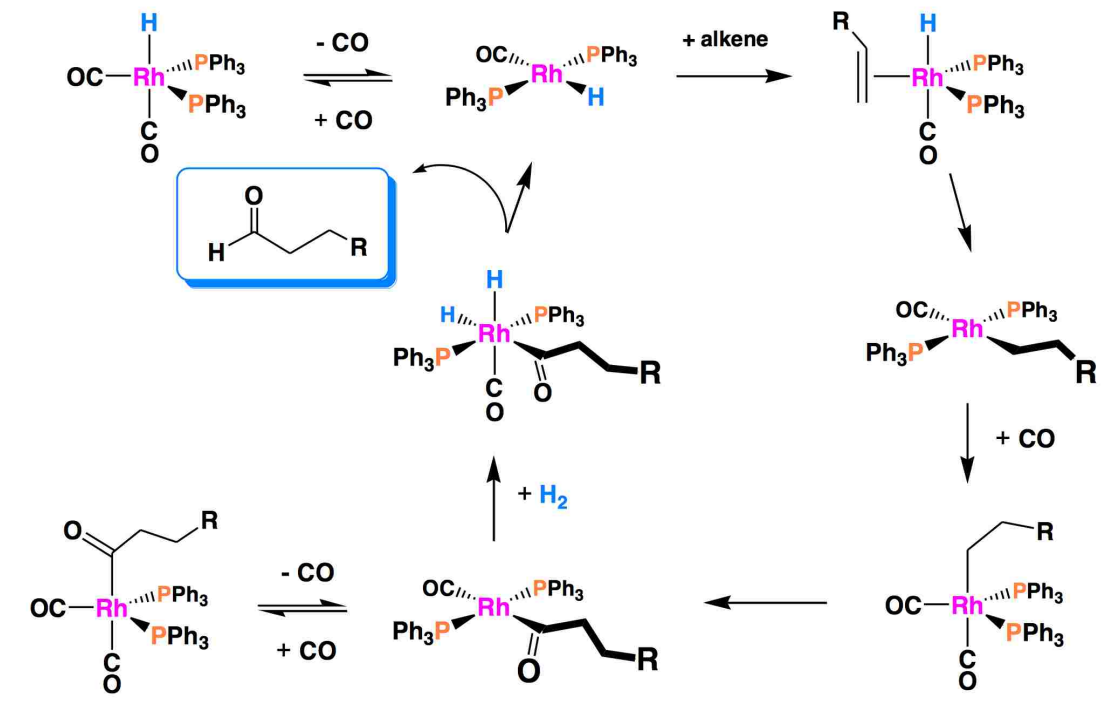


Figure 1.3. Mechanism of the Rh/PPh₃ system

Pruett (Union Carbide) and Booth (Union Oil) developed, patented, and licensed the first commercial process that used a large excess of PPh₃ within the reactor.¹² They proposed that PPh₃ coordinates relatively weakly to the rhodium center, especially when pressurized with CO. The CO and PPh₃ act as competitive ligands to bind one of three coordination sites on the rhodium metal. The complex can take the structure of HRh(CO)_x(PPh₃)_{3-x}, which is illustrated in Figure 1.4.

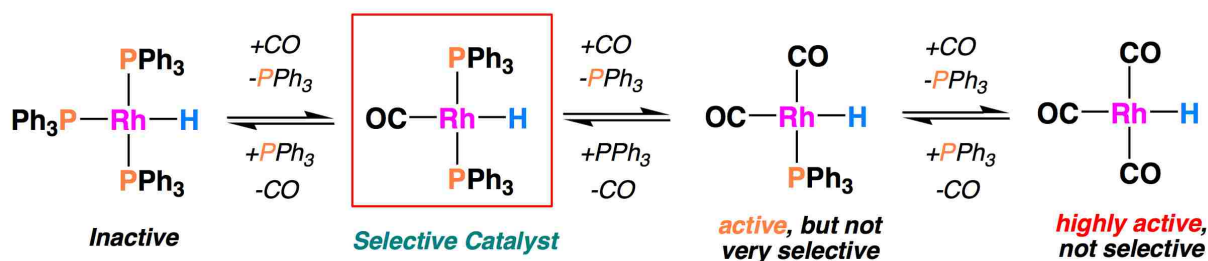


Figure 1.4. PPh₃/CO equilibrium for the rhodium catalyst

$\text{HRh}(\text{PPh}_3)_3$ is too sterically hindered to coordinate CO or alkene and is inactive for hydroformylation. Steric factors favor dissociation of PPh_3 from $\text{HRh}(\text{PPh}_3)_3$ allowing CO coordination, which forms the selective catalyst $\text{HRh}(\text{CO})(\text{PPh}_3)_2$. Under moderate pressure, another carbonyl will replace a second PPh_3 forming a less selective, but active catalyst. Finally under higher pressures of CO, the last PPh_3 is replaced by CO forming an unselective, extremely active catalyst, $\text{HRh}(\text{CO})_3$.

The $\text{HRh}(\text{CO})_3$ complex is believed to be the most active hydroformylation catalyst. With low sterics, nearly all alkenes can bind to $\text{HRh}(\text{CO})_3$; the thermodynamics of the catalyst begin to take over the reactivity of the substrates. As internally bound olefins are thermodynamically more stable than terminally bound ones, the internal or branched aldehyde is the thermodynamically stable product. This results in L:B of the $\text{HRh}(\text{CO})_3$ catalyst to be around 0.8:1. To preserve good L:B regioselectivity Pruetz found that a minimum of 0.4 M PPh_3 for every 1 mM of Rh was needed. This represents a 400 fold excess of PPh_3 for each rhodium center. The H_2/CO pressure used in the commercial Rh/ PPh_3 reactors is around 150 psi with operating temperatures around 125 °C, making the system much safer, and more energy efficient than the high pressure $\text{HCo}(\text{CO})_4$ catalyst.

Abatjodlou found that phosphine ligands, though helpful in making the catalyst selective, are not entirely stable themselves in the presence of rhodium.¹³ A rhodium center that is deficient in electron density will look to the ligands to gather additional electrons.

$\text{HRh}(\text{CO})(\text{PPh}_3)$ is formed when a PPh_3 dissociates from the rhodium, this is a highly reactive 14 electron complex. To counter the low density, the rhodium can pull more electrons from the phosphine ligand. Rhodium can intramolecularly attack one of the P-Ph bonds to oxidatively add a Ph^- group and a phosphide (PPh_2^-). This new 14 electron complex $\text{HRh}(\text{PPh}_2)(\text{Ph})(\text{CO})$

contains two new anionic ligands giving more electron density to the rhodium. H_2 can react with this complex to eliminate benzene. Alkenes can react with the rhodium-phosphide to eventually form alkyldiphenylphosphine, which is a poor ligand for hydroformylation. The phosphide ligand also has a strong tendency to bridge to another rhodium, and form inactive dimers and eventually clusters that precipitate out of solution.

1.3 Chelating Ligands

To maximize the steric bulk and stability of two phosphine groups without introducing 400 equivalents of the ligand to the reaction solution, and to minimize the loss of phosphines yielding unstable rhodium centers, research moved towards chelating phosphines. These chelating ligands were able to tether the labile phosphines to the metal center for easy re-association and often had larger cone angles on their own, which added to the sterics of the catalyst increasing the linear aldehyde selectivity. Slaugh's cobalt research demonstrated that these chelating ligands are generally poor choices for hydroformylation. Slaugh attained aldehyde yields of only 1.3 % for dppe ($Ph_2P(CH_2)_2PPh_2$), 4.5 % for $Ph_2P(CH_2)_3PPh_2$, but inactivity for dppb ($Ph_2P(CH_2)_4PPh_2$).

Like Slaugh, Matsumoto saw low activity for dppb when used as the sole ligand for rhodium in hydroformylation.^{14, 15} When Matsumoto used dppb, or similar ligands, as an additive to the Rh/ PPh_3 system he found it stabilized the material from degradation. Matsumoto began with the study of terminal substituted olefins such as allyl acetate and allyl alcohol. He initially found low conversion of the allyl acetate (12 %) when using 50 eq. of PPh_3 . Upon adding various chelating phosphines from $Ph_2PCH_2PPh_2$ (dppm) to dppb conversion would increase from 15 % with dppm, 47 % with dppe, 95 % with $Ph_2P(CH_2)_3PPh_2$ (dppp), and 82 % with dppb. Likewise, a similar trend was seen in the selectivity of the linear product with dppm

having 15 % linearity and dppb having 53 % linearity. Hydroformylation without the chelating phosphine only gave 33 % linear product. These chelating ligands also made the catalyst more stable as Matsumoto retested the same catalyst batch in multiple trials. He found that longevity of the catalyst, at the sacrifice of initial performance, was increased with the addition of the chelating phosphines. When allyl alcohol was tested for hydroformylation it was converted with 94 % efficiency. Dppb turned out to be the best overall ligand for rate, selectivity, and catalyst stability. Arco Chemical licensed this technology, and built the first hydroformylation plant in the US (Texas) to convert allyl alcohol to 1,4-butanediol.

Further exploration of chelating phosphines lead to the development of a second generation of ligands for hydroformylation. These new ligands were commercially designed to utilize the steric bulk of the ligand and chelate effect to produce active rhodium catalysts with excellent L:B selectivity. Some of these ligands are shown in the following figure (Figure 1.5).¹⁶

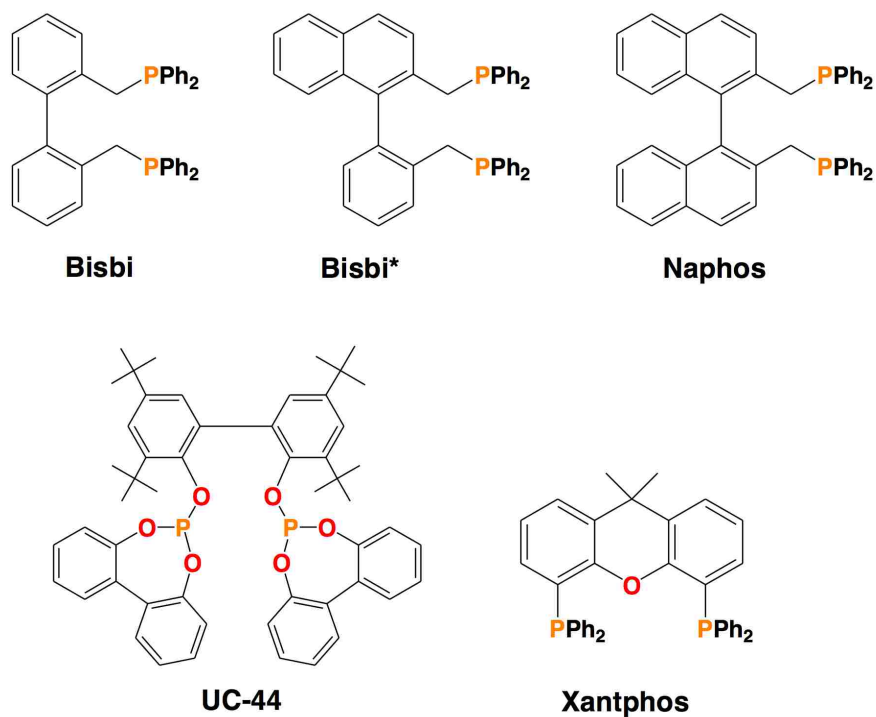


Figure 1.5. Commercially designed chelating phosphine ligands

These ligands were found to yield highly effective rhodium catalyst for hydroformylation. As these are chelating ligands, only 5 eq. are needed to bind effectively the rhodium while PPh₃ needs a minimum of 400 fold excess. Compared to PPh₃ these ligands gave better rates and selectivities, as seen in Table 1.2.¹⁷ One drawback was that UC-44 and Xantphos did more alkene isomerization. However, this could be used to the advantage of the catalyst to hydroformylate internal olefins to the linear product. A second disadvantage of these UC-44 and other phosphite ligands is that they are poor σ -donors to metal centers. This means that a rhodium center with π -backbonding to carbonyl ligands will be an electron-poor center. As was shown in Abatjodlou's work with phosphines, an electron deficient rhodium center can attack the P-O bond of a phosphite ligand leading to fragmentation and degradation. Though phosphites are highly active, their longevity suffers from this process.

Table 1.2. Hydroformylation of 1-hexene using Rh-ligand catalysts

Catalyst	Initial TOF (min ⁻¹)	L:B	% iso
Rh/PPh ₃ ^a	13	9:1	< 0.5
Rh/Bisbi ^b	25	70:1	< 0.5
Rh/Naphos ^b	27	120:1	1.5
Rh/Xantphos ^b	13	80:1	5.0

Hydroformylation was run at 90 °C and 6.2 bar 1:1 H₂/CO in acetone. 1 mM Rh(CO)₂(acac) was combined with ^a0.4 M PPh₃ (400 eq.) or ^b5 eq. of ligand.

1.4 Bimetallic Hydroformylation

Following the dual concepts of chelating ligands and bimetallic cooperativity from Heck's mechanistic proposals, the Stanley research group chose to explore the use of two metal centers to work in tandem as a hydroformylation catalyst. The group designed a tetraphosphine the ligand with two goals. The first goal was to chelate metal centers; two phosphines would be

tethered by an ethylene linkage allowing for a stable five-member chelate ring to form when bound to a metal center. The second goal was to bridge two chelate rings; a bis(phosphino)methane moiety would keep the metal centers in proximity, enhancing the potential for bimetallic cooperativity. Functionality was added to the phosphines giving them steric bulk for selectivity and electron-richness that could be σ -donated to the metal centers. When in closed-mode, there could be a Rh-Rh bond formed between the metal centers assisting the bimetallic cooperativity.

As the internal phosphines are chiral centers, the ligand exists in two diastereomeric forms: *racemic*, which is composed of two enantiomers (RR, SS), and *mesomeric* (RS). Both are excellent at forming bimetallic complexes, but form different geometries when the metals are adjacent to each other.

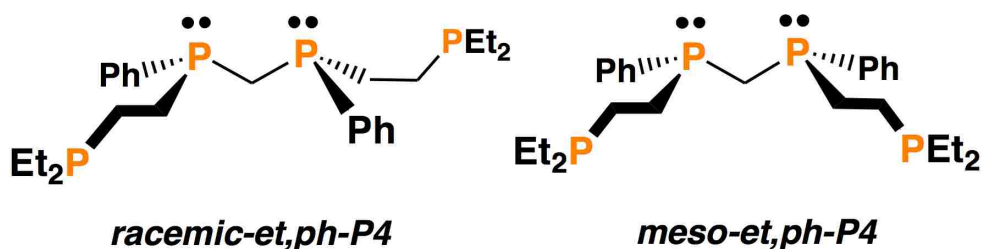
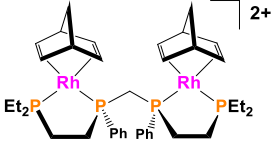
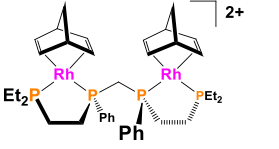


Figure 1.6. *Racemic* and *mesomeric* diastereomers of et,ph-P4

Utilizing this tetraphosphine ligand to bridge and chelate two rhodium centers the Stanley group was able to enhance the turnover frequency (TOF) of the reaction as well as the selectivity.¹⁸ Initial studies show the reactivity and selectivity of the *rac*-complex is far superior to the *meso*-complex. It was found that analogs of the et,ph-P4 ligand halves yield poor hydroformylation catalysts, which might indicate that the ligand itself would form an equally poor catalyst. When studying the *meso*-complex, this is true, but the *rac*-complex oddly yields something very different. As seen below in the Table 1.3, the $[\text{Rh}_2(\text{nbd})(\text{rac-et,ph-P4})]^{2+}$

catalyst precursor is twice as fast as PPh_3 and somewhat more selective, while the *meso*-catalyst precursor is a tenth the rate and slightly less regioselective selective but produces far more side products.

Table 1.3. Hydroformylation of 1-hexene using mono- and bimetallic Rh catalysts

Catalyst	Initial TOF (min^{-1})	L:B	iso %	hydro %
Rh/ PPh_3 (0.82 M)*	9	17:1	1	< 0.5
<i>meso</i> - 	0.9	14:1	24	10
<i>rac</i> - 	20	25:1	2.5	3.4

Hydroformylation was run at 90 °C and 6.2 bar 1:1 H_2/CO in Acetone. 1 mM $\text{Rh}(\text{CO})_2(\text{acac})$ was combined with *0.82 M PPh_3 (820 eq.). iso % is the percent of 2-hexene and 3-hexene in the product. hydro % is the percent of hexane in the product.

Before the injection of the olefin, the catalyst, unfortunately, is highly susceptible to fragmentation by H_2/CO pressures. It is believed that the catalyst fragments from an arm-on, arm-off mechanism. In the arm-off phase, one rhodium center is only bound to the internal phosphine giving it an open coordination site. A carbonyl can easily fill this site and block the re-binding of the external phosphine. The loss of the external phosphine can lead to dissociation of the internal phosphine. As a result one of two fragmentation complexes can form. The first contains one rhodium center bound to all four phosphines formed by the ligand wrapping entirely around the remaining rhodium center. The second is a bis-ligand species surrounding the two metal centers formed by a ligand detaching completely from both metal centers and embedding

itself into another arm-off system. Both species are inactive for hydroformylation and depicted below (Figure 1.7).

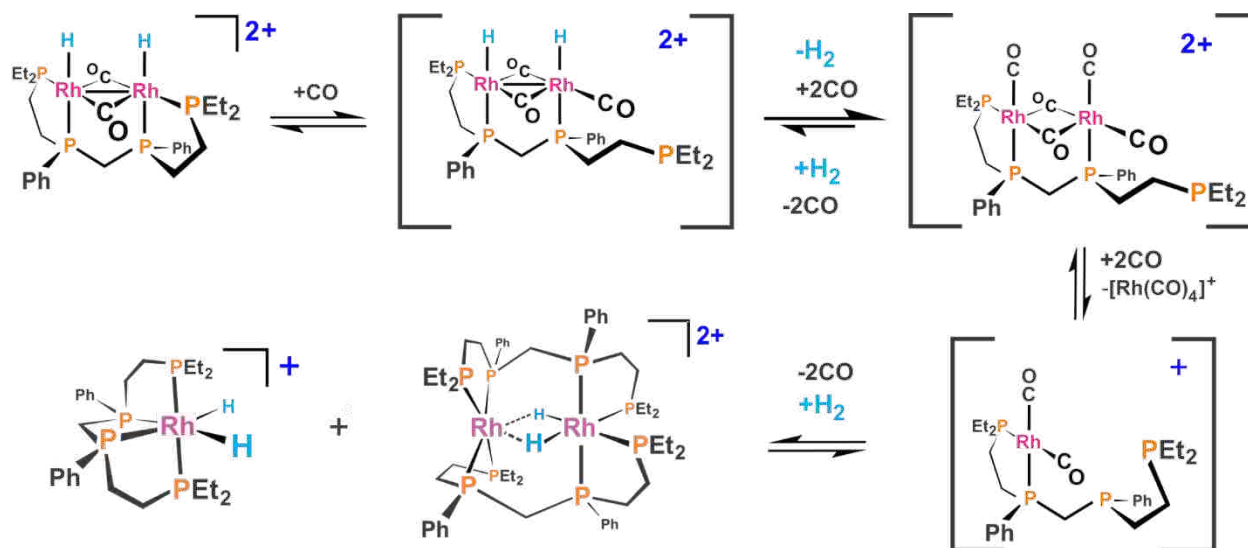


Figure 1.7. Proposed degradation mechanism of $[\text{Rh}_2(\text{nbd})_2(\text{et,ph-P4})]^{2+}$ catalyst

In an attempt to phase separate the product and catalyst after a hydroformylation reaction, David Aubry and Novella Bridges found that the addition of water to their acetone catalyst solution was able to stabilize the catalyst leading to higher turnovers and better linear selectivity. Darina Polakova tested the pH of the system and found that at reaction conditions (1 mM catalyst) the material had a pH of 3.1.¹⁹ $[\text{Rh}_2(\mu\text{-H})_2(\text{CO})_4(\text{rac-et,ph-P4})]^{2+}$, therefore, acts as a strong monoprotic acid in the presence of water. This creates a mono-cationic system, $[\text{Rh}_2(\mu\text{-H})(\text{CO})_4(\text{rac-et,ph-P4})]^+$. The phosphines of the et,ph-P4 ligand have partial positive charges to cause electrostatic repulsion from the metal center. With a lower charge on the mono-cationic system, there is less repulsion allowing for the phosphine arms to remain bound, which reduces fragmentation. When not actively hydroformylating alkenes, $[\text{Rh}_2(\mu\text{-H})_2(\text{CO})_4(\text{rac-et,ph-P4})]^{2+}$ is likely to convert into the deprotonated form. It is by the favorability of the complex in the presence of water to be deprotonated forming the more stable $[\text{Rh}_2(\mu\text{-H})(\text{CO})_4(\text{rac-et,ph-P4})]^+$ that the longevity of the catalyst is increased leading to greater turnovers. The group

hypothesizes from DFT calculations that the di-cationic catalyst is more reactive than the mono-cationic one.^{20, 21} Though water is present to deprotonate the metal center, some of the complex may be re-protonated and lead to some of the faster rates and higher selectivity.

1.5. Discovery of Aldehyde-Water Shift Reaction

Novella Bridges had an accidental leak in the autoclave during the testing of the water/acetone solvent systems. This, produced aldehyde and heptanoic acid during the hydroformylation of 1-hexene.²² When the leak was repaired, heptanoic acid no longer was produced. It was eventually postulated that the leak was small enough to allow the release of hydrogen gas faster than that of carbon monoxide in accords with Graham's Law of Effusion. This generated H₂-deficient conditions in the autoclave that shifted the catalyst equilibrium away from the dirhodium dihydride complex, which is active for hydroformylation, to a CO-bridged dirhodium carbonyl, [Rh₂(μ-CO)₂(CO)₂(*rac*-et,ph-P4)]²⁺, which is active for reacting aldehyde and water to make carboxylic acid and H₂. The reaction that was discovered by Bridges was the aldehyde-water shift reaction (AWS) (Figure 1.8).

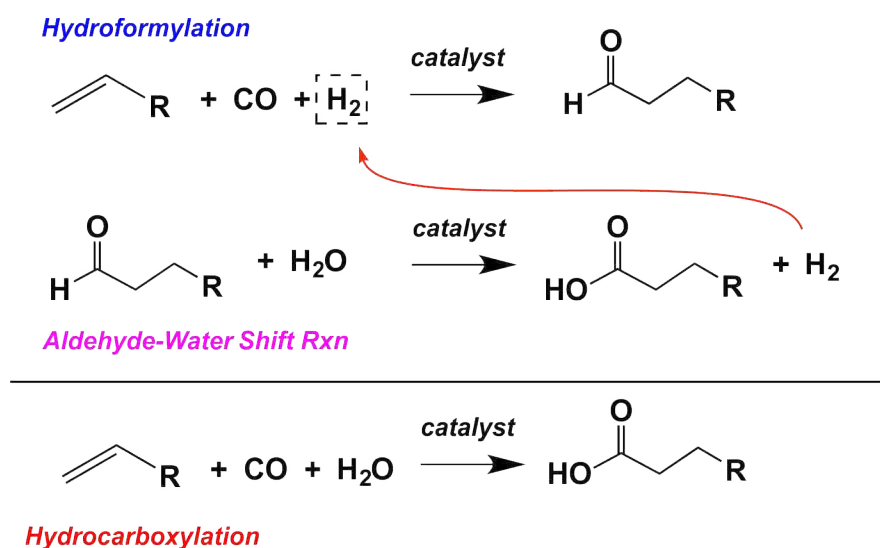


Figure 1.8. Reaction of hydrocarboxylation by tandem hydroformylation and AWS

Bridges and Aubry worked out leak-free reaction conditions where tandem hydroformylation and AWS would both operate. Hydroformylation was run for 10 mins to build up the concentration of aldehyde and reduce the amount of 1-hexene. The H₂/CO gas flow to the autoclave was then stopped, the stainless steel gas supply reservoir purged, refilled with pure CO gas, and then reopened to the autoclave. This typically took 5-10 mins. During this time the residual H₂/CO gas in the autoclave and solution continued to support hydroformylation of the 1-hexene, increasing the aldehyde concentration and almost completely consuming the 1-hexene. At this point almost all the H₂ was consumed in the autoclave, and AWS catalysis initiated, which converted aldehyde and water into carboxylic acid and H₂. As the H₂ concentration in the autoclave increased it eventually inhibited and stopped the AWS.

After the initial experiments by Aubry and Bridges, engineering modifications were made to the autoclave system used by the group for hydroformylation. Three new smaller gas reservoirs were added and connected to a manifold to allow quick changes in the composition of the gas being delivered to the autoclave. But these changes somehow made it very difficult for us to do AWS for reasons we still don't fully understand. Little to no success occurred for the AWS until Barnum made a few other modifications and created a more regimented way of running the experiments.²³ Barnum was able to do several hundred turnovers either via tandem hydroformylation and AWS, or by direct conversion of aldehyde and water to carboxylic acid and H₂. But AWS runs were still inconsistent, and higher turnovers were desired before any publication.

1.6. Design of a New Tetraphosphine Ligand

With the fragmentation issues of the $[\text{Rh}_2(\mu\text{-H})_2(\text{CO})_4(\text{rac-}et,\text{ph-P4})]^{2+}$ catalyst, the Stanley group proposed a new, modified version of the *et,ph-P4* ligand shown below (Figure 1.9).

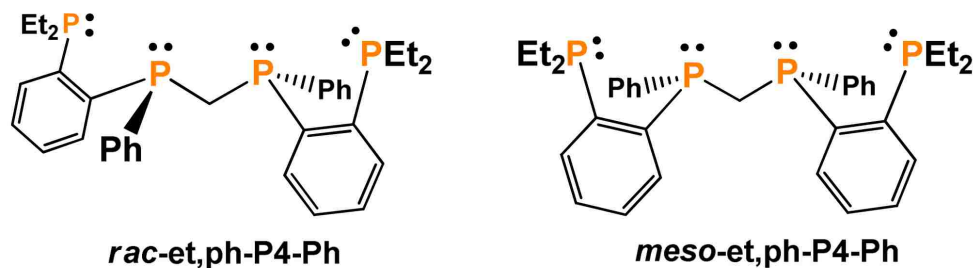


Figure 1.9. *Racemic* and *mesomeric* structures of *et,ph-P4-Ph*

This *et,ph-P4-Ph* ligand differs from the older one in that the internal and external phosphorus atoms are bound by a phenylene linkage rather than an ethylene one. This should dramatically increase the chelating effect of the ligand by giving it more rigid arms that would not be able to dissociate as easily from the rhodium centers. As such, the ligand should inhibit the previously observed fragmentation reactions and form highly active and long-lived hydroformylation catalysts. Synthesis of this ligand was built on the previous synthetic scheme of the *et,ph-P4* ligand with modifications by Alex Monteil.²⁴ Characterization of the ligand and the complexes it could form, optimization of the synthetic scheme for both the ligand and complexes, and uses of the ligand and complexes were not initially studied by Monteil. Other researchers in the Stanley group continued to examine the efficiency of the *et,ph-P4* ligand.

Bill Schreiter and Ekaterina Kalachnikova tackled the challenge of separating the *et,ph-P4-Ph* diastereomers.^{25, 26} While working with nickel mediated oxidative cleavage of olefins with O_2 , Schreiter found that the $\text{Ni}_2\text{Cl}_4(\text{meso-}et,\text{ph-P4-Ph})$ was soluble in *n*-butanol while the

$\text{Ni}_2\text{Cl}_4(\text{rac-}i\text{et,ph-P4-Ph})$ was not soluble. After filtering out the solid *rac*-complex, he proceeded to perform cyanolysis on the material, which yielded a metal cyanide complex and free *rac-}i\text{et,ph-P4-Ph}*. The process, however, was effective at gathering both forms of the ligand from the mixture of metal complexes, it was highly inefficient as it required over 280 eq. of cyanide to separate the ligand from the metal in low yields.

While Schreiter worked on the cyanolysis process, Kalachnikova examined another method for separating the ligand directly rather than first binding it in a metal complex. She found that column chromatography should be a far more efficient way to accomplish separation. As Kalachnikova worked on finding a good mobile and stationary phase, she too came across troubles with producing the ligand itself as key steps in the synthesis often produced yields below 50 % and in some cases below 10 %.

1.7. Continued Research on Hydroformylation and Aldehyde-Water Shift

With the tedious process of running hundreds of thin layer chromatography (TLC) plates and later columns for those solvent systems that worked, I was recruited by Ekaterina Kalachnikova to join her attempts at solving the separation of the *et,ph-P4-Ph* diastereomers. We eventually discovered two solvent systems to work with an alumina stationary phase, and achieved separation of the diastereomers as well as removal impurities and unreacted materials from the separated ligand.

In working towards separation, we were required to produce enough ligand to run additional TLC plates and columns. As such, our goals changed from making ligand to efficiently making ligand. To do this, optimization of some synthetic steps of the parts of the ligand was examined. Jointly, Kalachnikova and I probed into the chlorination of $\text{H(Ph)PCH}_2\text{P(Ph)H}$ (bridge) to make $\text{Cl(Ph)PCH}_2\text{P(Ph)Cl}$ (chlorobridge), the Grignard coupling

1-(diethylphosphino)-2-iodobenzene (I-small arm) with chlorobridge to make the et,ph-P4-Ph ligand, the Grignard coupling 1-(diethylphosphino)-2-bromobenzene (Br-small arm) with chlorobridge to make the et,ph-P4-Ph ligand.

After collaborating with Kalachnikova, I studied various aspects of both hydroformylation and AWS. I began with efforts to reproduce the work of Barnum with $[\text{Rh}_2(\text{nbd})_2(\text{rac-et,ph-P4})](\text{BF}_4)_2$. When separation of the et,ph-P4-Ph ligand was completed, I attempted to make the catalyst precursor $[\text{Rh}_2(\text{nbd})_2(\text{rac-et,ph-P4-Ph})](\text{BF}_4)_2$, and after characterization of the material, I began working towards finding suitable reaction conditions for hydroformylation and AWS with $[\text{Rh}_2(\text{nbd})_2(\text{rac-et,ph-P4-Ph})](\text{BF}_4)_2$.

The new complex had a number of problems beginning with the crystallization of the material. Efforts were made to produce a similar complex that might crystallize more readily as well as study the complex via nuclear magnetic resonance (NMR), so PF_6 was used as the counter anion and the $[\text{Rh}_2(\text{nbd})_2(\text{rac-et,ph-P4})](\text{PF}_6)_2$ was prepared and characterized. A second more serious issue was poor and unpredictable activity of both the BF_4 and PF_6 complexes in hydroformylation and AWS. *In situ* NMR and Fourier transform infrared (FT-IR) spectroscopic studies were performed to identify the active catalyst and note any degradation of the catalyst.

Finally, as the Stanley group is familiar with hydroformylation catalysis, we were hired to examine reaction conditions for the hydroformylation of 1-decene using the Rh/ PPh_3 system for industry. Though extensive studies have been performed on the Rh/ PPh_3 system, use of the system for industrial purposes required fine tuning of various conditions from solvents to temperature, run times to catalyst and ligand concentration, and total and partial pressures of syn-gas mixtures. The objective was to produce a linear decanal with minimal isomerization and

hydrogenation under the lowest amounts of both rhodium and PPh₃. The work is mentioned here, but will not be discussed in further chapters as the results are proprietary information of Centauri Technologies, LP.

1.8 References

1. Roelen, O. (to Ruhrchemie A.-G.), *Verfahren zur Herstellung von sauerstoffhaltigen Verbindungen*, Patent DE 849,548, 1938 & U.S. Patent 2327066, 1943.
2. Whyman, R., *Applied Organometallic Chemistry and Catalysis*. Oxford University Press: 2001.
3. Cornils, B.; Herrmann, W. A. *Applied Homogeneous Catalysis with Organometallic Compounds*. Wiley: 2002.
4. Heck, R. F.; Breslow, D. S., The Reaction of Cobalt Hydrotetracarbonyl with Olefins. *J. Am. Chem. Soc.* **1961**, 83, 4023.
5. Mirbach, M. F., On the Mechanism of the Co₂(CO)₈ Catalyzed Hydroformylation of Olefins in Hydrocarbon Solvents. A High Pressure UV and IR Study. *J. Organomet. Chem.* **1984**, 265 (2), 205.
6. Slauch, L. H.; Mullineaux, R. D., Novel Hydroformylation Catalyst. *J. Organomet. Chem.* **1968**, 13 (2), 469.
7. Unruh, J. D.; Christenson, J. R., A Study of the Mechanism of Rhodium/Phosphine Catalyzed Hydroformylation: Use of 1,1'-Bis(diarylphosphino)ferrocene Ligands. *J. Mol. Catal.* **1982**, 14, 19.
8. Osborn, J. A.; Wilkinson, G.; Young, J. F., Mild Hydroformylation of Olefins using Rhodium Catalysts. *Chem. Commun.* **1965**, 0, 17.
9. Evans, D.; Osborn, J. A., Hydroformylation of Alkenes by Use of Rhodium Complex Catalysts. *J. Chem. Soc. A.* **1968**, 0, 3133.
10. Brown, C. K.; Wilkinson, G., Homogeneous Hydroformylation of Alkenes with Hydridocarbonyltris(triphenylphosphine)rhodium(I) as Catalyst. *J. Chem. Soc. A.* **1970**, 0, 2753.
11. Gillard, R. D.; Osborn, J. A.; Stockwell, P. B.; Wilkinson, G., Activation of Molecular Hydrogen by Complexes of Rhodium (III). *Proc. Chem. Soc.* **1964**, 0, 284.
12. Pruett, R. L.; Smith, J. A. Hydroformylation of Unsaturated Organic Compounds US 3917661 A, November 4, 1975.

13. Abatjoglou, A. G.; Billig, E. Bryant, D. R., Mechanism of Rhodium-Promoted Triphenylphosphine Reactions in Hydroformylation Processes. *Organometallics*. **1984**, *3*, 923.
14. Matsumoto, M.; Tamura, M., Rhodium Catalyzed Low Pressure Hydroformylation of Substituted Terminal Olefins. Role of α,ω Bis(diphenylphosphino)alkane in Combination with Excess Triphenylphosphine. *J. Mol. Catal.* **1982**, *16*, 195.
15. Matsumoto, M.; Tamura, M., Reinvestigation of Atmospheric Hydroformylation of 1-Octene Catalyzed by a Rhodium Complex. Some Advantages Given by Added α,ω Bis(diphenylphosphino)alkane. *J. Mol. Catal.* **1982**, *16*, 209.
16. Franke, R.; Selent, D.; Börne, A., Applied Hydroformylation. *Chem. Rev.* **2012**, *112*, 5675.
17. Aubry, D. A.; Bridges, N. N.; Ezell, K.; Stanley, G. G., Polar Phase Hydroformylation: The Dramatic Effect of Water on Mono- and Dirhodium Catalysts. *J. Am. Chem. Soc.* **2003**, *125*, 11180.
18. Broussard, M. E.; Juma, B.; Train, S. G.; Peng, W. J.; Laneman, S. A.; Stanley, G. G., A Bimetallic Hydroformylation Catalyst: High Regioselectivity and Reactivity Through Homobimetallic Cooperativity. *Science*. **1993**, *260*, 1784.
19. Polakova, D. Studies on a Dirhodium Tetrphosphine Hydroformylation Catalyst. Ph.D. Dissertation, Louisiana State University, Baton Rouge, LA, 2012.
20. Wilson, Z. S. Electronic Structural Investigations of Bi- and Polymetallic Complexes Using Quantum Mechanical Methods. Ph.D. Dissertation, Louisiana State University, Baton Rouge, LA, 2004.
21. Fernando, S. R. G. Computational Studies on Bimetallic Catalysis and X-Ray Absorption Spectroscopy. Ph.D. Dissertation, Louisiana State University, Baton Rouge, LA, 2015.
22. Stanley, G. G.; Aubry, D. A.; Bridges, N.; Barker, B.; Courtney, B. Aldehyde-Water Shift Catalysis: H₂ Production from Water and Aldehydes via a Homogeneous Dirhodium Tetrphosphine Catalyst. *Prepr. Pap. – Am. Chem. Soc., Div. Fuel Chem.* **2004**, *49*, 712.
23. Barnum, A. R. Studies of a Dirhodium Tetrphosphine Catalyst for Hydroformylation and Aldehyde-Water Shift Catalysis. Ph.D. Dissertation, Louisiana State University, Baton Rouge, LA, 2012.
24. Monteil, A. R. Investigation into the Dirhodium-Catalyzed Hydroformylation of 1-Alkenes and Preparation of a Novel Tetrphosphine Ligand. Ph.D. Dissertation, Louisiana State University, Baton Rouge, LA, 2006.

25. Schreiter, W. J. Investigations into Alkene Hydration and Alkene Oxidation Catalysis. Ph.D. Dissertation, Louisiana State University, Baton Rouge, LA, 2013.
26. Kalachnikova, E. Improved Synthesis, Separation, Transition Metal Coordination and Reaction Chemistry of a New Binucleating Tetrphosphine Ligand. Ph.D. Dissertation, Louisiana State University, Baton Rouge, LA, 2015.

Chapter 2: Ligand Synthesis and Complex Characterization

2.1 Introduction

Based on the proposed bimetallic cooperativity mechanism for cobalt hydroformylation by Heck and Brewslow, the Stanley group thus developed and examined the ability of the novel *et,ph*-P4 ligand to bind two rhodium centers that could cooperate and do hydroformylation better than monometallic catalysts (Figure 2.1).^{1,2} Although the two diastereomeric forms of the *et,ph*-P4 ligand are good at coordinating to two rhodium centers, the conformations of bimetallic complexes are quite different when the metals are adjacent. This should lead to differences in reactivity and selectivity between the diastereomers, which is what is observed.

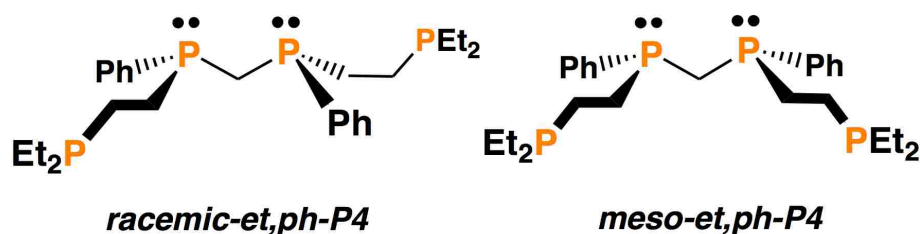


Figure 2.1. *Racemic* and *mesomeric* structures of *et,ph*-P4

The *rac*-dirhodium precursor generated a catalyst that was more than 20× faster and far more selective than the *meso*-complex. Comparisons with monometallic “half” analogs of $[\text{Rh}_2(\text{nbd})_2(\text{rac-}et,ph\text{-P4})](\text{BF}_4)_2$ like $[\text{Rh}(\text{nbd})(\text{dppe})](\text{BF}_4)$ demonstrated that they were terrible hydroformylation catalysts, and mainly did the alkene isomerization and hydrogenation side reactions.³ Interestingly, the addition of PPh_3 to $[\text{Rh}_2(\text{nbd})_2(\text{rac-}et,ph\text{-P4})](\text{BF}_4)_2$ leads to rapid deactivation and loss of selectivity.⁴ Prof. Stanley proposed that coordination of PPh_3 to the bimetallic catalyst dissociates the internal phosphine of *et,ph*-P4, and opens up the complex leading to a loss of cooperativity between the two metals. The more electron-donating terminal phosphine that remains coordinated deactivates the rhodium center for hydroformylation.

Though $[\text{Rh}_2(\text{kbd})_2(\text{rac-}i\text{-et,ph-P4})](\text{BF}_4)_2$ appears to be better than the best monometallic rhodium catalysts at hydroformylation, its longevity and reusability are lacking. NMR studies of the complex under 200 – 300 psig of H_2/CO show fragmentation of the complex.⁵ It is proposed that the fragmentation is due to flexibility of the ethylene linkage of the phosphine chelate that can lead to an arm-off dissociation. As shown below in Figure 2.2, the catalyst under H_2/CO pressure first dissociates an external phosphine to initiate the fragmentation reaction.

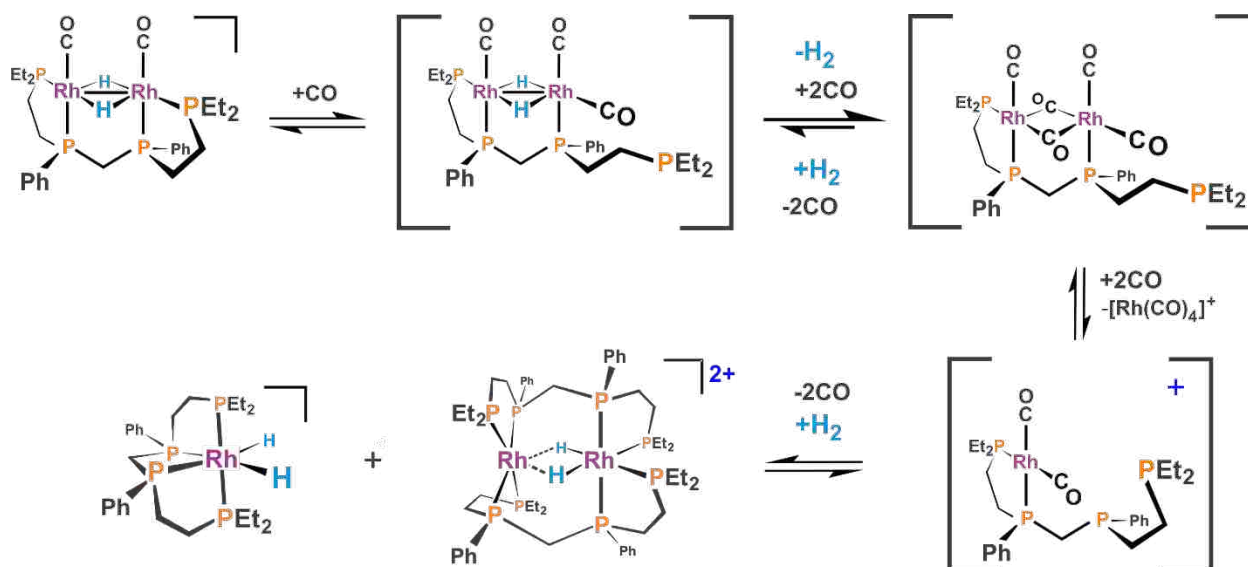


Figure 2.2. Proposed fragmentation of $[\text{Rh}_2(\mu\text{-H})_2(\text{CO})_2(\text{rac-}i\text{-}1,2\text{-bis(2-ethylphosphino)ethane})]^{2+}$

Once the external phosphine dissociates, the empty coordination site on the rhodium center can be filled with a free carbonyl, which blocks the re-association of the arm. The catalyst is now less electron-rich, having replaced the σ -donating phosphine with a π -backbonding carbonyl. This promotes reductive elimination of hydrogen gas and coordination of more carbonyl ligands. This CO-rich rhodium center can now dissociate, leading to fragmentation of the catalytically active bimetallic catalyst. From here, this complex can either find a second similar complex in solution and form a bis-ligand, di-rhodium species or the ligand can wrap around the single rhodium center, along with oxidative addition of H_2 , forming a saturated 18

electron octahedral complex. Both of these complexes have yet to be characterized directly, but crystal structure of similar complexes, $[\text{Rh}_2(\text{rac-}i\text{et,ph-P4})_2]^{2+}$ and $[\text{RhCl}_2(\kappa^4\text{-}i\text{rac-}i\text{et,ph-P4})]^+$, have been identified.^{6,7}

Bridges and Aubry studied the effect of adding water to the acetone solvent to generate a highly polar solvent system from which the less polar heptaldehyde product would phase separate to enable easy isolation from the catalyst solution.⁸ The addition of 30 % water (by volume) to the acetone solvent increased the initial TOF from 20 min^{-1} to 30 min^{-1} , increased the L:B aldehyde selectivity from 25:1 to 33:1, and decreased the production of side products from isomerization and hydrogenation from 5.9 % to 1 %.[†]

The group proposed a new mechanism for the reaction in which the deprotonation of a rhodium center aided by the presence of water would lead to a more stable form of the catalyst (Figure 2.3). DFT calculations performed by Ranelka Fernando back up the proposed structures and show reasonable energy barriers for the steps proposed in the mechanisms of both the monocationic and dicationic systems.^{9,10}

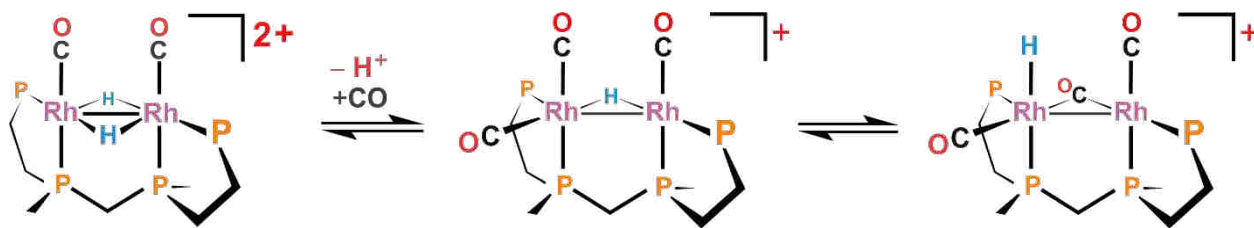


Figure 2.3. Deprotonation of the active *et,ph-P4* catalyst

The addition of water, though helpful in stabilizing the catalyst, does not fully prevent degradation. As the acidic proton is still in solution, it can rebind to the deprotonated rhodium center, and once again enter the fragmentation pathway in Figure 2.2.

[†]The TOF reported here is 30 min^{-1} unlike the reported 73 min^{-1} in the JACS paper as a problem occurred in the old autoclave controller and data collector that gave an incorrect initial TOF.

The Stanley group, therefore, proposed a more rigid, stronger chelating ligand to inhibit catalyst fragmentation. The et,ph-P4-Ph ligand (Figure 2.4) replaced the rotationally flexible ethylene linkage between the internal and external phosphines with an *o*-phenylene group. The rigid nature of the phenylene ring imposes a sterically directed chelate at the metal center with little or no conformational flexibility that can lead to the dissociation of either phosphine. The study of such *ortho*-phenylenebis(dialkylphosphine) ligands to stabilize transition metal complexes has been reported.¹¹

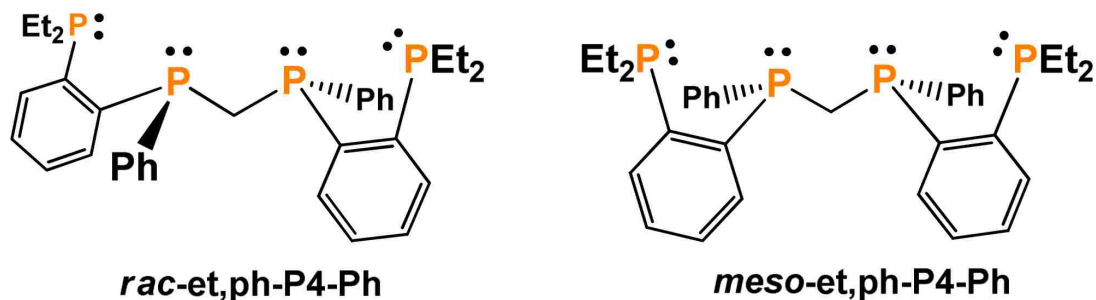


Figure 2.4. *Racemic* and *mesomeric* structures of et,ph-P4-Ph

This ligand's synthesis was first developed by Monteil.¹² His work diagrammed in Figure 2.5 is built from the synthetic scheme of the et,ph-P4 ligand with modification allowing for Grignard coupling of the external arms to the bridging internal phosphines.

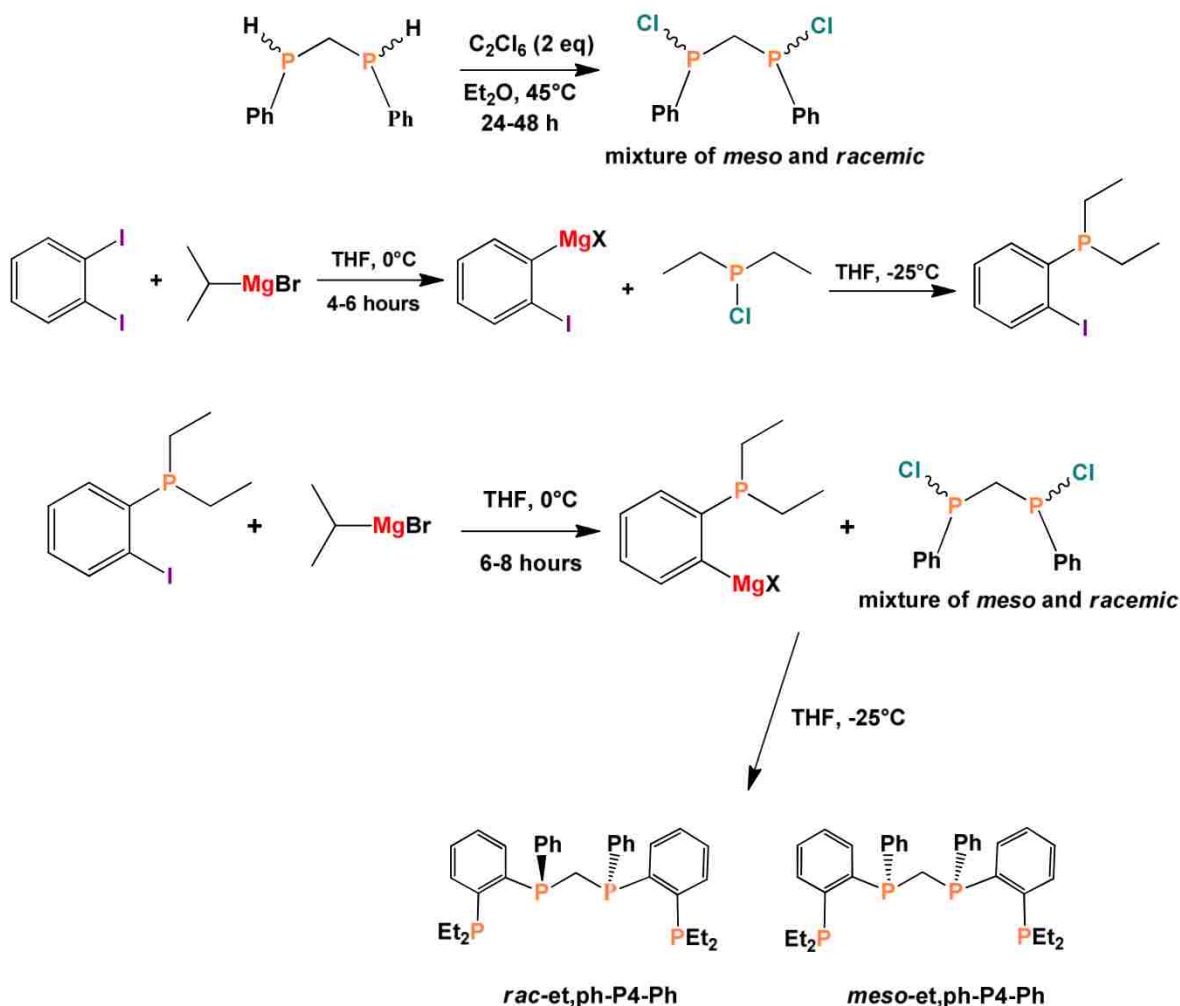


Figure 2.5. Synthesis developed by Alex Monteil of *et,ph-P4-Ph*

His synthesis was not optimized leading to some low yielding reactions. Furthermore, the two diastereomers of this ligand were never separated as the mixture is a gunky paste. With the older *et,ph-P4* ligand one separation was achieved by partially crystallizing the diastereomeric mixture in hexane.¹³ The *meso-et,ph-P4-Ph* would partially crystallize out of hexane at low temperatures overnight leaving the solution enriched in *rac*-diastereomer. Repeating this process gives pure *meso-et,ph-P4* and a solution enriched in *rac-et,ph-P4* to about an 80 – 85 % level. A second less efficient and less green method involving cyanolysis of a nickel complex can also

achieve separation. Here, the mixed ligands are added to NiCl₂ to form Ni₂Cl₄(et,ph-P4). The *meso*-complex is insoluble in ethanol while the *rac*-complex is soluble. After filtration of the materials, the two are treated with 150 – 250 eq. of NaCN yielding the ligand and [Ni(CN)₄]²⁻, which is soluble in water. The ligand is then isolated by extraction using an immiscible organic solvent.

Attempts were made to find an appropriate solvent in which the new et,ph-P4-Ph ligand could be crystallized without success. Schreiter was able to form the similar dinickel tetrachloride complexes and found a way to separate and isolate the new ligand diastereomers using cyanolysis.¹⁴ Compared to the old Ni₂Cl₄(et,ph-P4) complexes, he found the new Ni₂Cl₄(*rac*-et,ph-P4-Ph) complex is insoluble and the Ni₂Cl₄(*meso*-et,ph-P4-Ph) complex is soluble in 1-butanol. Once again after filtration, an excess of NaCN was added to the material to yield some free ligand that could be extracted in a water/benzene solution. Like the older method, the separation was neither efficient, nor green, as it required over 250 eq. of NaCN to release the ligand from the nickel in low yields. Finally, Mark Peterson attempted to functionalize the internally bound phenyl rings in hope that either a *para*-substituent of a *t*-butyl or NMe₂ group would allow for better crystallization, but he was unsuccessful.¹⁵

The older et,ph-P4 ligand had been reacted with [Rh(nbd)₂]BF₄ to form [Rh₂(nbd)₂(et,ph-P4-Ph)](BF₄)₂, the catalyst precursor, by Melanie Broussard.¹⁶ From this same procedure, Monteil worked to combine the newer et,ph-P4-Ph ligand to the same rhodium starting material. He may have succeeded in his efforts, but the ³¹P{¹H} NMR of his material was not clean, and he could not crystallize the material for an X-ray structure.

In hope of using the et,ph-P4-Ph ligand for our catalytic studies, Kalachnikova and the author worked jointly to optimize the synthesis of the ligand as well as form a more efficient

method for separation. After the ligand was obtained, the author separately used it to make $[\text{Rh}_2(\text{nbd})_2(\text{rac-}i\text{-et,ph-P4-Ph})](\text{BF}_4)_2$. The research into the new *et,ph-P4-Ph* ligand synthesis optimization, separation, and dirhodium catalyst characterization is described below.

2.2 Results and Discussion

2.2.1 Optimization of “Chlorobridge,” $\text{Cl}(\text{Ph})\text{PCH}_2\text{P}(\text{Ph})\text{Cl}$

Though we do not buy these materials, commercially available $\text{Cl}_2\text{PCH}_2\text{P}(\text{Cl})_2$ has been converted into $\text{Cl}(\text{Ph})\text{PCH}_2\text{P}(\text{Ph})\text{Cl}$, here in named chlorobridge, by Stelzer *et al.* and Schmidbaur and Schnatterer. Both methods are outlined below in Figure 2.6.¹⁷

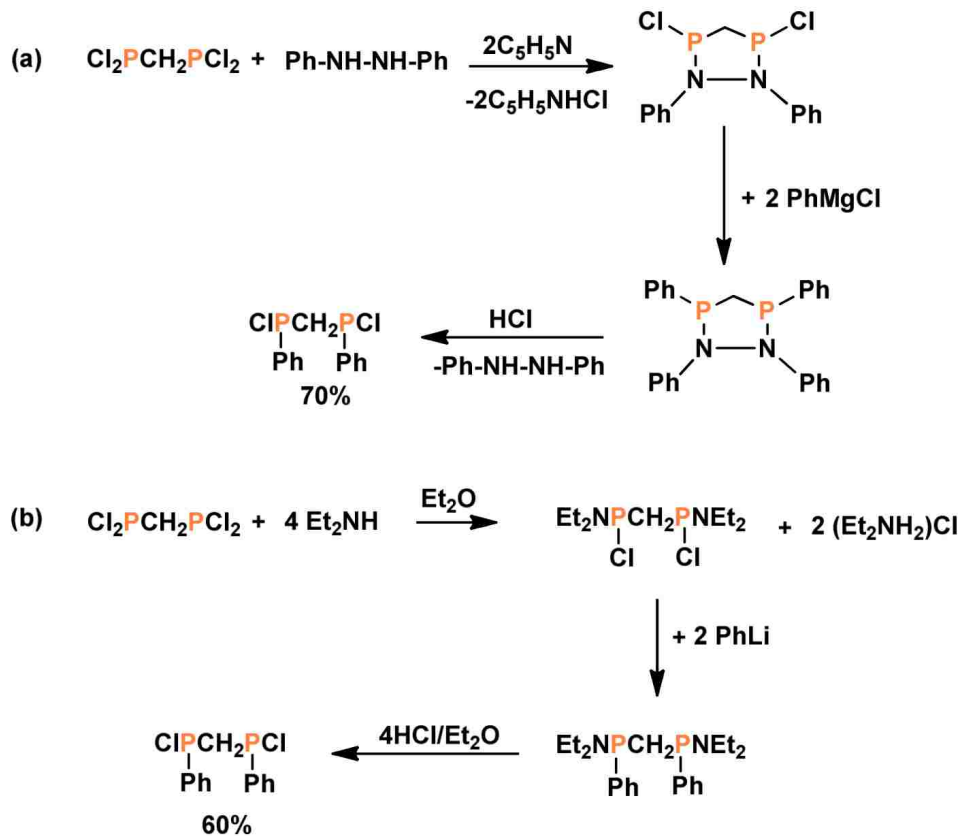


Figure 2.6. Synthesis of chlorobridge reported by ^aStelzer *et al.* and ^bSchmidbaur and Schnatterer

Though these syntheses give decent yields to the chlorobridge, each requires multiple steps with several intermediates. As we use H(Ph)PCH₂P(Ph)H, or bridge, as our starting material in the synthesis of et,ph-P4, Monteil described the efforts of Weferling as a potential way to directly chlorinate the bridge to chlorobridge.¹⁸ Weferling demonstrated the ability of C₂Cl₆ and PCl₅ to chlorinate primary and secondary phosphines. Monteil focused on using C₂Cl₆ as the chlorination agent of choice, and we followed his procedure, but found several issues that needed to be improved.

When C₂Cl₆ and the bridge were dissolved together in diethyl ether and allowed to react for 24 hours at ~45 °C, a pink material was obtained with a white precipitate. Filtration of the two materials would separate the solid from the chlorinated product, but when the product was dried additional white solid would come out of solution. Each subsequent filtration would lead to loss of material and more solid needing additional filtration. After considerable loss of material, our yield for this reaction was only 42 %. Examination of the materials via ³¹P {¹H} NMR showed the desired product as a single diastereomer with a chemical shift at 81.0 ppm (s) in the pink solution (Figure 2.7), and no chemical shifts for the white solid. Further examination of the white solid via ¹³C {¹H} NMR showed a chemical shift corresponding to unreacted C₂Cl₆.

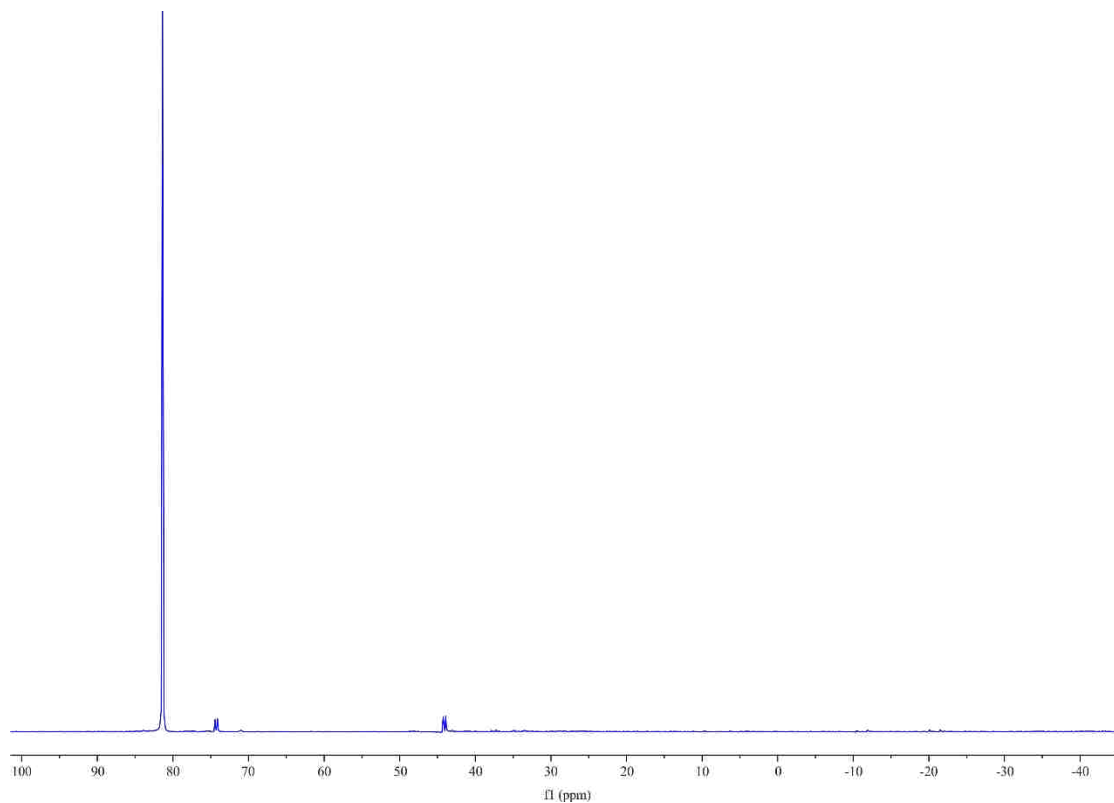


Figure 2.7. $^{31}\text{P}\{^1\text{H}\}$ NMR of $\text{Cl}(\text{Ph})\text{PCH}_2\text{P}(\text{Ph})\text{Cl}$ in CDCl_3 from the reaction of bridge with C_2Cl_6 in diethyl ether

The reaction requires 1 eq. of C_2Cl_6 to react with each P-H group of the bridge. As we used exactly 2 eq. of C_2Cl_6 , which would react with the two P-H groups to produce two P-Cl, and the ^{31}P NMR showed no sign of unreacted bridge, we were stumped as to why excess C_2Cl_6 precipitated out of solution under vacuum. Dropwise additions of the $\text{H}(\text{Ph})\text{PCH}_2\text{P}(\text{Ph})\text{H}$ to the C_2Cl_6 , and the C_2Cl_6 to the bridge were made with no change in the results for the reaction. Even a reduction of the C_2Cl_6 equivalents from 2 to 1.5 failed to change the precipitation of excess C_2Cl_6 after workup, causing the need for filtration, and lower yields of the $\text{Cl}(\text{Ph})\text{PCH}_2\text{P}(\text{Ph})\text{Cl}$ bisphosphine. Furthermore, attempts to vacuum distill the product away from the C_2Cl_6 would lead to degradation of the material at temperatures above $100\text{ }^\circ\text{C}$. The result of the excessive heating was decomposition of chlorobridge to PhPCl_2 and dimerization of the chlorobridge.

During vacuum distillation, a crystalline white material was seen at the top of the flask, which was found to be C_2Cl_6 . Upon examination, it was noticed that the C_2Cl_6 would sublime under the low pressure above 100 °C. By heating the product for a short time *in vacuo*, one could sublime the C_2Cl_6 away from the bulk product. With the C_2Cl_6 covering the top of the flask, the chlorobridge could be pipetted to a secondary flask. This allows one to avoid filtration of the C_2Cl_6 . However, with the degradation of the chlorobridge occurring at higher temperatures, sublimation of C_2Cl_6 could lead to lower yields. Instead of these simple fixes, movement to solvents in which the C_2Cl_6 is more reactive was examined.

Monteil reported using toluene as an alternate solvent for the reaction of C_2Cl_6 and the bridge. In this reaction, Monteil reports the use of 140 °C and an 18 hour reaction time. These conditions, unfortunately, resulted in degradation of the product due to too high a temperature. We ran the same reaction at 80 °C and found that after only 3 hours the $H(Ph)PCH_2P(Ph)H$ was completely converted to the chlorinated product. Furthermore, when vacuum distilling the solvent, we found little to no C_2Cl_6 remaining in the flask.

During this experimentation, the dropwise addition of both the C_2Cl_6 to the bridge and the bridge to the C_2Cl_6 were studied. In each case, the resulting yields and purities were similar. However, as the C_2Cl_6 is less soluble in toluene than the bridge, it was found that preheating the C_2Cl_6 in toluene would allow it to completely dissolve, so the addition of bridge to C_2Cl_6 was preferred. Also, during the addition of either material, a gas was produced. As the reaction was expected to yield byproducts of HCl and tetrachloroethene, the gas was presumed to be HCl. To keep the gas from remaining in the solution, a larger flask with ample headspace was determined to be necessary for the reaction. We also found that purging the flask with N_2 occasionally helped remove HCl.

$^{31}\text{P}\{^1\text{H}\}$ NMR was used to assess the purity of the material, and what appeared to be a single diastereomer of $\text{Cl}(\text{Ph})\text{PCH}_2\text{P}(\text{Ph})\text{Cl}$ was found. By happenstance, some NMR samples were prepared fairly dilute and in aromatic solvents such as benzene and toluene. These samples of $\text{Cl}(\text{Ph})\text{PCH}_2\text{P}(\text{Ph})\text{Cl}$, yielded two resonances with chemical shifts of 80.6 ppm and 80.8 ppm. At high concentrations or in non-aromatic solvents, the *rac*- and *meso*-diastereomers of the chlorobridge have the same chemical shift of 81.4 ppm (Figure 2.8). Low concentrations in aromatic solvents produce conditions that allow the resonances of each diastereomer to be observed. A full list of experimental data is shown in Table 2.1.

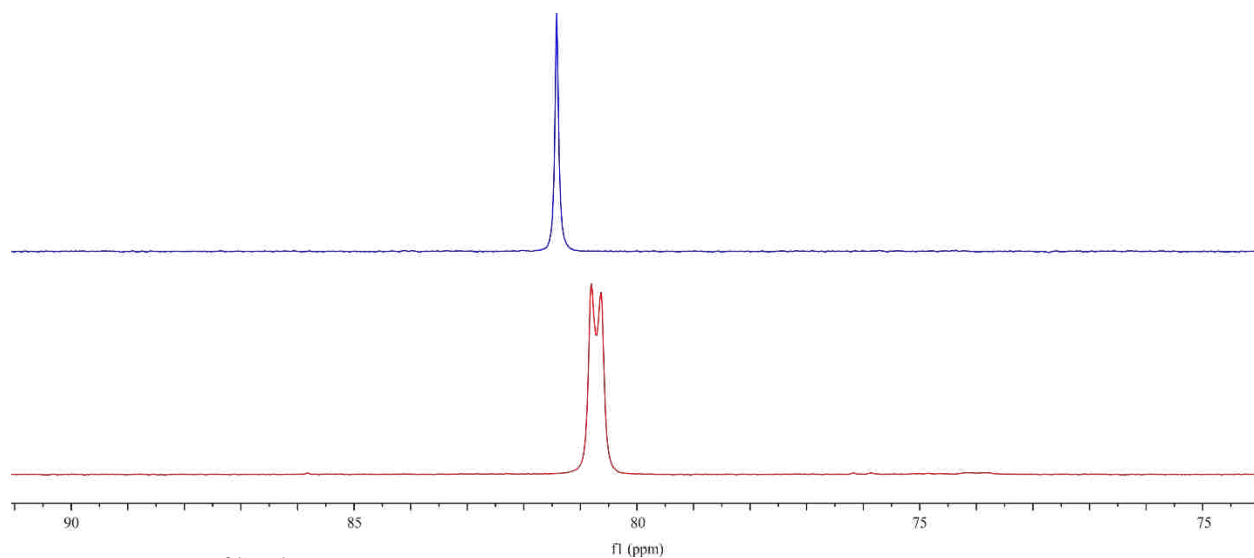


Figure 2.8. $^{31}\text{P}\{^1\text{H}\}$ NMR of the $\text{Cl}(\text{Ph})\text{PCH}_2\text{P}(\text{Ph})\text{Cl}$ in CD_2Cl_2 (top) and in benzene- d_6 (bottom), both *rac*- and *meso*-diastereomers can be seen in benzene.

Table 2.1. Results for Chlorination of Bridge via C₂Cl₆

Exp.	C ₂ Cl ₆ (eq.)	Reagent Added	Reaction Conditions	Results
1 ^a	2	Jointly Combined	Diethyl Ether 24 hours 45 °C	White ppt. No Isolated product
2 ^a	2	Bridge	Diethyl Ether 24 hours 45 °C	White ppt. No isolated product
3 ^a	2	C ₂ Cl ₆	Diethyl Ether 24 hours 45 °C	White ppt. No isolated product
4 ^a	1.5	C ₂ Cl ₆	Diethyl Ether 24 hours 45 °C	No isolated product 65 % Pure (by NMR)
5 ^b	2	Bridge	Toluene 3 hours 80 °C	87 % Yield 100 % Pure (by NMR)

^aSolutions were made with H(Ph)PCH₂P(Ph)H and C₂Cl₆ concentrations of 1 M. ^bSolutions were made with H(Ph)PCH₂P(Ph)H concentration being 10 M and C₂Cl₆ concentration being 2 M.

The optimization of the chlorobridge was achieved by the dropwise addition of H(Ph)PCH₂P(Ph)H to C₂Cl₆ dissolved in toluene at ~80 °C. The mixture was then allowed to react for 3 hours at ~80 °C, and then the chlorobridge product isolated by vacuum distillation.

2.2.2. Optimization of et,ph-P4-Ph via Grignard Coupling of “I-Small Arm,” 1-(diethylphosphino)-2-iodobenzene

The next step in the synthesis of the et,ph-P4-Ph ligand is to form 1-(diethylphosphino)-2-iodobenzene, or I-small arm. The goal of this synthesis was to utilize Grignard coupling reactions to combine the chlorobridge with the I-small arm creating the ligand. Both the experiments for the coupling of these materials as well as the coupling of the *o*-dihalobenzene with a phosphine were developed by Monteil from the original research of Boymond.¹⁹

In experiments by Boymond *et al.*, the use of $i\text{PrMgBr}$ as a mediating Grignard reagent has shown magnesium-iodine exchange of 1-bromo-2-iodobenzene to produce $\text{Br}(o\text{-C}_6\text{H}_4)\text{MgBr}$ in high yields and shown in Figure 2.9. Boymond reports on the use of this method to produce aromatic aldehydes and allylic compounds, while Gommermann reports on it forming polyfunctional unsaturated amines.²⁰ It is through this research that Monteil began examining the production of aryl phosphines.

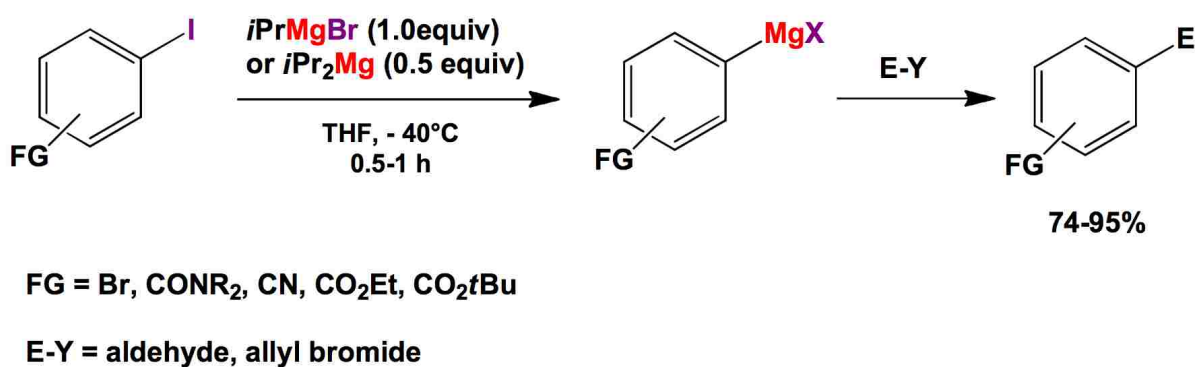


Figure 2.9. Extent of Boymond's magnesium-iodine exchange

The results of Monteil's studies show he was successful in first forming the *ortho*-substituted halobenzene Grignard that could then be treated with Et_2PCl to exchange the chloride forming the small arm. Monteil attempted to form F, I, and Br benzene Grignards and found that each were ideally made at 0°C over a 6 hour reaction time by reaction of the *o*-dihalobenzene with $i\text{PrMgBr}$. At the end of this period, the resulting Grignard would be reacted with Et_2PCl at -25°C , and then allowed to warm to room temperature and fully react overnight (Figure 2.10).

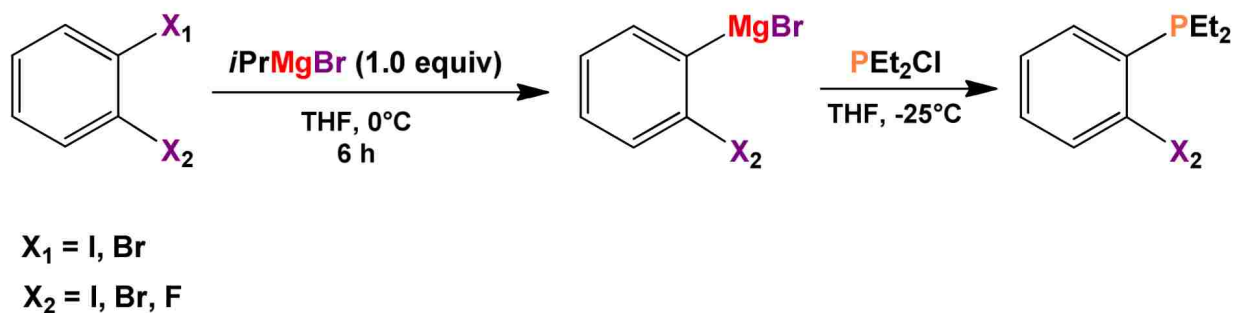


Figure 2.10. Monteil's preparation of aryl phosphines by Mg-I exchange

As Monteil found that the Br-small arm was unable to yield the et,ph-P4-Ph ligand when coupled to Et_2PCl by reaction with $^i\text{PrMgBr}$, the I-small arm became the preferred starting material for the coupling reaction. In making the I-small arm it is critically important to keep the reaction at $0\text{ }^\circ\text{C}$ over the full 6 hour period. Allowing the reaction to warm above $0\text{ }^\circ\text{C}$ during this time causes many side products to form.

The coupling of the chlorobridge and I-small arm was reported by Monteil to proceed in a similar fashion as seen for the formation of I-small arm. The I-small arm reacts with $^i\text{PrMgBr}$ for 8 hours at $0\text{ }^\circ\text{C}$. The resulting Grignard is then coupled with chlorobridge at $-25\text{ }^\circ\text{C}$ and allowed to heat to room temperature overnight (Figure 2.11).

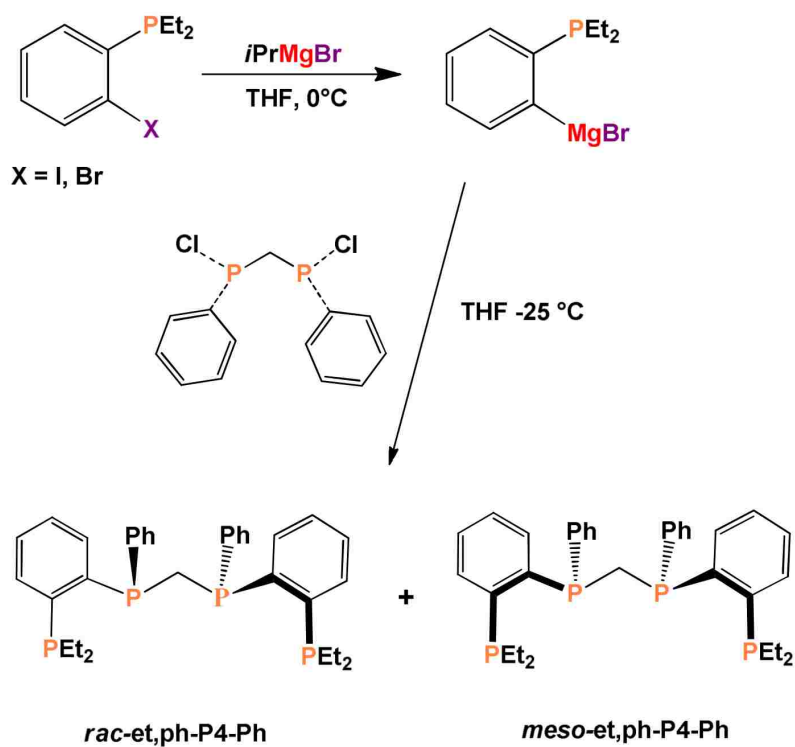


Figure 2.11. Monteil's preparation of et,ph-P4-Ph by Mg-I exchange of chlorobridge and I-small arm

Following preliminary workup, the resulting crude ligand was found to contain unreacted I-small arm. Monteil suggested the short-path distillation of the small arm from the ligand at 180 °C. If this step were skipped, the reaction is diastereoselective for the *meso*-ligand. An explanation for this selectivity is unknown at this time. Monteil did heat his sample and reported the mixed ligand product, which is what we normally do to get both diastereomers. Remember that the *rac-et,ph-P4* forms the active dirhodium hydroformylation catalyst. The *meso*-diastereomer is considerably less active and selective. So our group is most interested in the *rac-et,ph-P4-Ph* diastereomer.

The crude mixed *rac,meso-et,ph-P4-Ph* ligand has a physical appearance of a yellow paste. Kalachnikova found that column chromatography of the crude mixed ligand using dichloromethane as the mobile phase and neutral alumina as the stationary phase could remove

the majority of the yellow impurities.²¹ The $^{31}\text{P}\{^1\text{H}\}$ NMR of this material has a complicated second order pattern. The two diastereomers make the ^{31}P NMR even more complicated as their shifts are within 1 ppm of each other, and their second-order resonances overlap. This pattern occurs between -26 ppm to -32 ppm (Figure 2.12). If the crude ligand does not undergo distillation of the I-small arm, small phosphine impurities related to the I-small arm and unreacted I-small arm itself are often found in the “purified” ligand. This unreacted material averages $\sim 20\%$ of the integrated phosphine peaks.

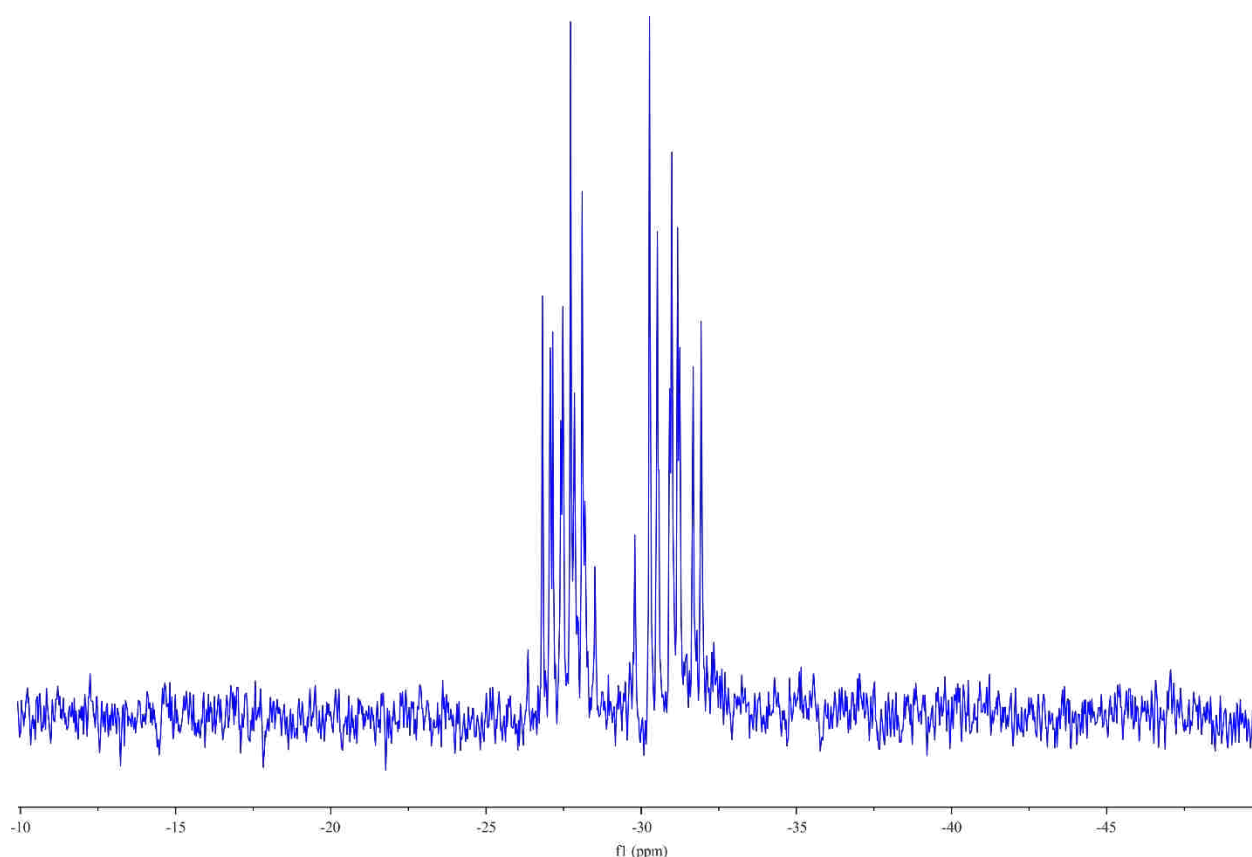


Figure 2.12. $^{31}\text{P}\{^1\text{H}\}$ NMR of mixed et,ph-P4-Ph

As a result of the overheating of the Grignard making the I-small arm and the presence of unreacted material, examination of temperatures and reaction times for the ligand reaction were studied. It was found that extending the reaction time of the small arm Grignard formation from 8 hours to 24 hours allowed for the complete conversion of the I-small arm to the Grignard

reagent. If the temperature were to rise too much during this period, then byproducts would form from the Grignard leading to lower yields of the ligand (Figure 2.13). As such, the Grignard was kept at 0 °C for the full 24 hour period before further cooling and reaction with the chlorobridge.

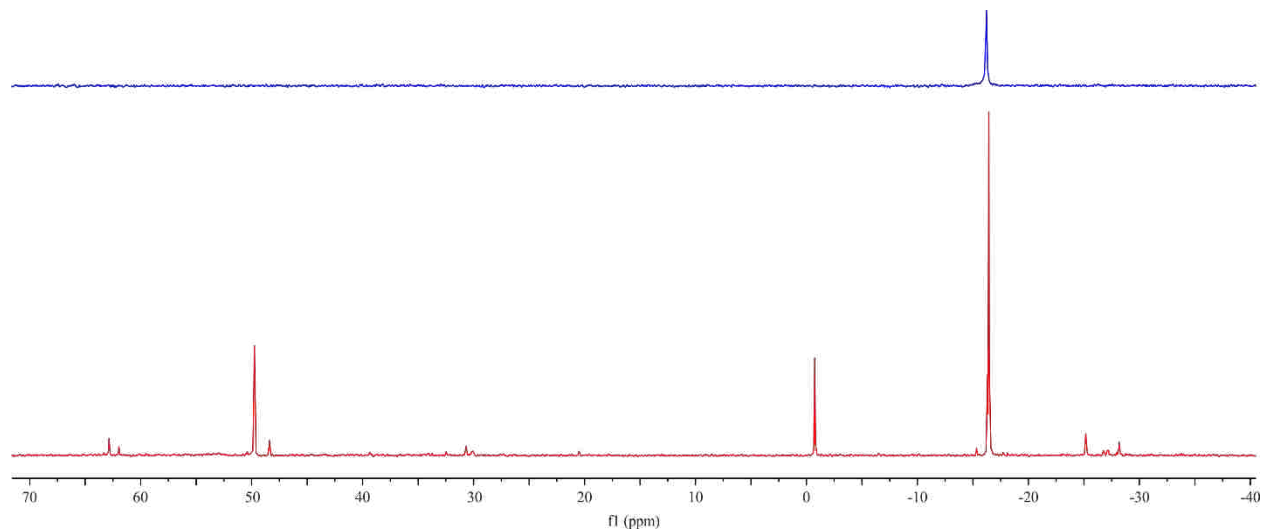


Figure 2.13. $^{31}\text{P}\{^1\text{H}\}$ NMR of I-small arm reacting with $^i\text{PrMgBr}$ after 24 hours (top) and 6 hours (bottom)

We found that allowing the I-small arm and $^i\text{PrMgBr}$ to fully react while at 0 °C for 24 hours would reduce the unreacted I-small arm from ~20 % to ~2 % – a substantial improvement in yield. Other optimizations were made to the workup of the ligand. Kalachnikova designed a column chromatography method using DCM and alumina to separate the bulk impurities from the ligand. Short-path distillation is still suggested to help remove the excess I-small arm, but this leads to epimerization, which is usually desired to make *rac*-et,ph-P4-Ph. If one only were to want *meso*-et,ph-P4-Ph, then I-small arm should be removed via the separation column in the next section.

2.2.3. Separation of *meso*- and *rac*-et,ph-P4-Ph

Monteil never was able to develop a separation technique for the *rac*- and *meso*-diastereomers of the et,ph-P4-Ph ligand. After hundreds of solvent mixtures and countless

experimentation of the stationary phase, it was found that two mobile phases could elute the *meso*- and *rac*-ligands separately from Grade IV alumina column. The first mobile phase is that of DCM/toluene/hexane in a 1:2:3 ratio. When eluted, the first fractions from the column are the impurities including unreacted I-small arm. They are closely followed by the *meso*-ligand. Finally, there is a decent gap between the *meso*-ligand and the subsequent *rac*-ligand fraction. The second mobile phase is that of DCM/hexane in a 1:4 ratio. Here, the materials elute in the same order, but with differences in the elution time. The unreacted small arm elutes separately from the impurities. There is the larger gap between the impurities and the *meso*-ligand. Instead of a gap between the pure *meso*- and *rac*-ligands, a mixed ligand set of fractions elutes between them.

Because the first solvent mixture fails to eliminate the impurities and requires higher temperatures to remove toluene from the ligand, which may result in epimerization, the second solvent mixture is the preferred mobile phase for the separation column.

Since the $^{31}\text{P}\{^1\text{H}\}$ NMR of either ligand diastereomer has such similar chemical shifts, ^1H NMR is used to determine the purity of the ligand fractions. The methylene bridging protons are in a clear region of the ^1H NMR spectrum and have different coupling patterns. The *meso*-*et*,*ph*-P4-Ph having non-equivalent protons forms two doublets of triplets centered at 2.8 ppm and 3.1 ppm (Figure 2.14). The *rac*-*et*,*ph*-P4-Ph having equivalent protons forms a triplet at 3.0 ppm (Figure 2.14).

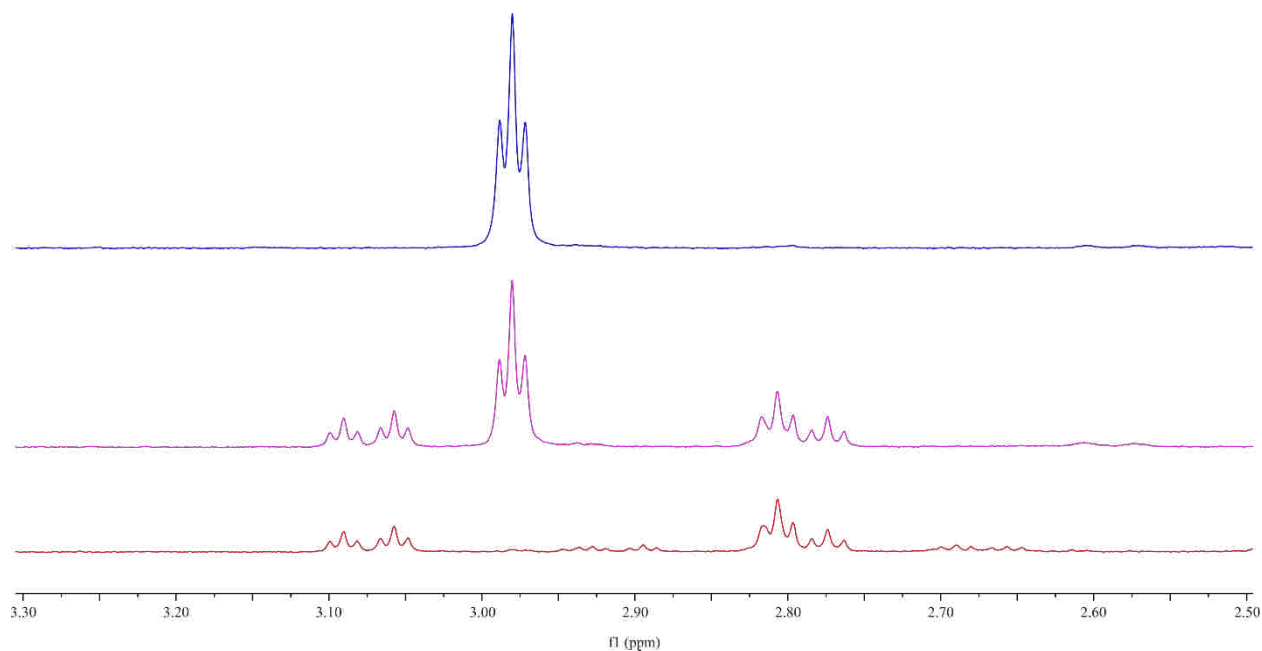


Figure 2.14. Expanded ^1H NMR of et,ph-P4-Ph
The top spectrum corresponds to the *rac*-ligand, the middle to the mixed ligand,
and the bottom to the *meso*-ligand.

2.2.4 Optimization of et,ph-P4-Ph via Grignard Coupling of “Br-Small Arm,” 1-(diethylphosphino)-2-bromobenzene

After running separation columns, it was found that several impurities needed to be removed from the ligand. Some of these were able to be eliminated with the modified temperature and reaction time of the I-small arm and the $^i\text{PrMgBr}$ to later form the et,ph-P4-Ph ligand. As a re-examination of Monteil’s work, attempts to form the ligand from the Br-small arm were studied.

The Br-small arm was made as described by Monteil with the addition of 1-iodo-2-bromobenzene and $^i\text{PrMgBr}$ at $0\text{ }^\circ\text{C}$ for 6 hours followed by the addition of Et_2PCl at $-25\text{ }^\circ\text{C}$ and a reaction overnight at room temperature. Monteil was unable to react the resulting Br-small arm with magnesium turning. Kalachnikova chose to heat the magnesium turning in hope of starting the reaction of the metal and Br-small arm. At $\sim 70\text{ }^\circ\text{C}$ the reaction started with magnesium dissolving into the Br-small arm solution.²² Within 3 hours, her mixture turned a red-brown

color, which she believed was the end of the reaction. When heated to 70 °C from the start, the color change occurs when the magnesium dissolves. By running GC/MS samples every ten minutes of the quenched reaction mixture, I found complete conversion took 60 minutes instead.

Kalachnikova followed by cooling the reaction mixture to room temperature and then adding it to a cooled chlorobridge (−35 °C). Though this works, the cannula used to transfer the Br-small arm Grignard often cools too much and makes it very difficult to transfer the solution to the chlorobridge. Instead, keeping the Grignard solution at 70 °C allows for easy flow of the material to the chlorobridge. Once added, the mixture is allowed to warm to room temperature and react overnight. Workup of the resulting ligand is the same as that of the I-small arm. The ligand contains ~3 % unreacted Br-small arm as the only phosphine impurity visible on ³¹P NMR.

Though suggested by Kalachnikova, the excess Br-small arm cannot be removed via short-path distillation at 100 °C. A temperature of 135 °C is needed to remove the Br-small arm from the ligand. Like the I-small arm reaction, distillation can remove the excess Br-small arm, but one epimerizes the et,ph-P4-Ph ligand in the process. If one were to want pure *meso*-et,ph-P4-Ph heating should be avoided and separation of the Br-small arm and the ligand should be via the DCM/Hexane column described above. Once the Br-small arm is removed, the ligand can be used or epimerized and the diastereomers separated as before. Improvements to the procedure over the I-small arm are significant as no impurities remain after the DCM cleanup column.

2.25. Synthesis of $[\text{Rh}_2(\text{nbd})_2(\text{rac-}\text{et,ph-P4-Ph})](\text{BF}_4)_2$

Based on Broussard's synthesis of $[\text{Rh}_2(\text{nbd})_2(\text{rac-}\text{et,ph-P4})](\text{BF}_4)_2$, the synthesis of the new complex featuring the et,ph-P4-Ph ligand was achieved.¹³ The scheme for this synthesis is below in Figure 2.15.

Table 2.2. Selected Bond Distances (Å) and Bond Angles (°) of $[\text{Rh}_2(\text{nbd})_2(\text{rac-}i\text{-et,ph-P4})](\text{BF}_4)_2$

Rh1-C34	2.257(2)	Rh2-C41	2.221(2)
Rh1-C35	2.229(2)	Rh2-C42	2.243(2)
Rh1-C37	2.207(2)	Rh2-C44	2.209(2)
Rh1-C38	2.227(2)	Rh2-C45	2.211(2)
Rh1-P1	2.2822(5)	Rh2-P3	2.2798(5)
Rh1-P2	2.2948(5)	Rh2-P4	2.2869(6)
P2-C7	1.839(2)	P3-C7	1.844(2)
P1-Rh1-P2	84.648(19)	P3-Rh2-P4	84.57(2)
P1-Rh1-C34	168.89(6)	P3-Rh2-C41	99.11(6)
P1-Rh1-C35	147.02(6)	P3-Rh2-C42	105.62(6)
P1-Rh1-C37	95.06(6)	P3-Rh2-C44	169.46(8)
P1-Rh1-C38	104.05(6)	P3-Rh2-C45	150.65(9)
P2-Rh1--C34	168.89(6)	P4-Rh2-C41	142.95(7)
P2-Rh1-C35	99.50(6)	P4-Rh2-C42	169.76(6)
P2-Rh1-C37	151.02(7)	P4-Rh2-C44	104.56(7)
P2-Rh1-C38	169.07(6)	P4-Rh2-C45	93.67(7)
C37-Rh1-C38	36.39(9)	C44-Rh2-C45	35.93(12)
C37-Rh1-C35	65.79(8)	C44-Rh2-C41	76.88(9)
C38-Rh1-C35	76.89(8)	C45-Rh2-C41	65.43(10)
C37-Rh1-C34	76.95(8)	C44-Rh2-C42	65.38(9)
C38-Rh1-C34	64.94(8)	C45-Rh2-C42	77.01(9)
C35-Rh1-C34	35.55(9)	C41-Rh2-C42	35.93(9)
P2-C7-P3	118.60(10)		

The X-ray crystallography shows that the complex is dicationic and bimetallic with each rhodium in the 1+ oxidation state and a d^8 configuration. The geometry is square planar with the ligand bound to the metal as anticipated. The structure is similar to the one reported for $[\text{Rh}_2(\text{nbd})_2(\text{rac-}i\text{-et,ph-P4})](\text{BF}_4)_2$. A distance of 6.010 Å is found between the metal centers, which is longer than the 5.527 Å distance for $[\text{Rh}_2(\text{nbd})_2(\text{rac-}i\text{-et,ph-P4})](\text{BF}_4)_2$; both distances indicate no interaction between the metals. P–CH₂–P angle is 118.6 °, which is similar to the 120.9 ° angle seen in $[\text{Rh}_2(\text{nbd})_2(\text{rac-}i\text{-et,ph-P4})](\text{BF}_4)_2$. Likewise, the Rh–P bonds for the two

complexes are very similar being $\sim 2.29 \text{ \AA}$ each. The norbornadiene bond lengths and angles are similar to those reported in other complexes.¹⁹

A sample of the crystals were dried and tested for solubility. It was found that the complex is soluble in acetone, acetonitrile, DMF, DMSO, benzene, toluene, DCM, methanol, and ethanol; it is slightly soluble in THF; and it is insoluble in diethyl ether and hexane.

The ^1H NMR shows a triplet at 3.83 ppm ($J_{\text{P-H}} = 9.7 \text{ Hz}$) indicative of the protons on the central methylene bridge (Figure 2.17).

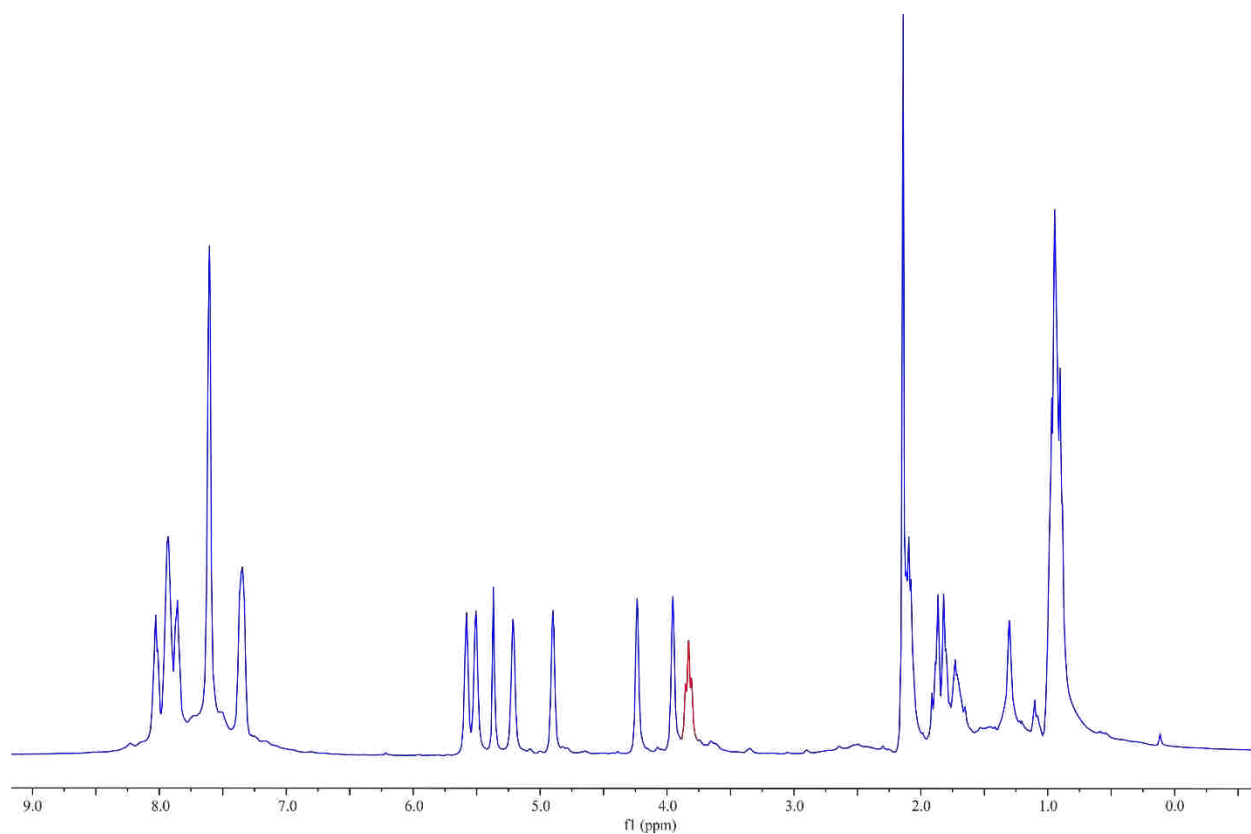


Figure 2.17. ^1H NMR of $[\text{Rh}_2(\text{nbd})_2(\text{rac-et,ph-P4})](\text{BF}_4)_2$

The $^{31}\text{P}\{^1\text{H}\}$ NMR has two doublets of doublets centered at 43.1 ppm ($J_{\text{Rh-P}} = 161.1$, $J_{\text{Pint-Pext}} = 28.6$) and 56.5 ppm ($J_{\text{Rh-P}} = 154.1 \text{ Hz}$, $J_{\text{Pint-Pext}} = 28.6 \text{ Hz}$) (Figure 2.18). Based on the older $[\text{Rh}_2(\text{nbd})_2(\text{rac-et,ph})](\text{BF}_4)_2$ complex, the external phosphines are assigned to the 56.5 ppm resonances and the internal phosphines are assigned to the 43.1 ppm peaks.

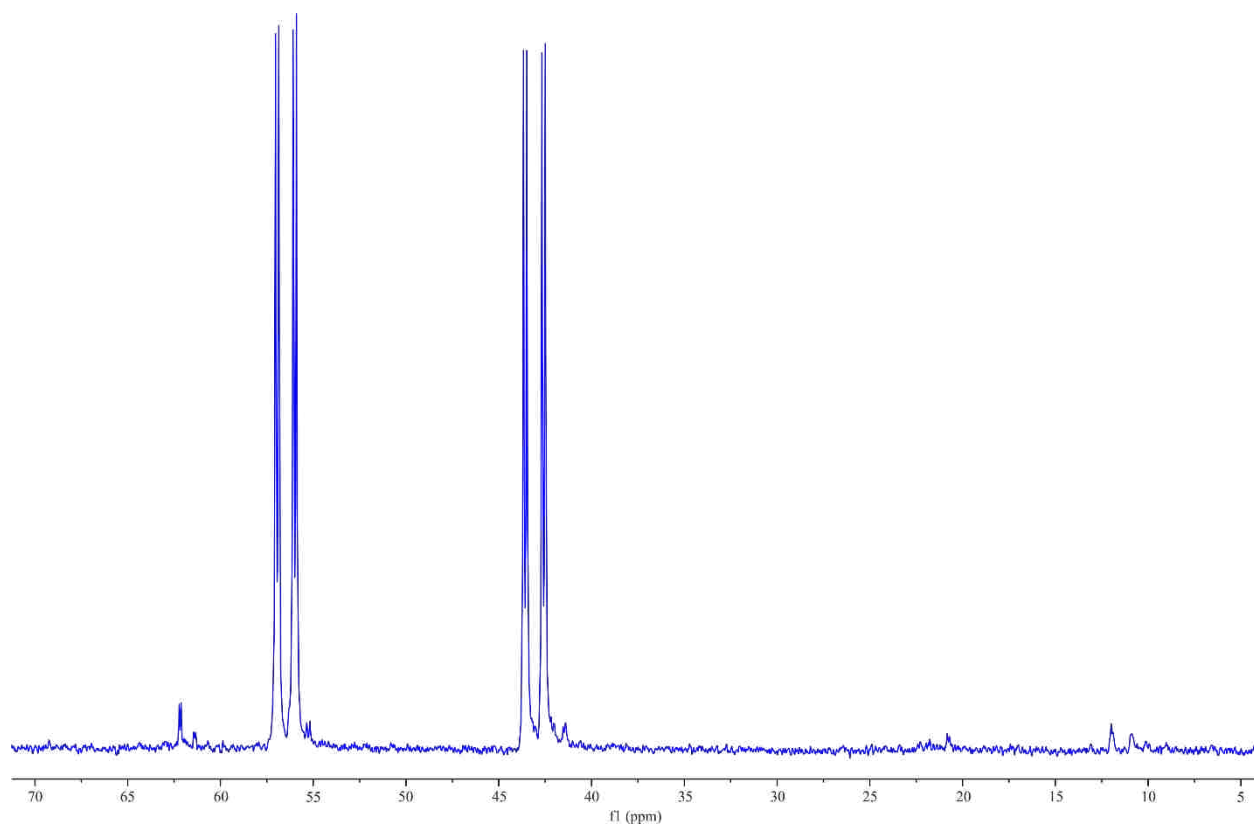


Figure 2.18. $^{31}\text{P}\{^1\text{H}\}$ NMR of $[\text{Rh}_2(\text{nbd})_2(\text{rac-et,ph-P4})](\text{BF}_4)_2$

2.3 References

1. Heck, R. F.; Breslow, D. S., The Reaction of Cobalt Hydrotetracarbonyl with Olefins. *J. Am. Chem. Soc.* **1961**, *83*, 4023.
2. Laneman, S. A.; Fronczek, F. R.; Stanley, G. G., Synthesis of Binucleating Tetratertiary Phosphine Ligand System and the Structural Characterization of Both *Meso* and *Racemic* Diastereomers of {Bis[diethylphosphinoethyl]phenylphosphino}methane} tetrachlorodinickel. *Inorg. Chem.* **1989**, *28*, 1872.
3. Broussard, M. E.; Juma, B.; Train, S. G.; Peng, W. J.; Laneman, S. A.; Stanley, G. G., A Bimetallic Hydroformylation Catalyst: High Regioselectivity and Reactivity Through Homobimetallic Cooperativity. *Science*. **1993**, *260*, 1784.
4. Aubry, D. A.; Monteil, A. R.; Peng, W.; Stanley, G. G., The Unusual Inhibition of a Dirhodium Tetrakisphosphine-based Bimetallic Hydroformylation Catalyst by PPh_3 . *R C Chimie*. **2002**, *5*, 473.

5. Matthews, R. C.; Howell, D. K.; Peng, W.; Train, S. G.; Treleaven, W. D.; Stanley, G. G., Bimetallic Hydroformylation Catalysis: *In Situ* Characterization of a Dinuclear Rhodium(II) Dihydrido Complex with the Largest Rh–H NMR Coupling Constant. *Angew. Chem., Int. Ed.* **1996**, *35*, 2253.
6. Hunt, C.; Nelson, B. D.; Harmon, E. G.; Fronczek, F. R.; Watkins, S. F.; Billodeaux, D. R.; Stanley, G. G., A Binuclear Rhodium (I) Complex with Two Tetraphosphine Ligands at 100 K. *Acta. Crystallogr., Sect. C: Cryst. Struct. Commun.* **2000**, *56*, 546.
7. Hunt, C.; Fronczek, F. R.; Billodeaux, D. R.; Stanley, G. G., A Monometallic Rh(III) Tetraphosphine Complex: Reductive Activation of CH₂Cl₂ and Selective Meso to Racemic Tetraphosphine Ligand Isomerization. *Inorgo. Chem.* **2001**, *40*, 5192.
8. Aubry, D. A.; Bridges, N. N.; Ezell, K.; Stanley, G. G., Polar Phase Hydroformylation: The Dramatic Effect of Water on Mono- and Dirhodium Catalysts. *J. Am. Chem. Soc.* **2003**, *125*, 11180.
9. Fernando, S. R. G. Computational Studies on Bimetallic Catalysis and X-Ray Absorption Spectroscopy. Ph.D. Dissertation, Louisiana State University, Baton Rouge, LA, 2015.
10. Fernando, R. G.; Gasery, C. D.; Moulis, M. D.; Stanley, G. G., Bimetallic Homogeneous Hydroformylation. *In Homo and Heterobimetallic Complexes in Catalysis*, 1; Kalck, P.; Springer: Switzerland, 2016.
11. (a) Warren, L. F.; Bennett, M. A., Stabilization of High Formal Oxidation States of the First-Row Transition Metal Series by *o*-Phenylenebis(dimethylphosphine). *J. Am. Chem. Soc.* **1974**, *96*, 3340; (b) Warren, L. F.; Bennett, M. A., Comparative Study of Tertiary Phosphine and Arsine Coordination to the Transition Metals. Stabilization of High Formal oxidation States by *o*-Phenylene-Based Chelate Ligands. *Inorgo. Chem.* **1976**, *15*, 3126; (c) Sethulakshmi, C. N.; Subramanian, S.; Bennett, M. A.; Manoharan, P. T., Electron Paramagnetic Resonance Studies of Two Low-Spin Hexacoordinate Di(tertiary phosphine) Complexes of Nickel(III). *Inorgo. Chem.* **1979**, *18*, 2520; (d) Roberts, N. K.; Wild, S. B., Metal Complexes Containing Diastereoisomers and Enantiomers of *o*-Phenylenebis(methylphenylarsine) and its Phosphorus Analog. 1. Stereochemistry and Dynamic Behavior of Square-Planar and Square-Pyramidal Complexes of Bivalent Nickel. *Inorgo. Chem.* **1981**, *20*, 1892; (e) Roberts, N. K.; Wild, S. B., Metal Complexes Containing Diastereoisomers and Enantiomers of *o*-Phenylenebis(methylphenylarsine) and its Phosphorous Analogue. 2. Stereochemistry and Dynamic Behaviour of Square-Planar and Square-Pyramidal Complexes of Bivalent Palladium and Platinum. *Inorgo. Chem.* **1981**, *20*, 1900; (f) Mashima, K.; Komura, N.; Yamagata, T.; Tani, K.; Haga, M. A., Synthesis and Crystal Structure of a Cationic Trinuclear Ruthenium(II) Complex, [Ru₃(μ²-Cl)₃(μ³-Cl)₂{1,2- bis(diphenylphosphino)benzene}₃]PF₆. *Inorgo. Chem.* **1997**, *36*, 2908; (g) McDonagh, A. M.; Humphrey, M. G.; Hockless, D. C. R., Selective Preparation of Cis-or Trans-Dichlorobis{(R,R)-1,2-phenylenebis(methylphenylphosphine-P)} osmium(II) from Dimethylsulfoxide Complex Precursors. *Tetrahedron: Asymmetry* **1997**, *8*, 3579.

12. Monteil, A. R. Investigation into the Dirhodium-Catalyzed Hydroformylation of 1-Alkenes and Preparation of a Novel Tetrphosphine Ligand. Ph.D. Dissertation, Louisiana State University, Baton Rouge, LA, 2006.
13. Aubry, D. A.; Laneman, S. A.; Fronczek, F. R.; Stanley, G. G., Separating the Racemic and Meso Diastereomers of a Binucleating Tetrphosphine Ligand System through the Use of Nickel Chloride. *Inorgo. Chem.* **2001**, *40*, 5036.
14. Schreiter, W. J. Investigations into Alkene Hydration and Alkene Oxidation Catalysis. Ph.D. Dissertation, Louisiana State University, Baton Rouge, LA, 2013.
15. Peterson, M. A. Toward the Advancement of Tetrphosphine Ligand Synthesis for Homogeneous Bimetallic Catalysis. Ph.D. Dissertation, Louisiana State University, Baton Rouge, LA, 2013.
16. Broussard, M. E. Bimetallic Hydroformylation Catalysis. Ph.D. Dissertation, Louisiana State University, Baton Rouge, LA, 1993.
17. (a) Schmidbaur, H; Schnatterer, S., Synthese und Eigenschaften Offenkettiger und Cyclischer $1\lambda^3, \lambda^3$ -Diphosphaalkane RR'P-CH₂-PR'R. *Chemische Berichte* **1986**, *119*, 2832; (b) Gol, F.; Hasselkuß, G.; Knüppel, P. C.; Stelzer, O. Z., *Naturforsch., B: Chem. Sci.* **1988**, *43*, 31.
18. Weferling, N., Neue Methoden zur Chlorierung von Organophosphorverbindungen mit P-H-Funktionen. *Zeitschrift für anorganische und allgemeine Chemie* **1987**, *548*, 55.
19. Boymond, L.; Rottländer, M.; Cahiez, G.; Knochel, P., Preparation of Highly Functionalized Grignard Reagents by an Iodine–Magnesium Exchange Reaction and its Application in Solid-Phase Synthesis. *Angew. Chem., Int. Ed.* **1998**, *37*, 1701.
20. Knochel, P.; Dohle, W.; Gommermann, N.; Kneisel, F. F.; Kopp, F.; Korn, T.; Sapountzis, I.; Vu, V. A., Highly Functionalized Organomagnesium Reagents Prepared through Halogen–Metal Exchange. *Angew. Chem., Int. Ed.* **2003**, *42*, 4302.
21. Kalachnikova, E. Improved Synthesis, Separation, Transition Metal Coordination and Reaction Chemistry of a New Binucleating Tetrphosphine Ligand. Ph.D. Dissertation, Louisiana State University, Baton Rouge, LA, 2015.
22. (a) Cano, M.; Heras, J. V.; Ovejero, P.; Pinilla, E.; Monge, A., Heterobimetallic Group 6 Rhodium Complexes: I. Formation of tribridges derivatives [(OC)₃M(μ-Cl)(μ-CO)(μ-dppm)Rh(NBD)] (M = Mo, W) by ring opening of [(CO)₄M(dppm-PP)]. Crystal structure of [(CO)₃Mo(μ-Cl)(μ-CO)(μ-dppm)Rh(NBD)]. *J. Organomet. Chem.* **1991**, *410*, 101; (b) Robertson, J. J.; Kadziola, A.; Krause, R. A.; Larsen, S., Preparation and Characterization of Four- and Five-Coordinate Rhodium(I) Complexes. Crystal structures of Chloro(2-phenylazo)pyridine)(norbornadiene)rhodium(I), (2,2'-

bipyridyl)(norbornadiene)rhodium(I) chloride hydrate, and Chloro(2,2'-bipyridyl)(norbornadiene)rhodium(I). *Inorgo. Chem.* **1989**, *28*, 2097.

Chapter 3: Hydroformylation and Aldehyde-Water Shift Catalysis

3.1 Introduction

The Stanley group has been studying bimetallic cooperativity, especially in regards to hydroformylation. The group designed and prepared a tetrakisphosphine ligand *et,ph-P4* that binds two metal centers and orients them in such a way that they can interact with each other.¹ The $[\text{Rh}_2(\text{nbd})_2(\text{rac-}et,ph\text{-P4})](\text{BF}_4)_2$ catalyst precursor is believed to react with syn-gas and shift to a closed-mode orientation forming the hydrido-carbonyl catalyst $[\text{Rh}_2(\mu\text{-H})_2(\text{CO})_4(\text{rac-}et,ph\text{-P4})]^{2+}$ (Figure 3.1).^{2,3} This catalyst has better rates and selectivity compared to the commercial Rh/PPh₃ system including an initial TOF of 20 min⁻¹, 25:1 L:B aldehyde regioselectivity, and low byproducts of 2.5 % alkene isomerization and 3.4 % hydrogenation in an acetone solvent.

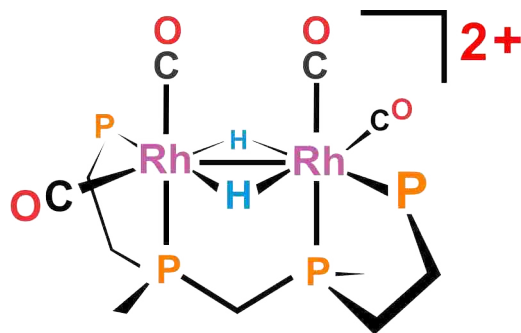


Figure 3.1. $[\text{Rh}_2(\mu\text{-H})_2(\text{CO})_4(\text{rac-}et,ph\text{-P4})]^{2+}$

The work to determine the nature of the catalyst and a mechanism for the catalytic cycle has taken over 25 years. The *in situ* FT-IR and NMR studies started in 1994 and lead to the formulation of the bimetallic catalyst as a dicationic Rh(II) species, not a neutral Rh(I) hydride as was originally proposed⁴ The FT-IR studies were particularly useful in showing the presence of both bridging carbonyls (1819 cm⁻¹ and 1834 cm⁻¹) and terminal carbonyls (between 1971 cm⁻¹ – 2095 cm⁻¹). The ¹H NMR studies in acetone-d₆ showed the existence of a hydrides at –5.6 ppm,

–6.3 ppm, –8.8 ppm, and –15.2 ppm at low temperature (Figure 3.2). COSY experiments demonstrated that these hydrides belong to three different rhodium complexes.

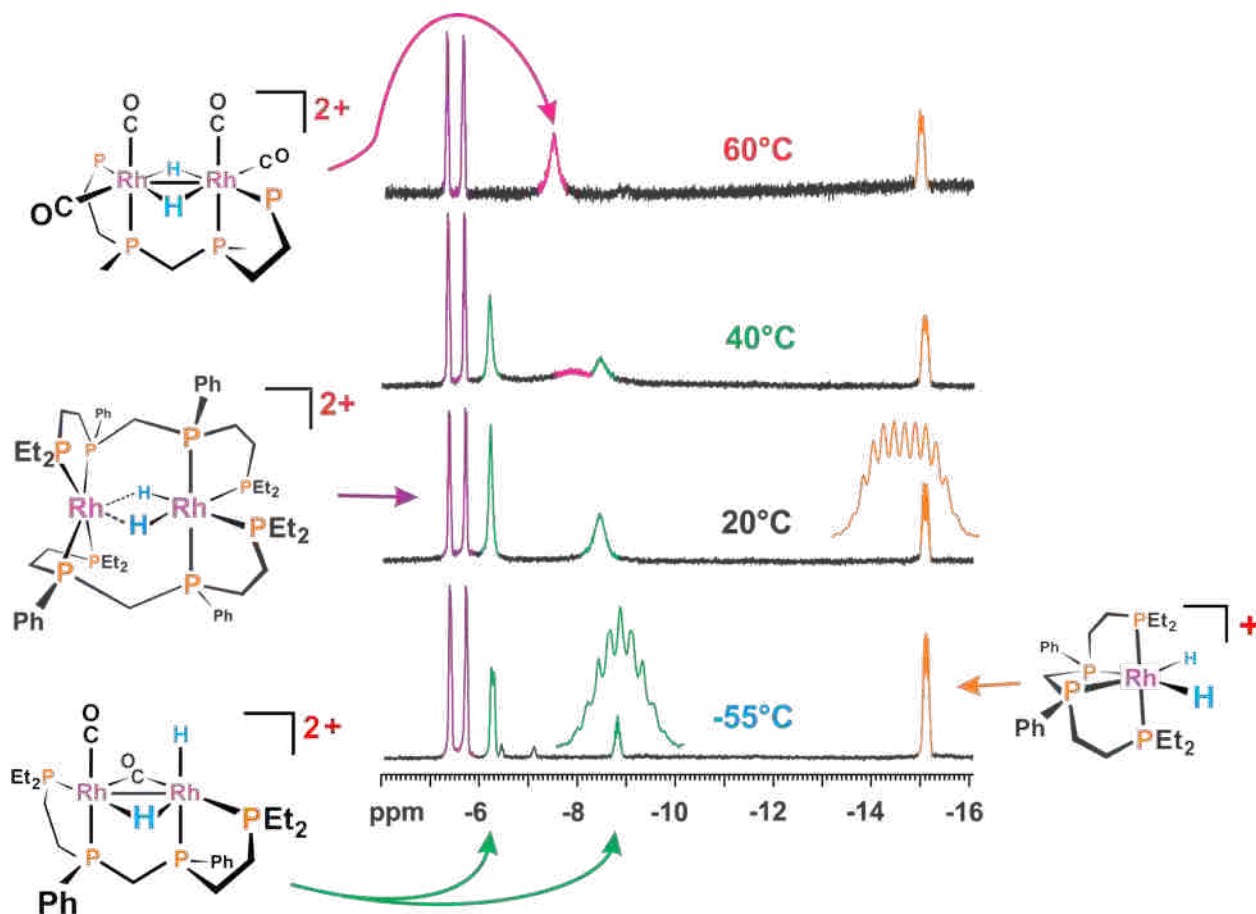


Figure 3.2. ^1H NMR of the hydride region of the mixture of complexes formed when $[\text{Rh}_2(\text{nbd})_2(\text{rac-}i\text{-et,ph-P4})]^{2+}$ is put under 200 psig of H_2/CO in acetone- d_6 .

The Stanley group mistakenly assigned the –5.6 ppm doublet of quartets as the dirhodium dihydride catalyst. Although they did extensive ^{31}P NMR decoupling experiments, they never got the 164 Hz coupled doublet to collapse. They, therefore, assigned this 164 Hz coupled pattern as Rh-H coupling. Polakova, however, showed later that this was P-H coupling, and assigned this as the double-P4 coordinated dirhodium dihydride complex, $[\text{Rh}_2\text{H}_2(\text{rac-P4})_2]^{2+}$, which forms from the fragmentation of the active dirhodium catalyst.⁵ This bis-*et,ph-P4* coordinated dirhodium species is inactive for hydroformylation.

The hydride resonance at -15.2 ppm is due to monometallic $[\text{RhH}_2(\kappa^4\text{-rac-P4})]^+$, which also is formed from the fragmentation of the dirhodium catalyst. This is a saturated 18 electron species that is very stable and unreactive. It represents the thermodynamic sink for catalyst decomposition. Finally, the low temperature hydride resonances at -6.3 and -8.8 ppm are due to the lowest energy isomer of the dirhodium catalyst, $[\text{Rh}_2\text{H}(\mu\text{-H})(\mu\text{-CO})(\text{rac-P4})]^{2+}$. The -6.3 ppm hydride is terminal, while the -8.8 ppm hydride is bridging with coupling to the two rhodium centers, at least three of the four phosphines, and the terminal hydride. The terminal hydride is not fully resolved at -55 °C. Both hydride resonances broaden as the temperature is raised to 20 °C. At 40 °C a new hydride resonance appears at -7.9 ppm, while the other two hydride resonances decrease in intensity. At 60 °C the -6.3 and -8.8 ppm resonances have disappeared, and have been replaced by a new broad hydride resonance at -7.5 ppm. Prof. Stanley believed for almost 20 years that this represented the symmetrical dirhodium species with two terminal hydrides and two bridging carbonyls.

An FT-IR study performed by Alexander used only CO pressure to study the carbonyl complexes that initially form in the absence of H_2 (Figure 3.3).⁵ The $[\text{Rh}_2(\text{nbd})_2(\text{rac-P4})]^{2+}$ catalyst precursor is extremely reactive to CO even at very low pressures. The carbonyl band at 2015 cm^{-1} represents the addition of a CO ligand to each Rh center of the catalyst precursor to form $[\text{Rh}_2(\text{nbd})_2(\text{CO})_2(\text{rac-P4})]^{2+}$. As the CO pressure and temperature increases, this complex loses the norbornadiene ligands completely to form the dirhodium pentacarbonyl complex, $[\text{Rh}_2(\text{CO})_5(\text{rac-P4})]^{2+}$. Interestingly no sign of the tetracarbonyl species is seen. This indicates that the dirhodium tetracarbonyl is quite reactive to CO and favors the pentacarbonyl complex. When the experiment was complete, colorless clear crystals lined the bottom of the autoclave. These were found to be a polymer of norbornadiene.

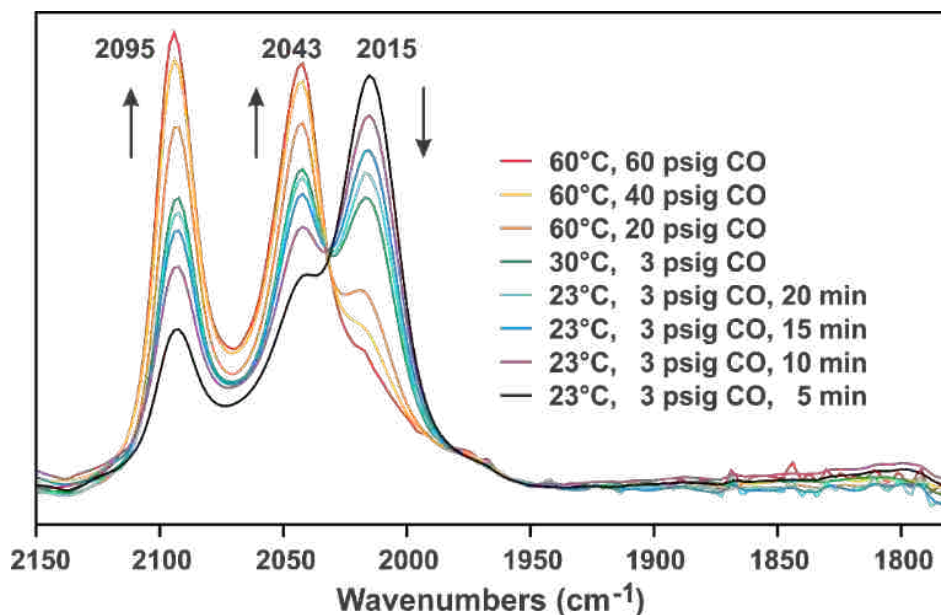


Figure 3.3. Stacked *in situ* FT-IR spectra of $\text{Rh}_2(\text{nbd})_2(\text{rac-et,ph-P4})](\text{BF}_4)_2$ under CO pressure

The reaction of $[\text{Rh}_2(\text{nbd})_2(\text{rac-P4})]^{2+}$ with 1:1 H_2/CO is shown in Figure 3.4. This was a recent study that I did with Prof. Stanley testing the new nitrogen-purged SpectraTech high pressure silicon-crystal ATR cell system that gives considerably better signal to noise relative to the unpurged configuration. At lower pressures (5 psig) the main species seen is the open-mode pentacarbonyl, $[\text{Rh}_2(\text{CO})_5(\text{rac-P4})]^{2+}$, with CO bands at 2094 and 2043 cm^{-1} . As the pressure increases CO bands at 2012, 1986, and 1949 cm^{-1} grow in, but then decrease as the temperature increases. Bridging CO bands at 1832 and 1820 cm^{-1} grow in as the temperature increases.

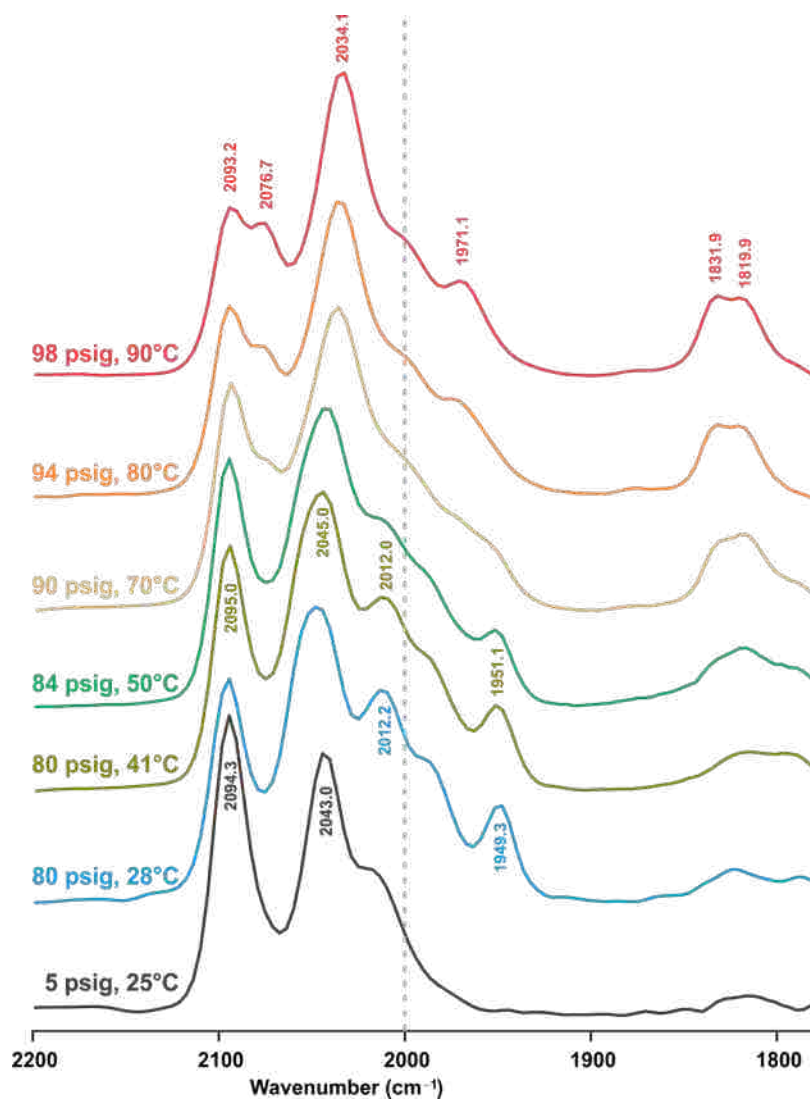


Figure 3.4. *In situ* FT-IR of the carbonyl region for $[\text{Rh}_2(\text{nbd})_2(\text{rac-P4})]^{2+}$ under 1:1 H_2/CO at various pressures and temperatures

The presence of the two bridging CO bands led Prof. Stanley to originally assign the catalyst as $[\text{Rh}_2\text{H}_2(\mu\text{-CO})_2(\text{CO})_2(\text{rac-et,ph-P4})]^{2+}$. Although there are no studies comparing the reactivity of bridging against terminal hydride ligands for a migratory insertion with an alkene ligand, the vast majority of organometallic chemists believe that terminal hydrides are more reactive than bridging hydrides. Prof. Stanley fell into this camp, which is why he proposed the higher temperature symmetrical hydride species from the NMR studies to be the terminal

dihydride. The two bridging carbonyl bands seen in the FT-IR appeared to support this proposed structure.

Dr. Zakyia Wilson did the first DFT calculations on these dirhodium catalyst species.⁶ Dr. Wilson's DFT calculations on four of the most likely isomeric structures for a dirhodium dihydride complex are shown in Figure 3.5. The calculated lowest energy isomer is the dirhodium complex with the one bridging and one terminal hydride, which is confirmed by the low temperature NMR study. The next highest energy isomer, by 1.5 Kcals, is the symmetrical species with two bridging hydrides. The complex with two terminal hydrides is 12.5 Kcals higher in energy and highly unlikely to play a role in catalysis.

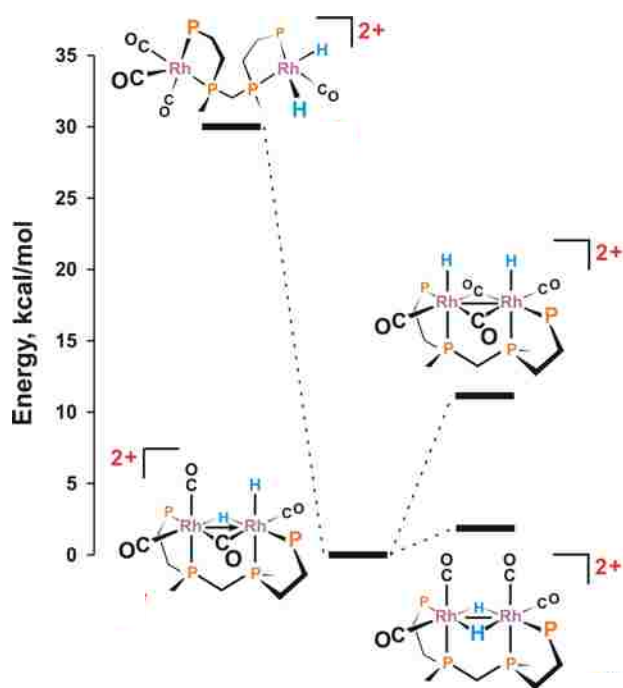


Figure 3.5. DFT relative energies for four different dirhodium dihydride isomers

Prof. Stanley, however, continued to believe that the terminal dihydride complex was the most likely catalyst species involved in the catalysis until Ranelka Fernando redid all the DFT calculations along with careful transition-state energy calculations for the mechanistic steps using the three lowest energy isomers.^{2,3} Dr. Fernando once again found the energy for the di-

bridging hydrides was considerably lower than that of the terminal hydride complex. The calculated relative energies from Dr. Fernando's DFT calculations are shown in Figure 3.6.

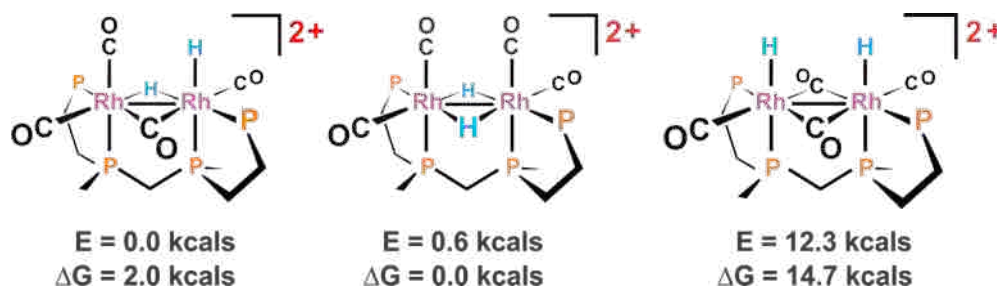


Figure 3.6. DFT relative energies for the three different closed-mode dirhodium dihydride isomers

Once again, the NMR work demonstrates that the lowest energy hydride is the bridged/terminal species. The electronic energy appears to predict this better than the zero point corrected ΔG energy. The bridged dihydride complex is only 0.6 Kcals higher in energy, which corresponds well to the variable temperature NMR that shows a new symmetrical hydride species at 60 °C. Once again, the terminal dihydride is significantly higher in energy and unlikely to play a role in catalysis.

What really convinced Prof. Stanley as to the importance of the bridged dihydride complex in the catalysis was Dr. Fernando's transition state calculations for the migratory insertion of alkene with the bridging vs. terminal hydride complexes. The energy barrier for the migratory insertion of the alkene with the bridging dihydride catalyst was a low 8.0 kcal/mol vs. 23.2 kcal/mol for the terminal dihydride (Figure 3.7). A similar trend was seen in her calculations on the monocationic monohydride dirhodium catalyst that forms in water. The consistency of these two calculations and re-examination of the spectroscopic data finally convinced Prof. Stanley that the bridging hydride species was indeed the key catalyst that reacts with alkene and starts the hydroformylation cycle.

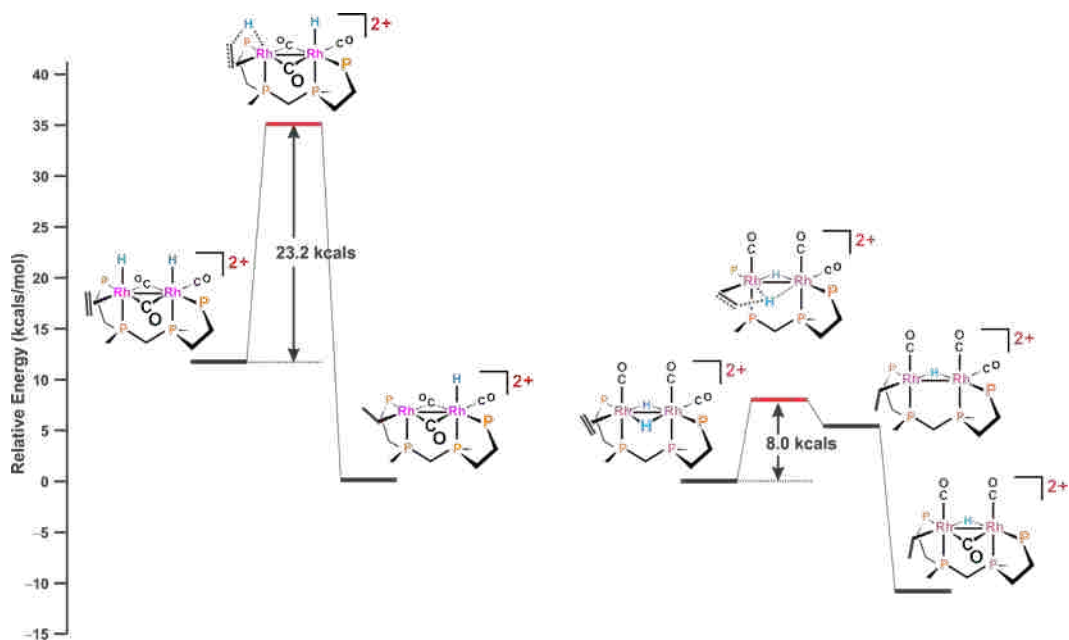


Figure 3.7. DFT transition state energies for the migratory insertion of an alkene with terminal and bridging hydrides

Our currently proposed hydroformylation cycle based on the dihydride bridged catalyst is shown in Figure 3.8. Starting with the active catalyst, a carbonyl dissociates from a rhodium center to allow for the addition of the olefin. A migratory insertion of a hydride to the olefin forms a linear alkyl ligand. A second migratory insertion of the terminal carbonyl and alkyl ligands creates the linear acyl group, and an additional carbonyl binds to the rhodium center. With a more electron-poor environment, the reductive elimination of the acyl group and the remaining bridging hydride leads to the production of the aldehyde. Several conformational changes occur in which the carbonyls move to bridging positions. The association of a carbonyl breaks open the system to an asymmetric pentacarbonyl complex. A carbonyl dissociates from a rhodium center as oxidative addition of H_2 takes place on the same center. With a final dissociation of a carbonyl, the terminal hydrides move to bridging positions, which closes the system and reforms the catalyst.

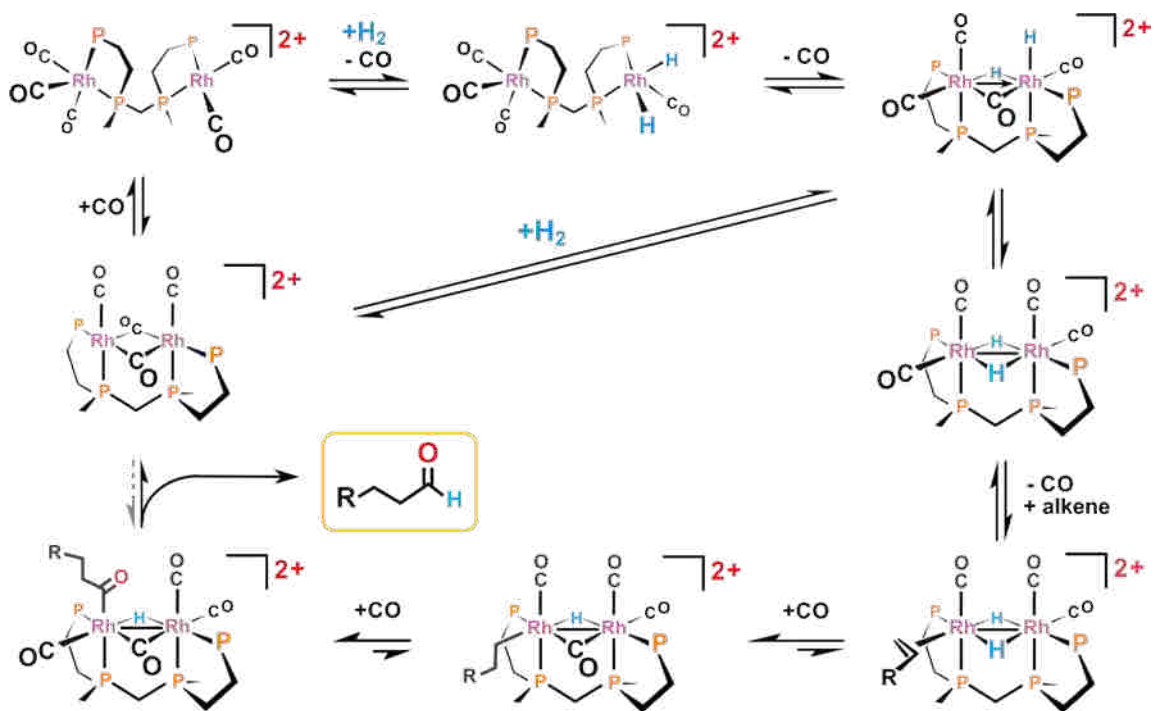


Figure 3.8. Proposed hydroformylation mechanism of $[\text{Rh}_2(\mu\text{-H})_2(\text{CO})_4(\text{rac-et,ph-P4})]^{2+}$

What is not shown in the mechanism is that the phosphine chelate arm is dissociating and reassociating. The broad resonances for the catalyst complex in the ^{31}P NMR support this on-off dissociation. Unfortunately, this phosphine-arm dissociation leads to catalyst fragmentation and deactivation, especially when alkene is not present. For example, letting the catalyst sit under reaction conditions (90 °C, 90 psig 1:1 H_2/CO , acetone solvent) without any alkene leads to complete deactivation of the catalyst after 80 mins. We believe there is a good bit of catalyst deactivation during the heating of the autoclave to reach operational conditions prior to injection of the alkene substrate to initiate hydroformylation.

In hopes to alleviate the classic homogeneous catalysis problem of separating the catalyst from the product, Bridges and Aubry tested the addition of the water to the acetone solvent to generate a very polar solvent from which heptaldehyde would phase separate.^{1,9} Although the heptaldehyde did phase separate from the very polar solvent, the dirhodium catalyst was actually

more soluble in the aldehyde product phase than the water/acetone layer. But, it was noted that a 30 % water/acetone system gave increased turnovers and higher selectivity as well as a decrease in the formation of side products from alkene isomerization and hydrogenation. The reasons for this increase in rate and selectivity described in their paper are not correct.

Almost 10 years passed before research in our group showed that deprotonation of one of the rhodium centers leads to a monocationic monohydride dirhodium catalyst system, $[\text{Rh}_2(\mu\text{-H})(\text{CO})_2(\text{rac-P4})]^+$. The more electron-rich rhodium centers in this catalyst should produce a catalyst that has lower activity due to the stronger coordination of the carbonyl ligands that can block empty coordination sites needed for binding the alkene and H_2 . We believe that the lower positive charge on the rhodium centers favors stronger coordination of the phosphines, far less chelate arm dissociation, and far less catalyst fragmentation and deactivation. This increases the amount of active bimetallic catalyst present in solution, which compensates for the lower activity of the monocationic catalyst.

The presence of cationic metal centers plays an important role in the phosphine dissociation. The phosphorus atom in a phosphine has a partial positive charge and this provides an electrostatic repulsion energy component when dealing with a metal center with a cationic charge. A DFT calculation on PMe_3 , for example, shows a Mulliken charge on phosphorus of +0.22. Donation of the phosphorus lone pair to a metal center increases the positive charge even more, along with an increased electrostatic repulsion with a positively charged metal center.

Walton and coworkers demonstrated that cationic dirhenium complexes readily dissociated phosphine ligands and coordinate chlorides (or bromides) to form neutral complexes.⁸ Reduction to make anionic rhenium dimers, on the other hand, favored dissociation of chlorides (or bromides) and coordination of phosphines, once again favoring the formation of

neutral dimer complexes. Facile phosphine dissociation from the rhenium centers occurred even with alkylated phosphines like PEt_3 . We believe the dicationic catalyst has enough localized positive charge residing on the rhodium centers to electrostatically weaken the Rh-P bonding and favor phosphine arm dissociation, which leads to catalyst fragmentation and deactivation.

Like the dicationic system, the monocationic one has been studied by *in situ* FT-IR and NMR. The bridging carbonyls in the acetone/water solvent are weaker in intensity and have slight shifts to lower wavenumbers, but the terminal peaks move considerably to lower frequencies by about 20 cm^{-1} . This shift points to a deprotonated monocationic complex that is more electron-rich. The ^1H NMR studies show a single broad resonance at -10.8 ppm ; believed to a hydride in dynamic equilibrium between a terminal and bridging position. A small hydride peak is also seen at -18.5 ppm , which is the monometallic fragmentation complex $[\text{RhH}_2(\kappa^4\text{-rac-P4})]^+$. The low intensity of this fragmentation product, coupled with no sign of the double-ligand coordinated dirhodium fragmentation complex, points to the stability of the monocationic dirhodium catalyst.

DFT calculations were performed on proposed structures of the deprotonated catalyst, and a mechanism for the hydroformylation was proposed (Figure 3.9).

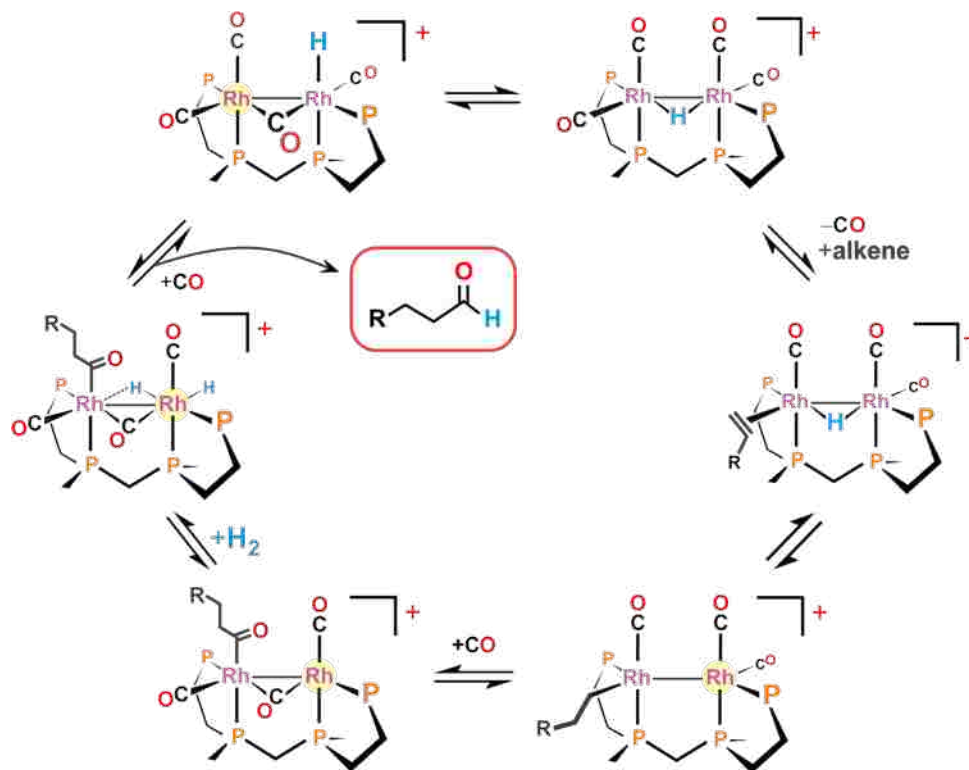


Figure 3.9. Proposed hydroformylation mechanism for $[\text{Rh}_2(\mu\text{-H})(\text{CO})_4(\text{rac-ct,ph-P4})]^+$, Rhodium centers highlighted in yellow are formally cationic and will have more labile carbonyl ligands.

Once again starting with the active catalyst, dissociation of a carbonyl and addition of the olefin to the same site occurs first. Next, the migratory insertion of the hydride and olefin form the linear alkyl ligand. A second migratory insertion of the alkyl ligand and the adjacent carbonyl form an acyl group, and another carbonyl adds to the open coordination site on the same rhodium. H_2 oxidatively adds to the second rhodium center, and rearranges to form a terminal and bridging hydride. The bridging hydride and the acyl group reductively eliminate to produce the aldehyde. A carbonyl adds to the complex and undergoes some conformational changes. This final complex has a small energy barrier to switch to the bridging hydride complex.

In Bridges and Aubry's water/acetone hydroformylation research, they also discovered a new reaction caused by a leak in their autoclaves that allowed H₂ to escape at a faster rate than CO leaving the system H₂ deficient. As a result, the aldehyde they were producing was converted into carboxylic acid via reaction with water. This also produced H₂ as the other product. When they finally noticed the leak, and fixed the autoclave, the reaction did not occur – just hydroformylation.

Prof. Stanley suggested running regular hydroformylation of 1-hexene for 10 minutes at which point the H₂/CO gas to the autoclave was turned off. The reservoir containing the H₂/CO mixture was vented, flushed with pure CO several times, and then pressurized with pure CO. While this was occurring the residual H₂/CO present in the autoclave was depleted via hydroformylation of the remaining alkene. This generated H₂-depleted conditions that shifted the catalyst equilibrium away from the hydride containing catalyst that was active for hydroformylation to a dirhodium complex with just carbonyls and our P4 ligand. This started aldehyde-water shift catalysis to produce carboxylic acid and H₂. Reopening the autoclave around this time to the pure CO kept the CO concentration high enough to maintain the dirhodium carbonyl species. The buildup of H₂ from the aldehyde-water shift catalysis reaction, however, shifted the catalyst equilibrium back to the hydride-containing complexes and stopped the aldehyde-water shift catalysis. Unfortunately, this reaction turned out to be very sensitive to the exact reaction conditions and proved to be difficult to reproduce consistently.

Barnum later reworked the autoclave system as well as the procedure for running the reactions to allow for some reproducibility, although with fewer turnovers than Bridges and Aubry had observed.⁹ I took over both the dirhodium hydroformylation and aldehyde-water shift

(AWS) catalysis projects, especially in regards to studying the new stronger coordinating *et,ph-P4-Ph* ligand.

3.2 Results and Discussion

3.2.1 Polar Phase Hydroformylation using Water-Solvent Mixtures

Studying the new $[\text{Rh}_2(\text{nbd})_2(\text{rac-}et,ph\text{-P4-Ph})](\text{BF}_4)_2$ catalytic precursor for hydroformylation was important because it should be far more resistant to fragmentation reactions, especially in its dicationic form. Most of my initial catalyst work was with the “old” *rac-}et,ph-P4* based dirhodium catalyst in order to learn how to use the autoclaves and analyze the products via GC/MS and NMR. An early problem that I encountered was an impurity that was leading to very poor hydroformylation results for 1-hexene, our standard test alkene. This was finally tracked down to a new batch of alumina that we use to remove peroxide impurities from 1-hexene. The alumina needed to be deactivated by the addition of the proper amount of water. The old alumina we were using had picked up enough water from the lab’s humidity, but the group didn’t realize this. So the new “dry” batch of alumina was not properly cleaning our alkene until it was deactivated by the proper amount of water. I prepared a new procedure for this for future students. I was now getting reasonably good and consistent results for the monocationic dirhodium catalyst based on the *rac-P4* ligand in 30% water/acetone: initial turnover frequency of 27 min^{-1} , L:B selectivity of 27:1, 4.6 % isomerization, and 1.3 % hydrogenation .

Hydroformylation with the new $[\text{Rh}_2(\text{nbd})_2(\text{rac-}et,ph\text{-P4-Ph})](\text{BF}_4)_2$ complex was now attempted. Initially, no reactivity occurred for this catalyst precursor. As the material was difficult to recrystallize in acetone, along with other solvents, an impure catalyst was used for these reactions, and it was believed that this caused the failure in reactivity. Prof. Stanley

suggested using a different counter anion that might allow for better recrystallization and purification.

PF₆ was selected as it was believed to work fine with the “old” *rac*-*et*,*ph*-P4 based dirhodium catalyst and provided a ³¹P NMR handle that might prove useful in characterizing the catalyst precursor. The procedure to produce the BF₄ salt by Broussard was used with the exchange of HBF₄ for HPF₆ to remove the acetylacetonate from Rh(acac)(nbd) to make [Rh(nbd)₂]PF₆.¹⁰ The reactivity of Rh(acac)(nbd) and HPF₆ was similar and allowed the exchange of the acetylacetonate for norbornadiene yielding the desired complex as determined by ¹H NMR (Figure 3.10).

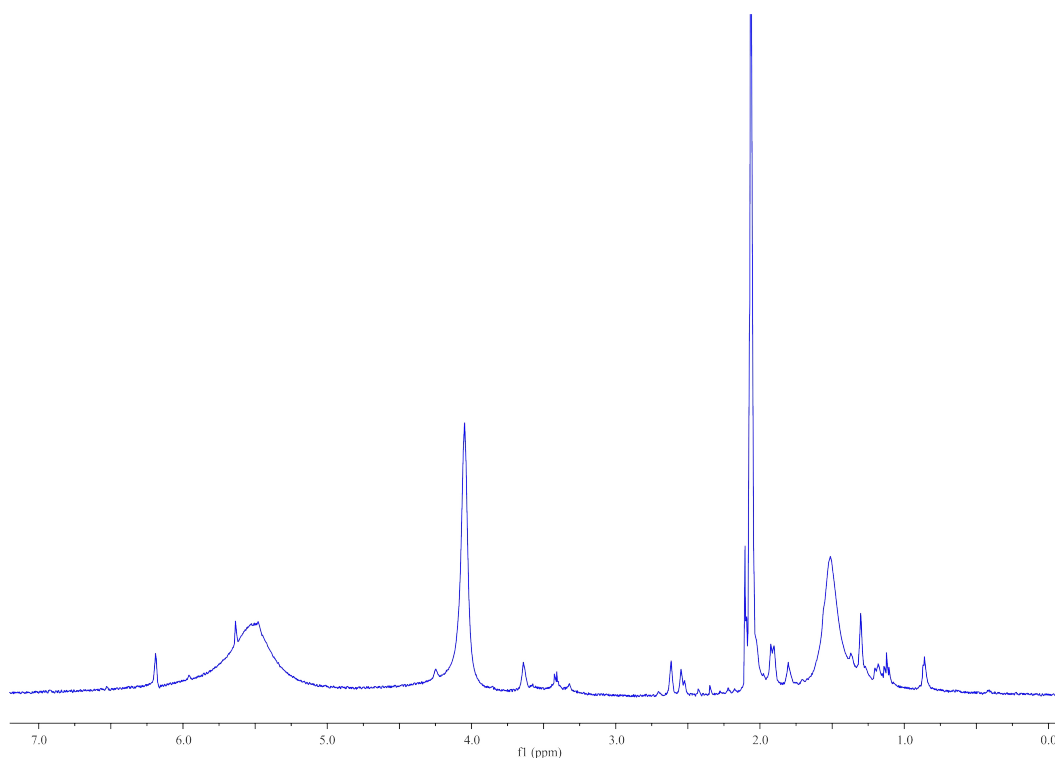


Figure 3.10. ¹H NMR of [Rh(nbd)₂]PF₆ in DCM-d₂

The reaction of the [Rh(nbd)₂]PF₆ with the *et*,*ph*-P4-Ph ligand proceeded as before and both ¹H NMR and ³¹P{¹H} NMR was used to confirm the formation of [Rh₂(nbd)₂(*rac*-*et*,*ph*-P4-Ph)](PF₆)₂ (Figure 3.11, Figure 3.12).

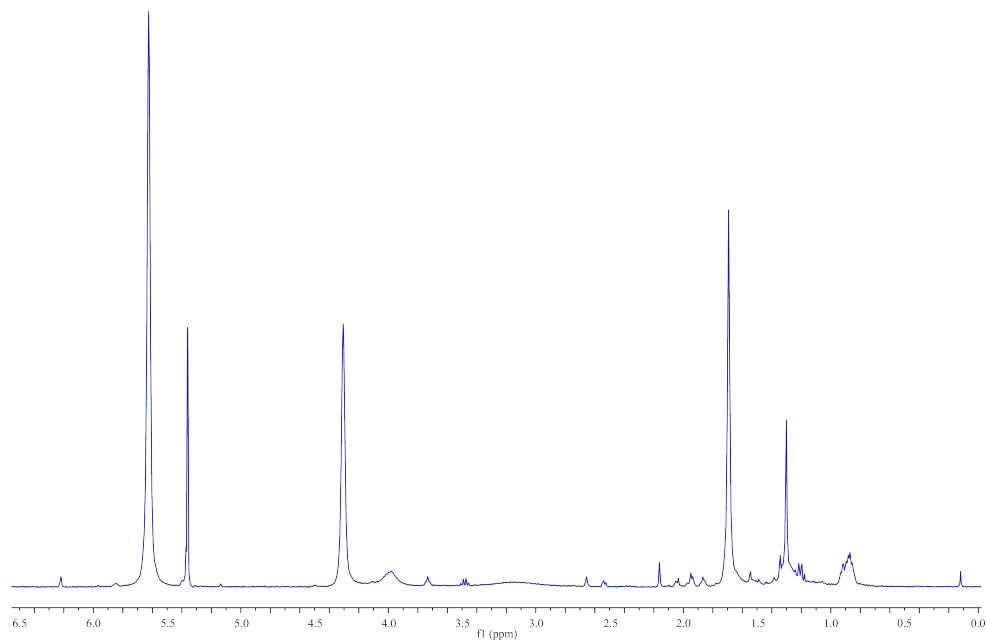


Figure 3.11. ^1H NMR of $[\text{Rh}_2(\text{nbd})_2(\text{rac-et,ph-P4-Ph})](\text{PF}_6)_2$ in DCM-d_2

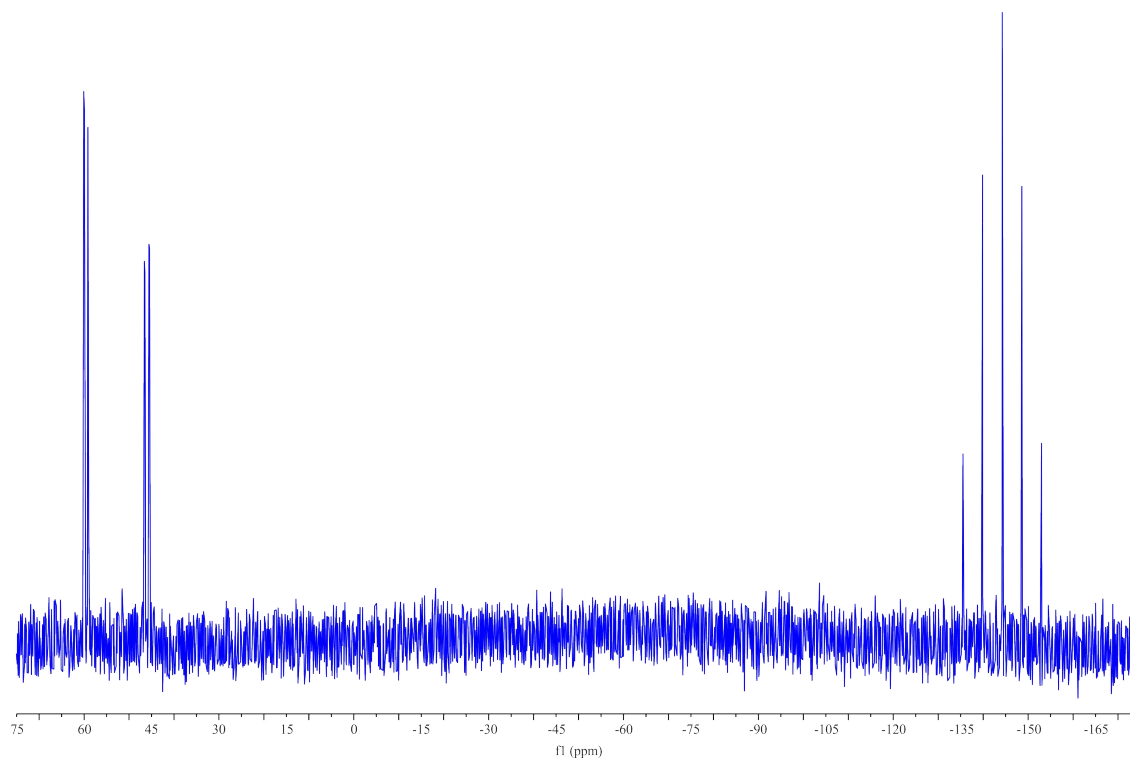


Figure 3.12. $^{31}\text{P}\{^1\text{H}\}$ NMR (bottom) of $[\text{Rh}_2(\text{nbd})_2(\text{rac-et,ph-P4-Ph})](\text{PF}_6)_2$ in DCM-d_2

The recrystallization of the new PF₆ salt was found to occur far more easily than the BF₄ salt. A slew of microcrystals would form within minutes of being dissolved in DCM. Though not ideal, these crystals were determined to be pure [Rh₂(nbd)₂(*rac*-*et*,*ph*-P4-Ph)](PF₆)₂ from X-ray crystallography.

When running the dried crystals in hydroformylation in acetone/water, the initial TOF of 19 min⁻¹ for the reaction was lower than the old [Rh₂(nbd)₂(*rac*-*et*,*ph*-P4)](BF₄)₂ catalyst precursor. We also found that the L:B selectivity dropped to 14:1 (compared to 28:1 for the old catalyst), and alkene isomerization started at 6.6 % and increased to 11.4 % over the course of the reaction. To further examine this anion effect, the PF₆ salt of the old catalyst was prepared and tested for hydroformylation. Similar to the new complex also in acetone/water, [Rh₂(nbd)₂(*rac*-*et*,*ph*-P4)](PF₆)₂ gave a lower TOF of 24 min⁻¹, slightly lower L:B selectivity of 26:1, and higher isomerization with initial levels of 5.3 % that rose to 10.9 %.

3.2.2 *In Situ* and Variable Temperature NMR Studies of [Rh₂(nbd)₂(*rac*-*et*,*ph*-P4-Ph)](PF₆)₂ and [Rh₂(nbd)₂(*rac*-*et*,*ph*-P4-Ph)](BF₄)₂

While examining the PF₆ salt for hydroformylation, we studied the *in situ* NMR under H₂/CO pressure. Following the procedures from Matthews and Alexander, the ¹H NMR and ³¹P{¹H} NMR were studied at -60 °C and room temperature (~20 °C).^{11, 12} The sample was initially dissolved in acetone-d₆ in a Wilmad “high-pressure” NMR tube. The tube was flushed of gas and filled with 120 psig of H₂/CO. After the NMR probe was cooled to -60 °C, the instrument started collecting data on the sample. Figure 3.13 shows the data for the ¹H NMR of the hydride region and the ³¹P NMR in figure 3.14.

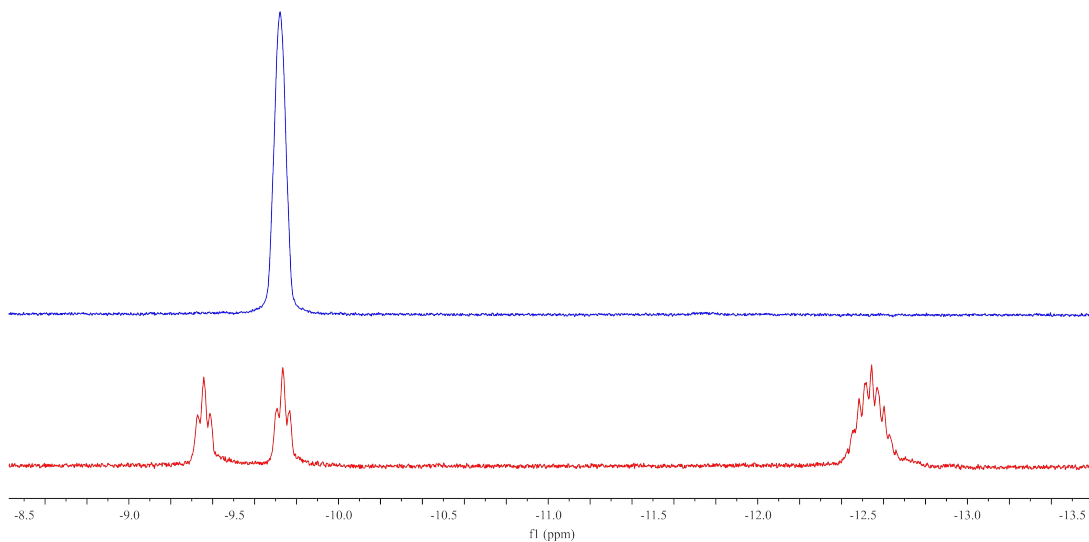


Figure 3.13. *In situ* ^1H NMR of the hydride region for $[\text{Rh}_2(\text{nbd})_2(\text{rac-et,ph-P4-Ph})](\text{PF}_6)_2$ at $-60\text{ }^\circ\text{C}$ (bottom) and $20\text{ }^\circ\text{C}$ (top) in acetone- d_6

The ^1H NMR at $-60\text{ }^\circ\text{C}$ contains a doublet of triplets centered at -9.6 ppm ($J_{\text{H-P}} = 151.1\text{ Hz}$, $J_{\text{H-H}} = 13.0\text{ Hz}$) and a triplet of triplets centered at -12.5 ppm ($J_{\text{H-H}} = 23.4\text{ Hz}$, $J_{\text{H-Rh}} = 11.6\text{ Hz}$). The *trans*- $J_{\text{H-P}}$ coupling indicates a terminal phosphine, which assigns it to the peaks centered at -9.6 ppm peaks. The “old” et,ph-P4 precursor does not show this coupling: likely from the dissociation of the terminal hydride. The bridging hydride is assigned to the -12.5 ppm peaks. When the sample is warmed to room temperature, the terminal and bridging hydrides coalesce to a single resonance at -9.7 ppm , which is likely the species with only bridging hydrides. An additional study of the hydride region of the $[\text{Rh}_2(\text{nbd})_2(\text{rac-et,ph-P4-Ph})](\text{PF}_6)_2$ precursor after an hour’s time shows no hydrides in the same sample. This was believed to be caused by H-D exchange between the rhodium hydride and the acetone- d_6 .

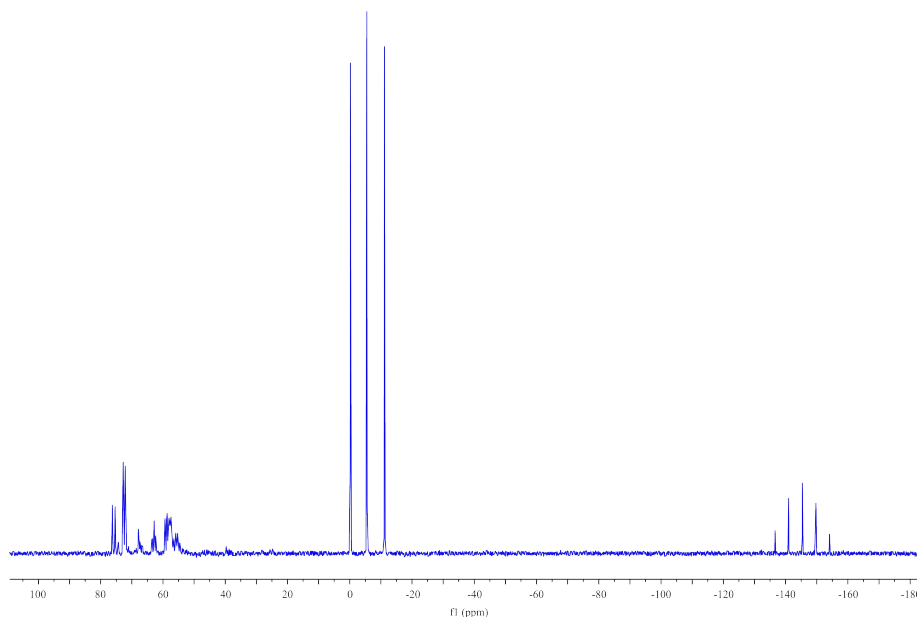


Figure 3.14. *In situ* $^{31}\text{P}\{^1\text{H}\}$ NMR $\text{Rh}_2(\text{nbd})_2(\text{rac-}et,\text{ph-P4-Ph})(\text{PF}_6)_2$ at $20\text{ }^\circ\text{C}$ (top) in acetone- d_6

The $^{31}\text{P}\{^1\text{H}\}$ NMR was not obtained for the lower temperature study. At room temperature, the septet at -145.5 ppm is due to the PF_6^- anion. The peaks ranging from 54 to 76 ppm are related to different dirhodium complexes. The triplet at -5.5 ppm is the $[\text{PF}_2\text{O}_2]^{2-}$ dianion formed from PF_6^- anion.

It was later found that rhodium is activated by the PF_6^- anion in acetone systems.¹³ The PF_6^- can undergo solvolysis with the acetone to produce a $[\text{PF}_2\text{O}_2]^{2-}$ dianion. The oxygens are presumed to be from the acetone solvent, perhaps producing 2,2-difluoropropane. The reactivity of the PF_6^- and acetone lead us to forgo our studies with the PF_6^- salt.

Although the PF_6^- anion is believed to interfere with hydroformylation, a study was performed in which the $[\text{Rh}_2(\text{nbd})_2(\text{rac-}et,\text{ph-P4-Ph})(\text{PF}_6)_2$ precursor was pressurized with 120 psig of H_2/CO in acetone- d_6 . Initially, broad resonances are seen at 59 and 74 ppm identified as the dynamic equilibrium of the bridging and terminal hydride species (Figure 3.15). After a week under pressure, those same resonances are still seen. If put under the same conditions, the

“old” $[\text{Rh}_2(\text{nbd})_2(\text{rac-}i\text{et,ph-P4})]^{2+}$ catalyst precursor would begin to deteriorate in an hour. The stability of the new $[\text{Rh}_2(\text{nbd})_2(\text{rac-}i\text{et,ph-P4-Ph})]^{2+}$ complex far exceeds the previous catalyst precursor, which gave hope for continued research without the PF_6^- anion.

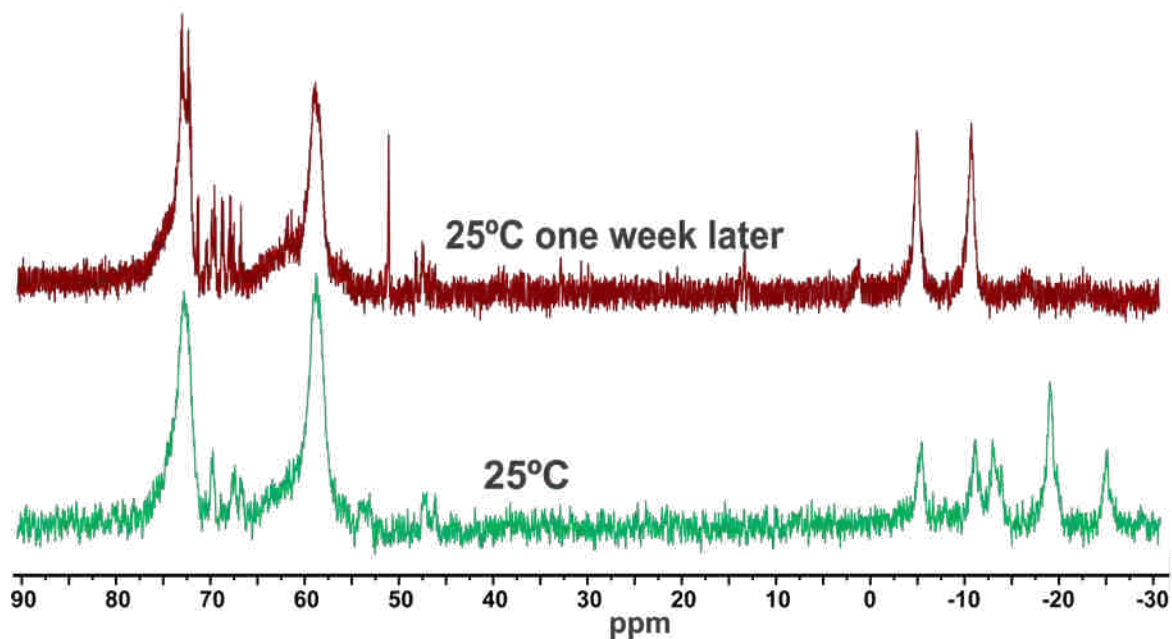


Figure 3.15. *In situ* $^{31}\text{P}\{^1\text{H}\}$ NMR of $[\text{Rh}_2(\text{nbd})_2(\text{rac-}i\text{et,ph-P4-Ph})](\text{PF}_6)_2$ in acetone-d_6

After consideration of the solvolysis of PF_6^- and acetone as well as the H-D exchange of the rhodium hydride and acetone- d_6 , Prof. Stanley proposed a mechanism for the H-D exchange that might help to explain the activation of acetone (Figure 3.16).

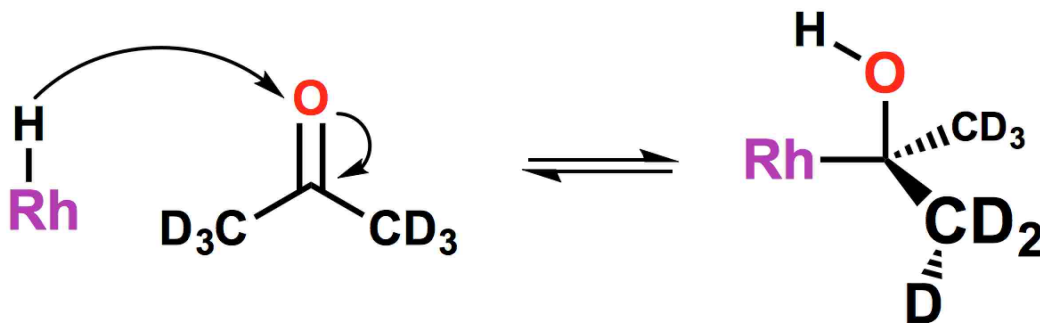


Figure 3.16. Proposed mechanism of H-D exchange

The hydride would attack the oxygen of the acetone-d₆, which in turn would break the double bond to the carbon. This produces a carbanion that can bind rhodium. Once bound, the rhodium can undergo β-hydride elimination with either one of six deuterium atoms or the original hydride. If any deuterium β-hydride eliminates, the exchange process has occurred producing the enol form of acetone that can tautomerize to acetone-d₅. In this process, the enol-acetone is a more active species that could more readily react with PF₆ to form the [PF₂O₂]²⁻ dianion.

After these studies, we believe we may have an explanation for the decomposition, and chose to return to the BF₄ salt for hydroformylation. To avoid any potential degradation, acetone was initially excluded from all research as the Rh₂(nbd)₂(*rac*-et,ph-P4-Ph)](BF₄)₂ precursor was able to activate it for H-D exchange and could lead to deterioration from interaction with PF₆. As Rh₂(nbd)₂(*rac*-et,ph-P4-Ph)](BF₄)₂ could not be crystalized, a crude sample was used in a similar study to the one above dissolved in DMF-d₇. The study was done beginning at -50 °C and moved to -30 °C, 0 °C, 30 °C, 60 °C, and 90 °C. Figure 3.17 illustrates the data of the hydride region for the ¹H NMR and figure 3.18 for ³¹P{¹H} NMR.

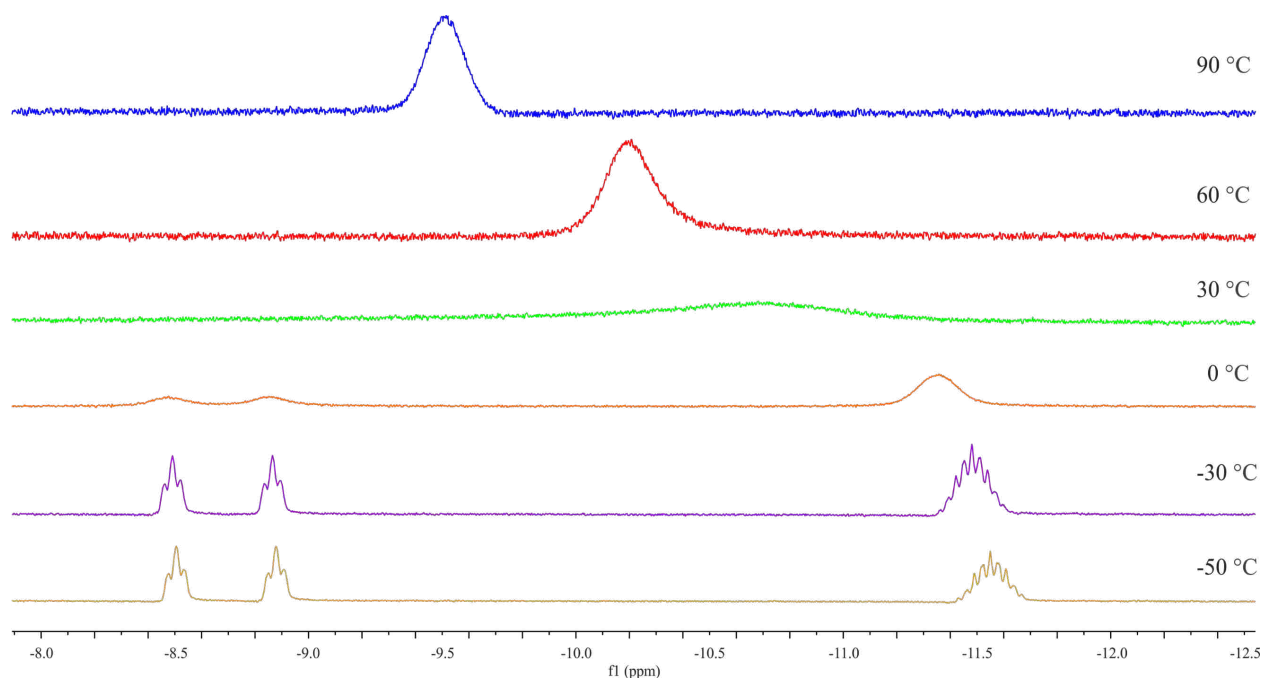


Figure 3.17. *In situ* ^1H NMR of the hydride region for $\text{Rh}_2(\text{nbd})_2(\text{rac-et,ph-P4-Ph})](\text{BF}_4)_2$ in DMF-d_7

The ^1H NMR at $-50\text{ }^\circ\text{C}$ contains a doublet of triplets centered at -8.7 ppm ($J_{\text{H-P}} = 149.5\text{ Hz}$, $J_{\text{H-H}} = 13.0\text{ Hz}$) and a triplet of quartets centered at -11.6 ppm ($J_{\text{H-H}} = 23.6\text{ Hz}$, $J_{\text{H-Rh}} = 11.6\text{ Hz}$). Like the PF_6 salt, the terminal hydride is assigned to the -9.6 ppm peaks, and the bridging hydride is assigned to the -12.5 ppm peak. As the temperature rose, the splitting began to broaden. At $0\text{ }^\circ\text{C}$, the splitting could no longer be discerned. At $30\text{ }^\circ\text{C}$, the peaks had merged to a single resonance near 10.7 ppm . This resonance shifted to 10.2 ppm at $60\text{ }^\circ\text{C}$ and 9.5 ppm at $90\text{ }^\circ\text{C}$. Also like the PF_6 salt, the broadening and reduction to a single peak is likely the bridging dihydride species.

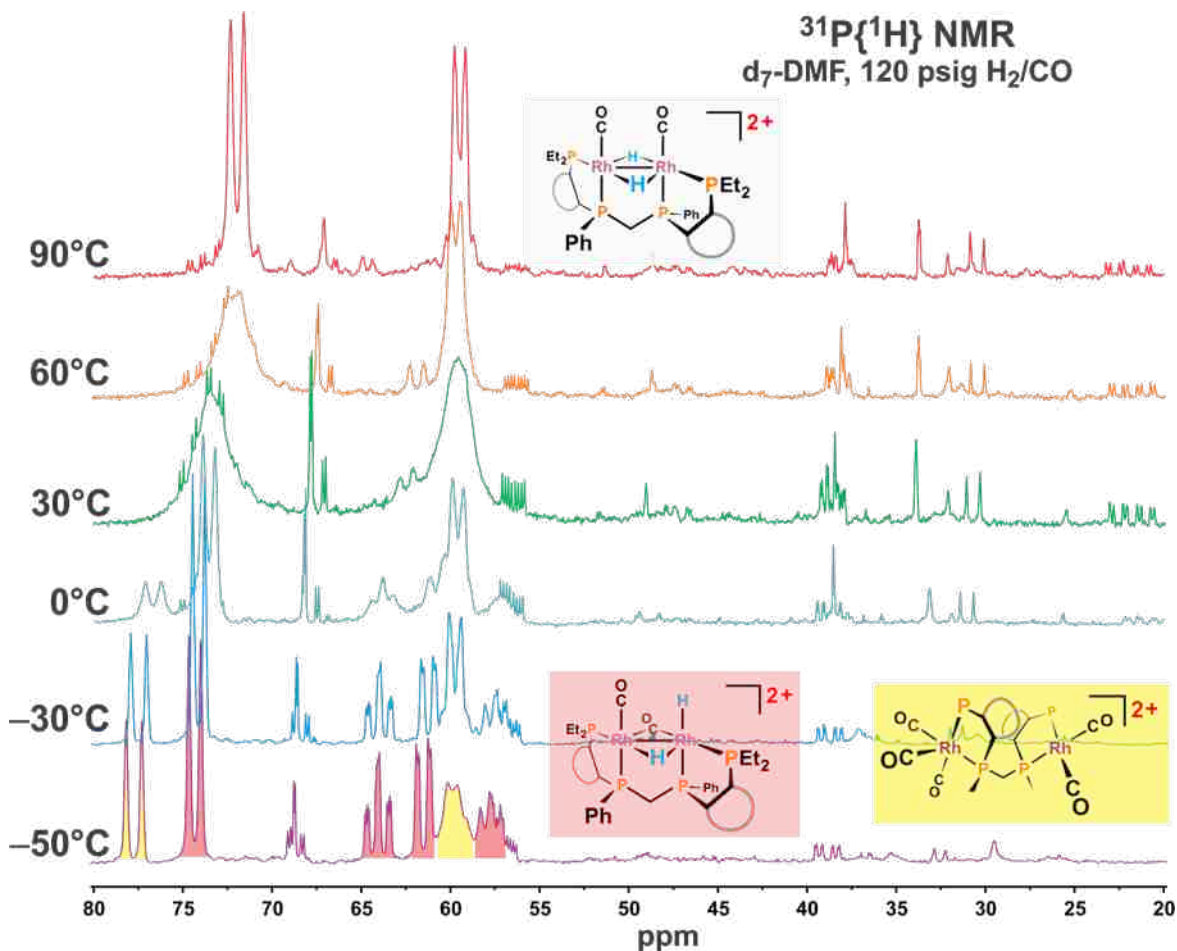


Figure 3.18. *In situ* variable temperature $^{31}\text{P}\{^1\text{H}\}$ NMR of $\text{Rh}_2(\text{nbd})_2(\text{rac-}\text{et,ph-P4-Ph})](\text{BF}_4)_2$ in DMF-d_7 at 120 psig H_2/CO

Upon examining the $^{31}\text{P}\{^1\text{H}\}$ NMR, “impurities” were found between 20 – 40 ppm. These are believed to be related to a DMF solvated complex. A second species believed to be another “impurity” is found between 68 – 69 ppm. At -50°C six major phosphine moieties resonances including a doublet of doublets at 77.7 ppm ($J_{\text{P-P}} = 142.7$ Hz, $J_{\text{P-H}} = 11.4$ Hz), a doublet of triplets at 74.3 ppm ($J_{\text{P-P}} = 111.2$ Hz, $J_{\text{P-H}} = 12.3$ Hz), a doublet of doublet of doublet of doublets (dddd) (as calculated by MestReNova) at 64.1 ppm ($J_{\text{P-P}} = 108.1$ Hz, $J_{\text{P-P}} = 97.2$ Hz, $J_{\text{P-Rh}} = 25.3$ Hz, $J_{\text{P-H}} = 12.3$ Hz), a doublet of doublets at 61.5 ppm ($J_{\text{P-P}} = 109.3$ Hz, $J_{\text{H-Rh}} = 25.6$ Hz) a doublet at 59.9 ppm ($J_{\text{P-P}} = 89.4$ Hz), and a multiplet between 56.7 – 59.7 ppm. As

illustrated in the figure above, the dd at 77.7 ppm and the multiplet at 58 ppm are believed to be the unsymmetrical pentacarbonyl species and the other four phosphines peaks are from $[\text{HRh}_2(\mu\text{-H})(\mu\text{-CO})(\text{CO})(\text{rac-}et,\text{ph-P4-Ph})]^{2+}$.

As the temperature rises, separate species begin to shift, broaden, and coalesce. At 30 °C, the double of triplets from 74.3 ppm has broadened into one resonance with the doublet of doublets from 77.7 ppm overlapping it as a multiplet. Likewise, the double of doublets from 61.5 ppm, doublet from 59.9 ppm, and multiplet from 58 ppm has broadened into a second resonance; and the dddd has started to become a doublet of doublets. It is thought that the species are in a dynamic equilibrium between the bridging H/CO and the bridging dihydride species.

By 60 °C the dddd has fully converted into a doublet of doublets at 59.7 ppm ($J_{\text{P-P}} = 91.6$ Hz); the broadened peaks at 60 ppm begins to switch back to a new double of doublets. Finally, at 90 °C, both broadened resonances have resolved into two doublet of doublets at 72.0 ppm ($J_{\text{P-P}} = 120.9$ Hz) and 59.5 ppm ($J_{\text{P-P}} = 98.1$ Hz), which is the bridged-dihydride species. Consistent with the NMR study of the PF_6 salt after a week under high pressure, little to no fragmentation was seen in the DMF-d_7 NMR study.

3.2.3 *In Situ* FT-IR Studies of $[\text{Rh}_2(\text{nbd})_2(\text{rac-}et,\text{ph-P4-Ph})](\text{BF}_4)_2$

After studying the NMR of $[\text{Rh}_2(\text{nbd})_2(\text{rac-}et,\text{ph-P4-Ph})](\text{BF}_4)_2$, similar *in situ* FT-IR experiments were performed. A procedure mimicking the work of Bridges and Alexander on the $[\text{Rh}_2(\text{nbd})_2(\text{rac-}et,\text{ph-P4})](\text{BF}_4)_2$ pre-catalyst was used examining the material. 10 mmol of $[\text{Rh}_2(\text{nbd})_2(\text{rac-}et,\text{ph-P4-Ph})](\text{BF}_4)_2$ was dissolved in 15 mL of DCM. The complex was loaded into the SpectraTech autoclave cell of the FT-IR. It then was flushed with a low pressure of CO. The species was then pressurized further to 40 psig and then 80 psig of CO. After formation of

the carbonyl species with 80 psig of CO, the system was heated to varying temperatures. At the end of the reaction the autoclave was allowed to purge to low CO pressure, and then flushed with N₂. Finally, to study the [Rh₂(nbd)₂(*rac*-*et*,*ph*-P4-Ph)](BF₄)₂ system further, it was put under 80 psig of H₂/CO and then heated back to 80 °C. Figure 3.19 depicts the FT-IR spectra for the experiment. The low signal to noise in these studies prompted Prof. Stanley to redesign the SpectraTech high pressure cell to include nitrogen flushing of the external path of the IR beam to minimize the interference by H₂O and CO₂. This study needs to be redone with the new cell configuration or the Mettler-Toledo ReactIR high pressure cell.

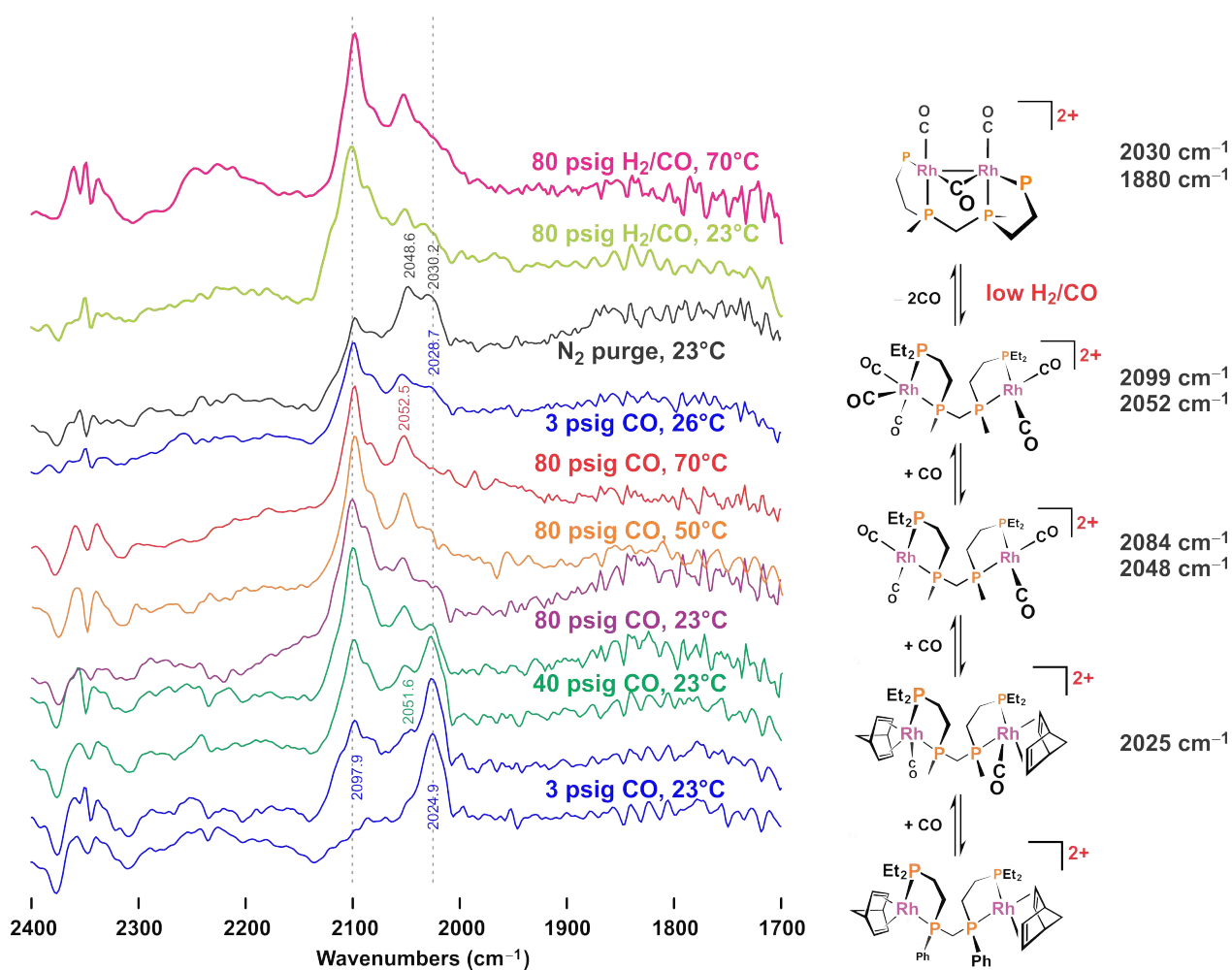


Figure 3.19. Stacked *in situ* FT-IR of [Rh₂(nbd)₂(*rac*-*et*,*ph*-P4-Ph)](BF₄)₂, the structures shown are drawn with the “old” *et*,*ph*-P4 ligand for clarity as the 1,2-phenylene chelate rings complicate the structure drawings.

The proposed structures along with their stretching frequencies are shown in the figure above. From the experiment, it was found that under low CO pressure the system barely binds CO. The system has a strong affinity for the norbornadiene ligands. As seen in Alexander's work, the old et,ph-P4 complex effectively competes with nbd within 20 minutes at 3 psig. It was not until the new system has sat under 40 psig of CO for about 20 minutes that carbonyls start to bind to the metal centers strongly enough to remove the nbd. Furthermore, when depressurized, the 2025 cm⁻¹ band grows back in, which indicates that nbd is able to recoordinate at lower pressures.

Unlike the old et,ph-P4 complex, norbornadiene does not appear to polymerize or hydroformylate *in situ*. The polymerization of nbd in the "old" [Rh₂(nbd)₂(*rac*-et,ph-P4)](BF₄)₂ catalyst precursor keeps the nbd from being a competitive ligand with the carbonyls as it removes the ligand from the solution. The new [Rh₂(nbd)₂(*rac*-et,ph-P4-Ph)](BF₄)₂ appears to bind nbd strongly enough that it acts as an inhibiting ligand.

The persistence of the norbornadiene ligand to coordinate to the rhodium centers leads the group to believe that this could be one of the critical flaws with the new Rh₂(nbd)₂(*rac*-et,ph-P4-Ph)](BF₄)₂ precursor complex. If the nbd were to rebind during hydroformylation, then it may not react as efficiently with alkene as the older et,ph-P4 based dirhodium catalyst. Although a polymer of nbd did not crystallize out of solution after the experiment, some red crystals did.

3.2.4 Characterization of [Rh₂(μ-CO)(CO)₃(*rac*-et,ph-P4-Ph)](BF₄)₂

A crystal from the FT-IR experiment was collected and given to Fronczek for X-ray diffraction. The crystal structure was determined to be [Rh₂(μ-CO)(CO)₃(*rac*-et,ph-P4-

Ph)](BF₄)₂. The ellipsoid plot is shown below in Figure 3.20. A selection of bond distances and angles are listed in Table 3.1.

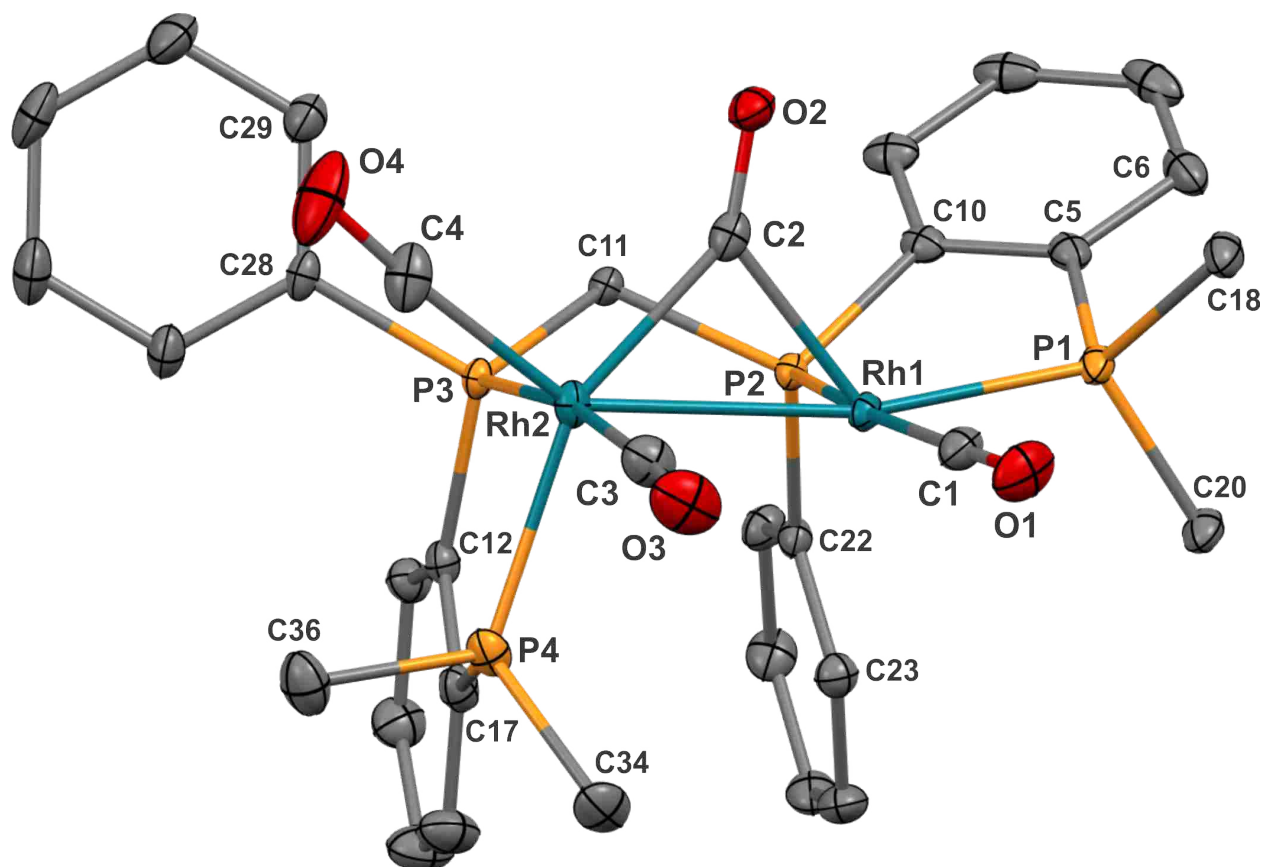


Figure 3.20. Plot with 50 % ellipsoids of [Rh₂(μ-CO)(CO)₃(rac-et,ph-P4-Ph)](BF₄)₂ (hydrogens and BF₄ counter-anions omitted for clarity)

The X-ray crystallography shows that the complex is dicationic and bimetallic with each rhodium in the 1+ oxidation state and a d⁸ configuration. The geometry for one rhodium is octahedral and the second is octahedral using an empty d-orbital as one of the sites. The ligand is bound to the metals as anticipated. A distance of 2.7702 Å is found between the metal centers; this distance points to a covalent bond between the metals. The proposed Rh-Rh bond makes Rh1 an unsaturated 16 electron metal center and Rh2 a saturated 18 electrons.

Table 3.1. Selected Bond Distances (Å) and Bond Angles (°) of $[\text{Rh}_2(\mu\text{-CO})(\text{CO})_3(\text{rac-}i\text{et,ph-P4-Ph})](\text{BF}_4)_2$

Rh1-C1	1.934(2)	Rh2-C2	2.075(2)
Rh1-C2	2.070(2)	Rh2-C3	1.934(2)
Rh1-P1	2.3018(5)	Rh2-C4	1.992(2)
Rh1-P2	2.2967(5)	Rh2-P3	2.3147(5)
Rh1-Rh2	2.7702(2)	Rh2-P4	2.3434(6)
P2-C11	1.8222(19)	P3-C11	1.8217(19)
C1-Rh1-C2	96.80(8)	C2-Rh2-P4	151.18(6)
C1-Rh1-P1	89.58(7)	C2-Rh2-Rh1	47.97(6)
C1-Rh1-P2	170.41(7)	C3-Rh2-C4	93.72(10)
C1-Rh1-Rh2	96.63(6)	C3-Rh2-P3	170.51(7)
C2-Rh1-P1	120.46(6)	C3-Rh2-P4	88.00(7)
C2-Rh1-P2	90.06(5)	C3-Rh2-Rh1	88.46(7)
C2-Rh1-Rh2	48.13(6)	C4-Rh2-P3	91.61(6)
P1-Rh1-P2	81.152(18)	C4-Rh2-P4	110.09(7)
P1-Rh1-Rh2	167.501(15)	C4-Rh2-Rh1	146.17(7)
P2-Rh1-Rh2	92.941(13)	P3-Rh2-P4	82.795(19)
C2-Rh2-C3	95.39(8)	P3-Rh2-Rh1	91.483(14)
C2-Rh2-C4	98.26(9)	P4-Rh2-Rh1	103.719(16)
C2-Rh2-P3	91.60(5)	P2-C11-P3	108.17(9)

A sample of the crystals were dried and tested for solubility. Though initially red in color, the dried sample was yellow; the original red color believed to be due to the size of the crystal. When smaller, and in a powder form, the material's color is less intense. It was found that the complex is soluble in acetone, acetonitrile, DMF, DMSO, DCM, methanol, and ethanol; it is slightly soluble in THF; and it is insoluble in diethyl ether, benzene, toluene, and hexane. When dissolved, the complex bubbles in solution and undergoes a color change from yellow to red. The gas being let off is likely one of the terminal carbonyls, and with a more electron-rich rhodium center the color changes. The ^1H NMR shows a triplet at 3.75 ppm ($J_{\text{P-H}} = 11.6$ Hz) indicative of the protons on the central methylene bridge (Figure 3.21).

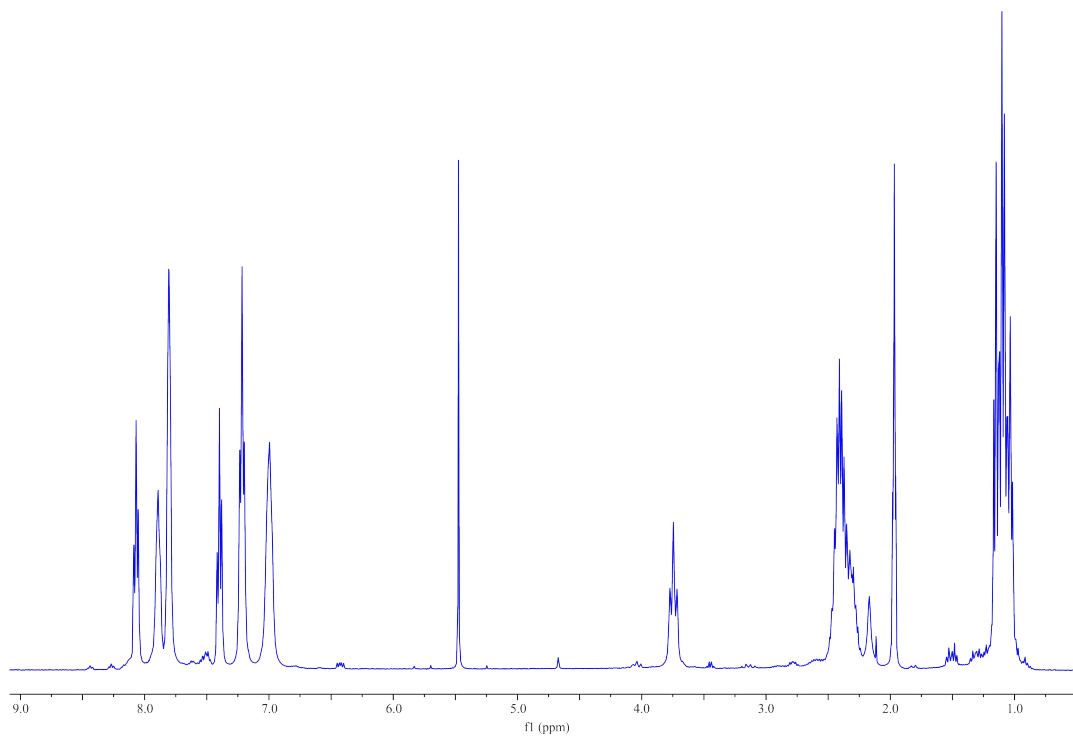


Figure 3.21. ^1H NMR of $[\text{Rh}_2(\mu\text{-CO})(\text{CO})_3(\text{rac-et,ph-P4-Ph})](\text{BF}_4)_2$ in DCM-d_2

The $^{31}\text{P}\{^1\text{H}\}$ NMR has two broad doublets the first centered at 63.9 ppm ($J_{\text{Rh-P}} = 137.1$ Hz) and 65.8 ppm ($J_{\text{Rh-P}} = 115.1$ Hz) (Figure 3.22). The smaller peaks are believed to be impurities of other carbonyl complexes from the FT-IR experiment. These impurities have yet to be identified. The crystals from the FT-IR experiment were gathered from a deep red solution. When this solution was dried, similar peaks to those in Figure 3.22 were seen.

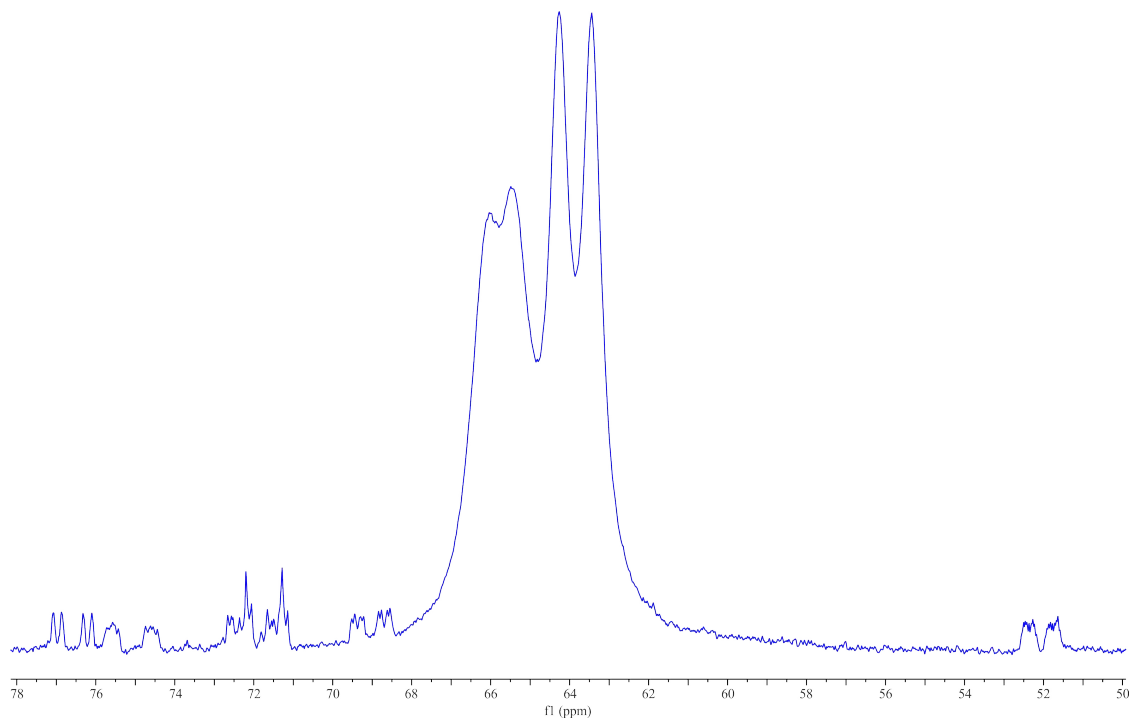


Figure 3.22. $^{31}\text{P}\{^1\text{H}\}$ NMR of $[\text{Rh}_2(\mu\text{-CO})(\text{CO})_3(\text{rac-et,ph-P4-Ph})](\text{BF}_4)_2$ in DCM-d_2

A sample of $[\text{Rh}_2(\mu\text{-CO})(\text{CO})_3(\text{rac-et,ph-P4-Ph})](\text{BF}_4)_2$ was examined on FT-IR (Figure 3.23). The band at 1900 cm^{-1} is from the bridging CO. The band is unusually intense and at a rather high frequency for a bridging carbonyl. The other three bands at 2044, 2073, and 2099 cm^{-1} are from the terminal carbonyls of the complex.

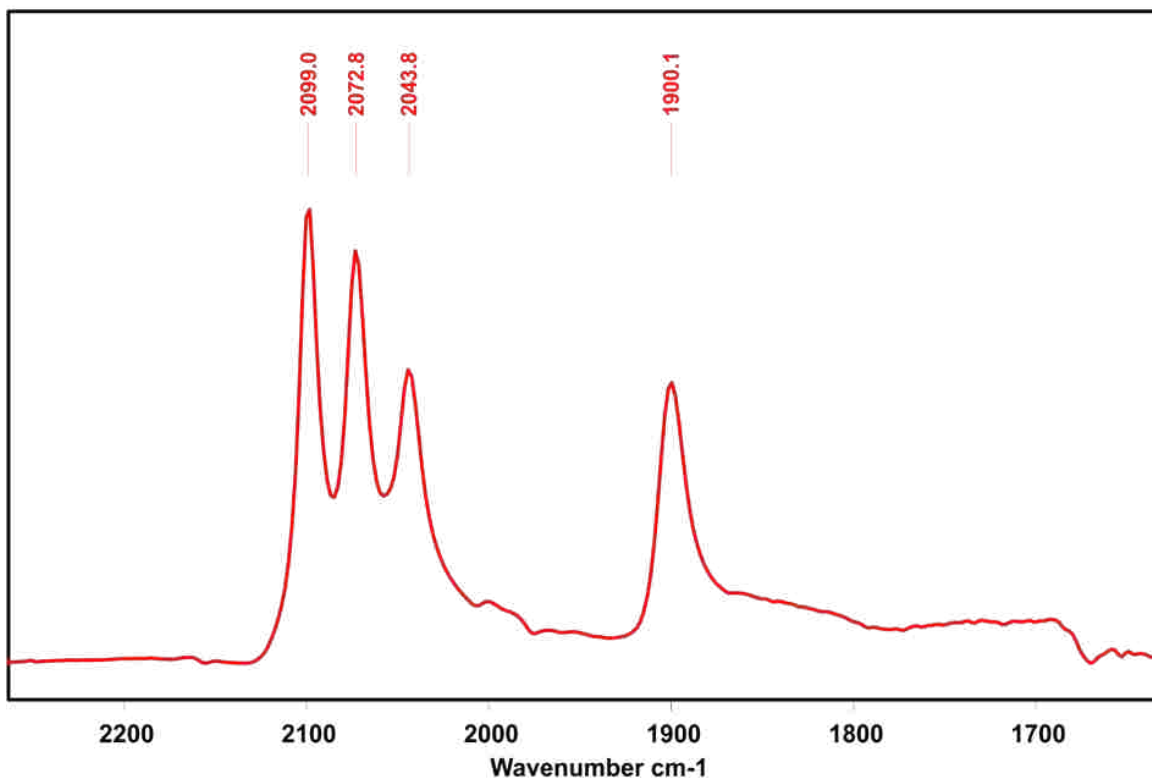


Figure 3.23. FT-IR of $[\text{Rh}_2(\mu\text{-CO})(\text{CO})_3(\text{rac-et,ph-P4-Ph})](\text{BF}_4)_2$

3.2.5 Hydroformylation with $[\text{Rh}_2(\mu\text{-CO})(\text{CO})_3(\text{rac-et,ph-P4-Ph})](\text{BF}_4)_2$ and AWS reactions

Some of the crystallized $[\text{Rh}_2(\mu\text{-CO})(\text{CO})_3(\text{rac-et,ph-P4-Ph})](\text{BF}_4)_2$ was tested for hydroformylation and showed remarkable results. In the acetone/water system, it was found that the initial TOF was 29 min^{-1} , the L:B was 17:1, the alkene isomerization was 4.7 %, and alkene hydrogenation was 1.1 %. However, in pure acetone, the system fared worse; the initial TOF was 20 min^{-1} , the L:B was 13.6, the alkene isomerization was 1.1 %, and the alkene hydrogenation was a very high 30.7 %. Once again, the use of acetone was believed to be the problem, so further runs were made in DMF and DMF/water systems.

Hydroformylation in DMF and DMF water systems with were quite good. When pure DMF was used the initial TOF were found to be 34 min^{-1} , the L:B selectivity was 16.4:1, isomerization was 3.3 % and hydrogenation was 1.2 %. When a DMF system with 25 % (by

vol) water was used[†], the initial TOF was 35 min⁻¹, the L:B selectivity was 17.6:1, isomerization was 1.9 %, and hydrogenation was < 1 %.

With the success of [Rh₂(μ-CO)(CO)₃(*rac*-et,ph-P4-Ph)](BF₄)₂, a procedure to make more crystals for subsequent reaction was proposed based on the conditions of the FT-IR experiment. Higher loadings of the complex from 10 mmol to 25 mmol were found to give better yields. So 25 mmol of [Rh₂(nbd)₂(*rac*-et,ph-P4-Ph)](BF₄)₂ was dissolved in 25 mL of DCM and loaded into an autoclave system under vacuum. Once loaded with the complex, autoclave was then pressurized to 80 psig of H₂/CO and heated to 70 °C. The complex would react for an hour and then the solution would be moved to a flask in which it could recrystallize.

The crystals were removed from a deep red solution as with the FT-IR experiment. Both the [Rh₂(μ-CO)(CO)₃(*rac*-et,ph-P4-Ph)](BF₄)₂ crystals and the red solution were dried and tested for hydroformylation. The crystals performed like above, but the red solution would only isomerize 1-hexene and hydrogenate it to hexane.

The [Rh₂(μ-CO)(CO)₃(*rac*-et,ph-P4-Ph)](BF₄)₂ crystals were also tested for tandem AWS. Keeping to Barnum's protocol, I attempted to run the hydroformylation reaction until 80 % conversion of the olefin to aldehyde was achieved. At this point I turned off the syn-gas inlet to the autoclave and opened a CO gas feed. The reaction was then monitored for acid production by GC-MS. As the hydroformylation reactions averaged 800 turnover (80 % conversion) at 60 minutes, the gas switch was tested between 50 – 70 minutes in 5 minute increments. The CO feed was also varied between 30 – 50 psig, and some attempts at purging the autoclave prior to

[†]Other levels including 10 %, 20 %, and 30 % (by vol.) of water were tested, but none performed as well as the 25 %.

opening the CO feed were also made. In all cases, hydroformylation took place, but slowed due to the switch of gases. At no point was heptanoic acid produced.

3.3 References

1. Aubry, D. A.; Bridges, N. N.; Ezell, K.; Stanley, G. G., Polar Phase Hydroformylation: The Dramatic Effect of Water on Mono- and Dirhodium Catalysts. *J. Am. Chem. Soc.* **2003**, *125*, 11180.
2. Fernando, S. R. G. Computational Studies on Bimetallic Catalysis and X-Ray Absorption Spectroscopy. Ph.D. Dissertation, Louisiana State University, Baton Rouge, LA, 2015.
3. Fernando, R. G.; Gasery, C. D.; Moulis, M. D.; Stanley, G. G., Bimetallic Homogeneous Hydroformylation. *In Homo and Heterobimetallic Complexes in Catalysis*, 1; Kalck, P.; Springer: Switzerland, 2016.
4. Matthews, R. C.; Howell, D. K.; Peng, W.; Train, S. G.; Treleaven, W. D.; Stanley, G. G., Bimetallic Hydroformylation Catalysis: *In Situ* Characterization of a Dinuclear Rhodium(II) Dihydrido Complex with the Largest Rh–H NMR Coupling Constant. *Angew. Chem., Int. Ed.* **1996**, *35*, 2253
5. Polakova, D. Studies on a Dirhodium Tetrphosphine Hydroformylation Catalyst. Ph.D. Dissertation, Louisiana State University, Baton Rouge, LA, 2012.
6. Wilson, Z. S. Electronic Structural Investigations of Bi- and Polymetallic Complexes Using Quantum Mechanical Methods. Ph.D. Dissertation, Louisiana State University, Baton Rouge, LA, 2004.
7. Bridges, N. N. Kenetic and Mechanistic Studies of a Bimetallic Hydroformylation Catalyst. Ph.D. Dissertation, Louisiana State University, Baton Rouge, LA, 2001.
8. Brant, P.; Salmon, D. J.; Walton, R. A., Electrochemical Oxidations of Complexes of Rhenium(II) Containing Metal-Metal Triple Bonds. Synthesis and Characterization of Paramagnetic Cations of the Type $[\text{Re}_2\text{X}_4(\text{PR}_3)_4]^+$, Where X = Cl or Br, Possessing Metal-Metal Bonds of Order 3.5. *J. Am. Chem. Soc.* **1978**, *100*, 4424.
9. Barnum, A. R. Studies of a Dirhodium Tetrphosphine Catalyst for Hydroformylation and Aldehyde-Water Shift Catalysis. Ph.D. Dissertation, Louisiana State University, Baton Rouge, LA, 2012.
10. Broussard, M. E. Bimetallic Hydroformylation Catalysis. Ph.D. Dissertation, Louisiana State University, Baton Rouge, LA, 1993.
11. Matthews, R. C. *In Situ* NMR and FT-IR Studies on a Bimetallic Hydroformylation Catalyst. Ph.D. Dissertation. Louisiana State University, Baton Rouge, LA, 1999.

12. Alexander, C. L. T. Studies of Dirhodium Homogeneous Catalyst System. Ph.D. Dissertation, Louisiana State University, Baton Rouge, LA, 2009.
13. (a) Thompson, S. J.; Bailey, P. M.; White, C.; Maitlis, P. M., Solvolysis of the Hexafluorophosphate Ion and the Structure of [Tris(μ -difluorophosphato)bis(pentamethylcyclopentadienylrhodium)] Hexafluorophosphate. *Angew. Chem. Int. Ed.* **1976**, *15*, 490. (b) White, C.; Thompson, S. J.; Maitlis, P. M., Pentamethylcyclopentadienylrhodium and -iridium Complexes XIV. The Solvolysis of Coordinated Acetone Solvent Species to Tris(μ -difluorophosphato)bis[η^5 -pentamethylcyclopentadienylrhodium(III)] Hexafluorophosphate, to the η^5 -(2,4-dimethyl-1-oxapenta-1,3-dienyl)(pentamethylcyclopentadienyl)iridium Cation, or to the η^5 -(2-hydroxy-4-methylpentadienyl)(η^5 -pentamethylcyclopentadienyl)iridium Cation. *J. Organomet. Chem.* **1977**, *134*, 319.

Chapter 4: Experimental Procedures

4.1 General Considerations

Unless notated, all reactions were carried out under a nitrogen environment using Schlenk lines or glove boxes and their corresponding techniques. All solvents were purchased from Sigma-Aldrich, aside from H₂O, which was deionized in house. Similarly, most all other chemicals were purchased from Sigma-Aldrich with the following exceptions. The Et₂Zn was procured from Strem Chemicals. The 1,2-diiodobenzene and the 1-bromo-2-iodobenzene were purchased from Matrix Scientific. Shell Neodene 10 was acquired from Shell through Centauri Technologies, LP. PPh₃ was obtained from BASF through Centauri Technologies, LP as well as directly from Sigma Aldrich. Both [Rh(nbd)₂](BF₄) and Rh(CO)₂(acac) were purchased from Umicore, Precious Metals Chemistry. N,N-DMF-d₇ and THF-d₈ were purchased from Cambridge Isotope Laboratories, Inc. The et,ph-P4 ligand as well as H(Ph)PCH₂P(Ph)H and Et₂PdCl were prepared as previously described.^{1,2} The synthesis of *rac*-[Rh₂(nbd)₂(et,ph-P4)](BF₄)₂ followed past research.³ Solvents were obtained dry and under N₂ or degassed with N₂; they were used without additional purification.

NMR spectra were recorded on one of three instruments including: Bruker Avance 400 MHz spectrometer, Avance III with three channels 400 MHz spectrometer, or Avance III Nanobay 400 MHz spectrometer. All FT-IR spectra were recorded on a Bruker Tensor 27 FT-IR. NMR data was analyzed and simulated using MestRenova (v 10.0) and FT-IR data was collected and analyzed using Bruker Opus (v 7.2). ¹H NMR chemical shifts were reported relative to TMS, and ³¹P NMR chemical shifts were reported relative to the external signal of 85 % H₃PO₄.

GC-MS data was collected on an Agilent Technologies 6890N Network GC system/5975 B VL MSD with a HP-5MS (30 m × 0.25 mm × 0.25 μm) column. X-ray crystallography analyses were performed by Dr. Frank Fronczek using either a Nonius KappaCCD diffractometer with Mo Kα radiation and graphite crystal monochromators or a Bruker Kappa APEX-II DUO diffractometer with Mo Kα or Cu Kα radiation and graphite crystal monochromators.

4.2 General Hydroformylation Procedures

Following the procedures from the literature, all reactions were carried out in modified Parr stainless steel autoclaves equipped with packless magnetic stirrers, thermocouples, and pressure transducers.⁴ The autoclave reactor was connected to Parr process controller 4875 and power controller 4870 to operate the heating and stirring components. The reactor is assembled and evacuated under a vacuum for fifteen minutes. Into a 125 mL Erlenmeyer flask, 0.093 g *rac*-[Rh₂(nbd)₂(et,ph-P4)](BF₄)₂ or 0.101 g *rac*-[Rh₂(nbd)₂(et,ph-P4-Ph)](BF₄)₂ is added with 54.6 mL H₂O, 23.4 mL acetone, and 0.646 g toluene. Through a column of Grade IV alumina, 11.25 mL of 1-hexene passed and is collected into a finger vial. While under negative pressure, the catalyst solution is added to the main reactor vessel and the 1-hexene to the olefin reservoir arm. The autoclave is pressurized separately from the reservoir to 90 psig of syn-gas and vented down to 45 psig. The main reactor is then allowed to heat up to 90 °C while stirring at 1000 rpm over the course of 20 minutes. The reactor is vented to 45 psig once again with the pressure above the reservoir at 90 psig. This extra pressure is used to inject the olefin at once into the reactor. The reaction's progress is monitored by SpecView (v 2.5) for gas consumption along with sampling analyzed by GC-MS.

4.3 General Aldehyde-Water Shift Procedures (Tandem Hydroformylation)

Following the procedures from the literature, all reactions are performed similarly to the reactions described above in 4.2.⁴ At some point in the reaction based on the predicted 80 % conversion of olefin, the gas feed is switched from syn-gas to pure CO. The pressure of the CO varied for the reactions. Some purging of the main reactor may be needed to gain desired CO pressure.

4.4 Synthesis of Cl-Bridge

Toluene is added to the previously made bridge as follows:

$$x \text{ g Bridge} \times \frac{1 \text{ mol}}{232.197784 \text{ g}} \times \frac{1000 \text{ mL}}{10 \text{ M}} = y \text{ mL Toluene}$$

A two-necked Schlenk flask charged with C₂Cl₆ (2.1 eq.) and Toluene as follows:

$$a \text{ g hexachlorethane} \times \frac{1 \text{ mol}}{236.7394 \text{ g}} \times \frac{1000 \text{ mL}}{2 \text{ M}} = b \text{ mL Toluene}$$

The two-necked flask is heated to ~80° C (up to 90° C) using an oil-bath while the upper neck is attached to a condenser. The bridge is added over 30 minutes to the C₂Cl₆ with periods of N₂ flowing into the two flask to help remove the HCl being produced. Once added, the solution reacts for 2-3 hours. If shown to be done via NMR, the toluene is reduced under vacuum pressure leaving behind Cl-bridge. Note: The Cl-bridge needs to be moved to a second flask for weighing; this process helps to remove excess C₂Cl₆ and H₂O if carefully transferred (heat-gun optional). Also reducing the toluene, do not heat the Cl-bridge above 85° C. Removal of toluene must be done promptly after the reaction is complete.

4.5 Synthesis of I-Small Arm

Day 1

THF is added to Et₂PCl as a solvent (9.25 mL/g) and the flask is put into the freezer until needed (1 eq.). A 500 mL (or 1000 mL) Schlenk flask containing a stir-bar that is covered in foil and is charged with I₂Bz and THF as the solvent (3.2 mL/g) (0.97 eq.). A round bottom flask is filled with ⁱPrMgBr (0.97 eq.) in THF as follows:

$$x \text{ mol} \times \frac{1000 \text{ mL}}{2.9 \text{ mol}} = y \text{ mL } i\text{PrMgBr}$$

Extra THF (1-2 mL) is used to wash all ⁱPrMgBr into the flask. The I₂Bz solution is cooled to 0° C with an ice-bath for 30 minutes. The ⁱPrMgBr is then added to the I₂Bz (slowly based on viscosity). The resulting Grignard solution is allowed to stir at 0° C for 4-6 hours. After the wait, Et₂PCl is added to the Grignard over the course of 30 minutes at -25° C. Then the solution slowly warms to room temperature overnight while still stirring. Some Na₂SO₄ is put into a 1000 mL Schlenk Flask and evacuated overnight.

Day 2

75 mL H₂O are degassed and added to the Grignard to quench the reaction. The flask is shaken and allowed to rest forming two layers in the solution. The organic layer is extracted into the Na₂SO₄ and further extracted with 150 mL diethyl ether (3-5 times). This solution is filtered in the glovebox, and the solvent is boiled off under vacuum. Note: The compounds produced are light sensitive. The small arm is then purified via short-path distillation. For this an oil-bath is heated to 130° – 135° C.

4.6 Synthesis of Br-Small Arm

The same method previously described in 4.5 is used here only using I-Br-Bz instead of I₂Bz. The Grignard from the I-Br-Bz and ⁱPrMgBr can be tested via GCMS to shorten the 4-6

hour period. Take a sample of the Grignard, add H₂O, and run it on GCMS after 1.5 hours (instead of 4-6 hours). Short-path distillation can be done at a lower temperature, but may not work at that lower one. The prescribed temperature for this is 84° – 86° C.

4.7 Synthesis of et,ph-P4-Ph via I-Small Arm

Day 1

Cl-Bridge are added to a Schlenk Flask with THF as the solvent and stored in the freezer until needed (2.43 mL/g) (1 eq.). A 500 mL pear-shaped Schlenk Flask that is covered in foil and containing a stirbar has small arm added to it with THF as the solvent (2.5 mL/g) (2 eq.). A round bottom flask is charged with ⁱPrMgBr (2 eq) in THF as with the Small Arm using extra THF as a wash. The small arm is cooled to 0° C in an ice-bath for 30 min. The ⁱPrMgBr is then added to the flask and the two mix overnight at a continuous 0° C.

Day 2

The Grignard is cooled further to -25° C using an acetone/dry ice-bath. The Cl-bridge is then added to the Grignard over a 30 min period. The solution then reacts overnight while warming back to room temperature. Some Na₂SO₄ is put into a 1000 mL Schlenk Flask and evacuated overnight.

Day 3

10 mL H₂O are degassed and added to the et,ph-P4-Ph to quench the reaction. The flask is shaken and allowed to rest to form two layers in the solution. The organic layer is extracted into the Na₂SO₄ and further extracted with 150 mL diethyl ether (3-5 times). The solution is filtered in the glovebox and the solvent boiled off via vacuum. The ligand is epimerized by heating it for 3 hours on an oil bath at 130° C.

4.8 Synthesis of et,ph-P4-Ph via Br-Small Arm

Day 1

Mg turnings are added to a two-necked Schlenk Flasks with a balloon wrapped to the top neck (2 eq. + 30 % or 2.6 eq.). The flask is purged and the balloon filled with Ar. The flask is then set on a stir-plate overnight.

Day 2

The balloon is removed and a refluxing condenser is attached to the top of the flask. The whole apparatus is then flame-dried to remove any H₂O. The flask is set in an oil bath heated to 70° C. Once hot Br-small arm in THF (4 mL/g) (2 eq.) is added to the Mg and allowed to react for 60 min. Cl-bridge in THF (3.3 mL/g) (1 eq.) is cooled to -35° C via an acetone/dry ice-bath. The Grignard solution is added to the Cl-bridge slowly while still hot leaving any excess Mg behind. Note: The Grignard may clog the cannula if too cold or added too slowly, but it should not all be added at once. The solution then reacts overnight while warming back to room temperature. Some Na₂SO₄ is put into a 1000 mL Schlenk Flask and evacuated overnight.

Day 3

10 mL H₂O are degassed and added to the et,ph-P4-Ph to quench the reaction. The flask is shaken and allowed to rest to form two layers in the solution. The organic layer is extracted into the Na₂SO₄ and further extracted with 150 mL diethyl ether (3-5 times). The solution is filtered in the glovebox and the solvent boiled off via vacuum. The ligand is epimerized by heating it for 3 hours on an oil bath at 130° C.

4.9 Column Chromatography for the Removal of Impurities from et,ph-P4-Ph

Into a 400 mL beaker, ~200 mL of alumina are poured. DCM is slowly added to the alumina until fully absorbed and about 1 mm of DCM rest atop the surface. The alumina is

agitated and poured into a glass column with a diameter of 4 cm. Sand is added to the top of the alumina and the ligand is added to the sand. DCM is used to elute the ligand from the column; the impurities do not travel in DCM. The solvent is boiled off under vacuum.

4.10 Column Chromatography for the Separation of *meso*- and *rac*-*et,ph*-P4-Ph

Method A

Into a 500 mL Erlenmeyer flask, 210 – 240 g of dry (Grade I) alumina are added. A volume of H₂O equaling 10 % of the mass of the alumina is added to the same flask and allowed agitated until the H₂O is evenly mixed. 40 mL of DCM and 160 mL of hexane are added to a second Erlenmeyer and shaken. The solvent mixture is added to the alumina, and once mixed, the alumina is poured into a glass column with a diameter of 4 cm fitted with glass wool and sand. Sand is added to the top of the alumina and the ligand is added to the sand. The same solvent mixture of DCM/Hexane in a 1:4 are used to elute the ligand from the column. Once the ligand comes off the column, fractions are collected 10 mL at a time. Sampling of the fractions by TLC is done to pull the appropriate fractions together. The solvent is boiled off under vacuum. Note: DCM can degrade the ligand if left to interact with it for extended periods. The solvent must be boiled off as soon as possible.

Method B

The same method previously described in 4.10 A is used here only using a solvent mixture of 1:2:3 DCM/Toluene/Hexane instead of 1:4 DCM/Hexane to elute the ligand.

4.11 Synthesis of [Rh(nbd)₂]PF₆

THF is added to the powder Rh(nbd)acac (15 mL/g) in a 250 mL Schlenk flask. The flask is put in a recrystallization dish with acetone and allowed to stir to better dissolve. The acetone is then cooled to -20 °C using dry ice. While cooling, into a tubular Schlenk flask HPF₆

(55 wt. % in water) (2 eq.) is added. Into a second tubular Schlenk flask nbd (4.5 eq.) is added. Using a cannula, the contents of both flasks are added dropwise to the cooled Rh(nbd)acac beginning with the acid. Once the second addition is finished, the mixture is brought into the glovebox and placed in the freezer for exactly 2 hours. Note: If the time period is exceeded, the acid will begin to “polymerize” making a mess, causing subsequent steps to be challenging. After the 2 hours, the solid that precipitates out of solution is filtered in the glovebox using vacuum filtration. The solid is then put into a vial and dried overnight.

4.12 Synthesis of $[\text{Rh}(\text{nbd})_2(\text{rac-}i\text{et,ph-P4-Ph})](\text{BF}_4)_2$

DCM is added to both $[\text{Rh}(\text{nbd})_2]\text{BF}_4$ (20 mL/g) (2 eq.) and *rac-}i\text{et,ph-P4-ph}* (10 mL/g) (1 eq.). The $[\text{Rh}(\text{nbd})_2]\text{BF}_4$ is set to stir while the *rac-}i\text{et,ph-P4-Ph}* is added dropwise via cannula to the $[\text{Rh}(\text{nbd})_2]\text{BF}_4$. Note: The reaction is complete once the ligand is added, but it is best to let the solution mix for an extra 30 min.

Remove the solvent from the mixture under vacuum pressure. Then recrystallize the material using acetone and hexane in the freezer for a few days (up to a few months) in a 500 mL Schlenk flask.

4.13 Synthesis of $[\text{Rh}(\text{nbd})_2(\text{rac-}i\text{et,ph-P4-Ph})](\text{PF}_6)_2$

The same method previously described in 4.12 is used here only using $[\text{Rh}(\text{nbd})_2]\text{PF}_6$ instead of $[\text{Rh}(\text{nbd})_2]\text{BF}_4$. Recrystallization is performed in DCM and can take between 2 hours up to 24 hours in the freezer.

4.14 Synthesis of $[\text{Rh}_2(\mu\text{-CO})(\text{CO})_3(\text{rac-}i\text{et,ph-P4-Ph})](\text{BF}_4)_2$

The modified Parr stainless steel autoclaves equipped with packless magnetic stirrers, thermocouples, and pressure transducers is assembled and evacuated under a vacuum for fifteen minutes. The *rac-}i\text{et,ph-P4-Ph}* $[\text{Rh}(\text{nbd})_2](\text{BF}_4)_2$ (0.025 mol) complex is added to a round

bottom flask with DCM as the solvent. While under negative pressure, the complex solution is added to the main reactor vessel. The autoclave is pressurized to 80 psig of syn-gas. The reactor is heated up to 70 °C while stirring at 1000 rpm. After an hour the reactor is cooled to room temperature and the gas inlet is lowered to 5 psig. The system is slowly purged to 5 psig. A syringe is evacuated with the gas flowing from the reactor a few times before it is used to remove the liquid from the reactor. This red solution is transferred to an evacuated Schlenk flask that is then concentrated down under a flow of syn-gas. The solution is placed into a freezer to recrystallize. After some time, yellow crystals precipitate out of the red solution.

4.15 References

1. Laneman, S. A.; Fronczek, F. R.; Stanley, G. G., Synthesis of Binucleating Tetratertiary Phosphine Ligand System and the Structural Characterization of Both *Meso* and *Racemic* Diastereomers of {Bis[diethylphosphinoethyl]phenylphosphino}methane} tetrachlorodinickel. *Inorg. Chem.* **1989**, *28*, 1872.
2. Aubry, D. A.; Laneman, S. A.; Fronczek, F. R.; Stanley, G. G., Separating the Racemic and Meso Diastereomers of a Binucleating Tetrachosphine Ligand System through the Use of Nickel Chloride. *Inorg. Chem.* **2001**, *40*, 5036.
3. Broussard, M. E.; Juma, B.; Train, S. G.; Peng, W. J.; Laneman, S. A.; Stanley, G. G., A Bimetallic Hydroformylation Catalyst: High Regioselectivity and Reactivity Through Homobimetallic Cooperativity. *Science.* **1993**, *260*, 1784.
4. Barnum, A. R. Studies of a Dirhodium Tetrachosphine Catalyst for Hydroformylation and Aldehyde-Water Shift Catalysis. Ph.D. Dissertation, Louisiana State University, Baton Rouge, LA, 2012.

Vita

Marshall Douglas Moulis is one of two son's of Mark Douglas Moulis and Vicki Neff Moulis born in July 1989 in Lafayette, LA. He attended the University of Dallas to receive a Bachelor's of Science in Chemistry with a concentration Music, which was completed in May of 2011. He became part of the Louisiana State University's graduate school to study chemistry in 2012. Marshall is expecting to graduate from LSU with a Doctor of Philosophy in chemistry in December of 2017.